PROCESS TOMOGRAPHY Ltd.

ELECTRICAL CAPACITANCE TOMOGRAPHY SYSTEM

TYPE PTL300E

OPERATING MANUAL

Issue 7

September 2010

VOLUME 1. FUNDAMENTALS OF ECT

ECT32v2 Software Version 2.38
Firmware version 1.47
System hardware .DLL DAM200E_2_27

PROCESS TOMOGRAPHY LTD
86 Water Lane, Wilmslow, Cheshire. SK9 5BB United Kingdom.
Phone/Fax 01625-549021
(From outside UK +44-1625-549021)
email: enquiries@tomography.com Web site: www.tomography.com

Registered in England No. 2908507. Registered Office 15, Croft Road, Wilmslow, Cheshire. SK9 6JJ United Kingdom.

*** IMPORTANT ***

*** OPERATING AND SAFETY PRECAUTIONS ***

*** STATIC CHARGE WARNING ***

The use of an ECT sensor with moving dielectric fluids in an insulating pipe can give rise to the development of **high electrostatic potentials** on the **sensor and pipe** which could create a safety hazard for both the **operator** and the **plant**. Any implications for the safety of the plant being monitored should be carefully considered before using the ECT system. In particular, the sensor metalwork should be solidly grounded and connected electrically to any adjacent metallic pipework to protect the operator. If installation of the sensor causes an insulated break in a run of metallic pipework, the two sections of pipe should be bonded together using a substantial electrical link which must also be connected electrically to the outer shield of the sensor.

The input channels of the DAM200E Capacitance Measurement Unit (CMU) contain CMOS circuitry. Because of the nature of the measurement of very small values of capacitance used in the system, it is not possible to fully protect these inputs. It is therefore very important that any sensors connected to the inputs of this unit are fully discharged before connections are made. **All sensors used with the DAM200E unit should include built-in discharge resistors of no more than 1 Mohm in value, connected between the individual sensor electrodes and the screens of the coaxial connecting leads, to ensure that static charge cannot build up on the sensor electrodes.**

ELECTROMAGNETIC COMPATIBILITY

The **PTL300E ECT** system is a sensitive scientific instrument. Under normal operating conditions, the system will not cause problems to other electronic equipment provided that the ECT sensor used with the system is adequately screened and grounded.

However, the **PTL300E system** may be adversely affected by high levels of electrical interference because of its high measuring sensitivity. If these problems persist, please contact PTL for advice on solutions to these problems.

INTRINSIC SAFETY DISCLAIMER

The PTL300E ECT system has not been certified for use in applications which require intrinsic safety certification and must not be used in applications where intrinically-safe equipment is mandatory.

ACKNOWLEDGEMENTS

The PTL300E Electrical Capacitance Tomography System is manufactured under licence from the University of Manchester Institute of Science and Technology (UMIST). The design is protected by British and foreign patents.

WARRANTY

This equipment is warranted by Process Tomography Ltd., (the Company) against any defects of materials or workmanship for a period of one year from the date of despatch. In the case of components employed in this equipment but not manufactured by the Company, the manufacturer's warranty will apply.

During the warranty period, the Company will repair or, at the Company's option, replace any warranted item that proves on examination to be defective, provided the equipment is returned, carefully packed and carriage prepaid to the Company, together with full details of the claimed fault.

This warranty is in all cases limited to the cost of making good the defect in the equipment itself. It does not apply to defects caused by abnormal conditions of working, accident, misuse, neglect, wear and tear, or to equipment which has been repaired or altered other than by a person authorised by the Company.

In no event shall the Company be liable for any damages or injury which may result from the use or misuse of this product by the purchaser, his employees or others, or for any incidental or consequential damages.

To register a claim under the provisions of this warranty, please contact the Company for instructions for returning the equipment.

COPYRIGHT

ELECTRICAL CAPACITANCE TOMOGRAPHY

Electrical Capacitance Tomography (ECT) is a technique for measuring the **permittivity distribution** of a **mixture of 2 dielectric materials** inside a **closed vessel**, from which the **concentration distribution** can be found. It is a research tool which allows measurements to be made on process plant which were previously either difficult or impossible to realise. This instruction manual contains a broad spectrum of information about electrical capacitance tomography, as well as specific operating instructions for the **PTL300E single and twin-plane ECT systems**. The **PTL300E-SP-G** system allows data from **one axial plane of electrodes** to be imaged while the **PTL300E-TP-G** system allows data from **one or two planes to be imaged simultaneously**.

HOW TO USE THIS MANUAL

The PTL300E Operating Manual is in **4 volumes** and applies to both **single** and **twin-plane PTL300E ECT systems**. Where appropriate, **data which applies only to twin-plane systems is contained within square brackets [ ]** and **should be ignored** by users of **single-plane systems.**

The manual is divided into **4 volumes** containing **nine main sections** as follows:

Volume 1 (sections 1 to 4) gives information about the **theoretical backgound to ECT**

Section 1, consisting of chapters 1 and 2 contains basic information about how to set up the ECT system and check it for correct operation. Full **detailed operating instructions** are given in **section 5 in volume 2.**

Section 2, consisting of the single chapter 3, contains an overview of ECT technology and provides a brief introduction to **Electrical Capacitance Tomography**.

Section 3 (chapters 4-7) gives further detailed information about the **PTL300E ECT system**, including the principle of operation of the ECT hardware and explains how the ECT system **measures the inter-electrode capacitances of the ECT sensor**.

Section 4, which contains chapters 8 to 15, explains how **ECT images** are reconstructed from the **capacitance measurements**.

Volume 2 (sections 5 to 8) contains detailed information about the operation of the **PTL300E ECT system.**

Section 5, consisting of chapters 16 to 30, gives detailed information about the **operation of the ECT system using the ECT32v2 software**.

Section 6 (Chapter 31) Describes the operation of a **file conversion utility** for converting data files from previous versions of PTL ECT systems into **ECT32v2** format.

Section 7 (Chapter 32) describes the **ECT Toolkit utilities** which provide diagnostic and maintenance facilities for the ECT system software and firmware and which allow the ECT system to be used directly for capacitance and other measurements.

Section 8 Contains a set of **Frequently Asked Questions (FAQs)** and answers about ECT technology.

Volume 3 contains a number of **Appendices** which give further detailed information about the ECT system, including data file formats, circuit constants and additional software utilities for use with the ECT system.

Appendix 1 contains the **specification** of the PTL300E ECT system.
Appendix 2 gives details of the **demonstration sensors** supplied with the ECT system.
Appendix 3 defines the various **data file formats** in use.
Appendix 4 describes the **electronic measurement circuitry.**
Appendix 5 gives information about the **triggering circuitry**.
Appendix 6 explains how **absolute capacitance values** can be calculated from the normalised values.
Appendix 7 details the s**ofware installation**.
Appendix 8 describes the **Recal advanced calibration software**
Appendix 9 describes the **IU2000 Image reconstruction software**.
Appendix 10 describes the **Plot3d Image reconstruction software**.
Appendix 11 describes the **Makemap sensitivity matrix generation software**.
Appendix 12 describes the **MatECT Matlab ECT utilities**.
Appendix 13 describes the **BCPconvert file conversion software**.

Volume 4 contains a number of **PTL Application notes** as follows:

AN1. Generation of ECT images from capacitance measurements
AN2. Calculation of volume ratio for ECT sensors
AN3. Engineering design rules for ECT sensors
AN4. An iterative method for improving ECT images
AN10. Linearising ECT sensors

First time users should read read sections 1 and 2. When the system has been successfully set up and tested, the remainder of the manual should be read to familiarise the user with the details of the ECT system and its operation. Most of the functions of the system can be checked using the demonstration sensor[s] supplied with each system. Once the ECT hardware and software have been mastered using the demonstration sensor[s], users will want to apply the system to custom sensors on their own plant. Process Tomography Ltd can provide advice to users to enable them to design their own custom sensors or can arrange for custom sensors to be designed and supplied to customers on request.

PTL300E OPERATING MANUAL

CONTENTS

VOLUME 1

SECTION 3 THE PTL300E ECT SYSTEM

SECTION 4 PERMITTIVITY IMAGES AND CONCENTRATION DISTRIBUTION

VOLUME 2

SECTION 5 OPERATING INSTRUCTIONS

SECTION 6. FILE CONVERSION SOFTWARE

SECTION 7. THE ECT TOOLKIT SOFTWARE

SECTION 8. FREQUENTLY ASKED QUESTIONS ABOUT ECT

SECTION 9 APPENDICES 1 to 7

VOLUME 3 SUPLEMENTARY SOFTWARE

SECTION 9 (continued) **APPENDICES 8 to 13**

Appendix 8 Recal advanced calibration software

Appendix 9 IU2000 Image reconstruction software

Appendix 10 Plot3d Image reconstruction software

Appendix 11 Makemap sensitivity matrix generation software

Appendix 12 MatECT Matlab ECT utilities

VOLUME 4 PTL APPLICATION NOTES

AN1. Generation of ECT images from capacitance measurements

AN2. Calculation of volume ratio for ECT sensors

AN3. Engineering design rules for ECT sensors

AN4. An iterative method for improving ECT images

AN10. Linearising ECT sensors

FIGURES

SECTION 1 BASIC INFORMATION

SECTION 2 INTRODUCTION TO ECT TECHNOLOGY

SECTION 3 THE PTL300E ECT SYSTEM

SECTION 4 CALCULATION OF PERMITTIVITY AND CONCENTRATION IMAGES

SECTION 5 OPERATING INSTRUCTIONS

SECTION 1 BASIC INFORMATION

This initial section, consisting of chapters 1 and 2 , explains how to unpack and set up the ECT system and gives simplified instructions for testing the system using one of the demonstration sensors supplied with the system.

1. POST-DELIVERY INSTRUCTIONS

1.1 UNPACKING THE SYSTEM

Following delivery of the ECT system, the system components should be unpacked, identified and checked for shortages against the delivery note. Any damage or shortages should be notified to the carrier and to PTL immediately.

1.2 SYSTEM COMPONENTS

Figure 1.1 shows the main components of a Twin-plane PTL300E ECT system. Figure 1 shows a DAM200E Capacitance Measurement Unit (CMU) a personal computer and two 12 element demonstration capacitance sensors.

A standard **PTL300E ECT system** consists of the following items:

[Desktop or Notebook personal computer loaded with PTL ECT software.] *

DAM 200E single [or twin-plane] Capacitance Measurement Unit.

1 [2] X demonstration 12 element capacitance sensor[s].

1 [2] X 5 metre crossed ethernet cable.

3 X IEC mains leads (for PC, monitor and DAM200E).

This Operating manual (4 volumes).

ECT32v2 software User Guide.

Software installation CD ROM

*** optional item**

1.3 POWER SUPPLY INFORMATION

The **DAM200E** unit will accept voltages from 90-240V, 50 or 60Hz. The control PC (where applicable) will be supplied with a power supply suitable for the country in which the PC is to be used.

1.4 SUMMARY OF SUPPLIED SOFTWARE

The ECT system is supplied with a comprehensive suite of control and analysis software. The primary software which is used used to control the ECT system and to capture and image data is the **ECT32v2 software.** However, additional software for use before and after capturing data is also supplied and a brief summary of each software item is given here for future reference.

1.4.1 **ECT32v2:** The main control and data capture software for use with PTL ECT systems. Full details are given in sections 2 and 5 of this manual.

1.4.2 **Recal.** Advanced calibration software suitable for constructing sensor C/K files. Full details in Appendix 8 of this manual.

1.4.3 **IU2000** Supplementary image reconstruction software for producing a range of enhanced ECT images from data files captured using the ECT32v2 software. Full details are given in Appendix 9 of this manual.

1.4.4 **Plot3d:** 2 and 3-dimensional plotting software for use with data files generated by the ECT32 software. Full details in Appendix 10 of this manual.

1.4.5 **Makemap:** Sensitivity Matrix generation software for circular ECT sensors. Full details in Appendix 11 of this manual.

1.4.6 **MatECT:** Set of Matlab utilities for ECT. Requires Matlab (not supplied) to be installed on the PC before use. Full details in Appendix 12 of this manual.

1.4.7 **BCPconvert:** File conversion software which converts data files captured using ECT32v2 into a range of other file formats. Full details in chapter 31 of this manual.

1.4.8 **ECT Toolkit.** Diagnostic and maintenance software for the PTL300E ECT system. Full details in Section 7 of this manual.

1.4.8 **ECTcon**: Software for converting files captured using previous versions of PTL software into the current ECT32v2 format. Full details in section 6 of this manual.

1.4.9 **ECTRemote:** Software for exporting live data (streaming) from the control PC to a second PC. Full details in Section 5 (chapter 30) of this manual.

1.4.10 **Flowan:** (Optional purchase). Comprehensive flow measurement and analysis software for use with PTL ECT systems. Full details in separate Flowan User Guide and Tomoflow User Manual.

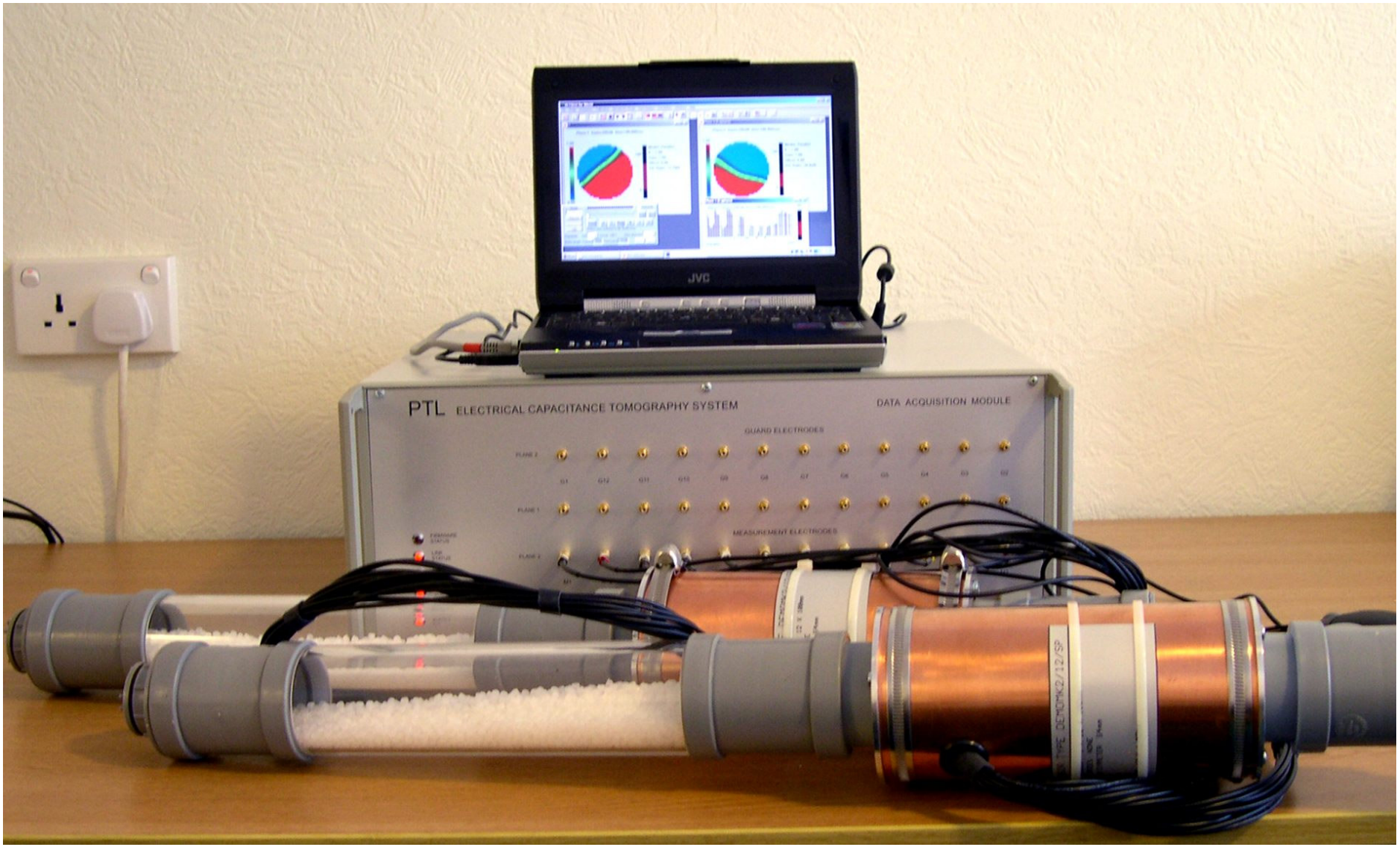

Figure 1.1 A PTL300E Twin-plane ECT system

2. QUICK START INSTRUCTIONS

This chapter gives a **quick tour** of some of the **important features** of the **PTL300E ECT system and demonstrates how to calibrate, capture** and **playback data** using the **ECT32** software and **one** of the **demonstration sensors** supplied with the ECT system. **Full details** of the **ECT system hardware** and **software** are given in **subsequent sections of this manual**. **Detailed and comprehensive operating instructions are given in section 5.**

********* STATIC CHARGE PRECAUTIONS *********

The input channels of the **DAM200E CMU** contain sensitive **CMOS** electronic circuitry. Because of the nature of the measurement of very small values of capacitance used in the system, it is not possible to fully protect these inputs. It is therefore **very important** that the **electrodes** of **capacitance sensors** are not allowed to become electrically charged with respect to earth before they are connected to the **DAM200E** unit. All capacitance sensors used with the **DAM 200E** unit must include built-in **discharge resistors** of no more than 1 Mohm in value, permanently connected between the individual sensor electrodes and the screens of the coaxial connecting leads, to ensure that static charge cannot build up on the sensor electrodes.

2.1 THE DAM200E CAPACITANCE MEASUREMENT UNIT (CMU)

The **front panel layout** of the **CMU** is shown in figure 2.1.1. There are **5 indicator lamps** (**LEDS**) and **4 sets of 12 x SMB miniature coaxial connectors**, **two sets** for the **Plane 1 and Plane 2 Measurement Electrode channels** and a further **two sets** for the **Plane 1 and Plane 2 Driven Guard Electrode channels**.

The **connectors** for the **Capacitance Measurement channels** are located on the **lower half** of the **front panel** and are labelled **M1 to M12**. The **Plane 1 set** are at the **bottom** of the panel with the **Plane 2 set** located directly above those for **Plane 1**.

The **connectors f**or the **Driven Guard channels** are located on the **top half of the panel** and are labelled **G1 to G12**. Again the **Plane 1** set is located below the **Plane 2** set.

The **rear panel** of the CMU is shown in figure 2.1.2. The **mains power input (IEC) socket, switch** and **fuse** are located at the RHS of the panel when viewed from the rear of the unit. Other items on the rear panel are a **LAN 10/100 MB/S Ethernet connector**, a **3-pin DIN trigger input/output connector** and and a **diagnostic serial (RS232) port**.

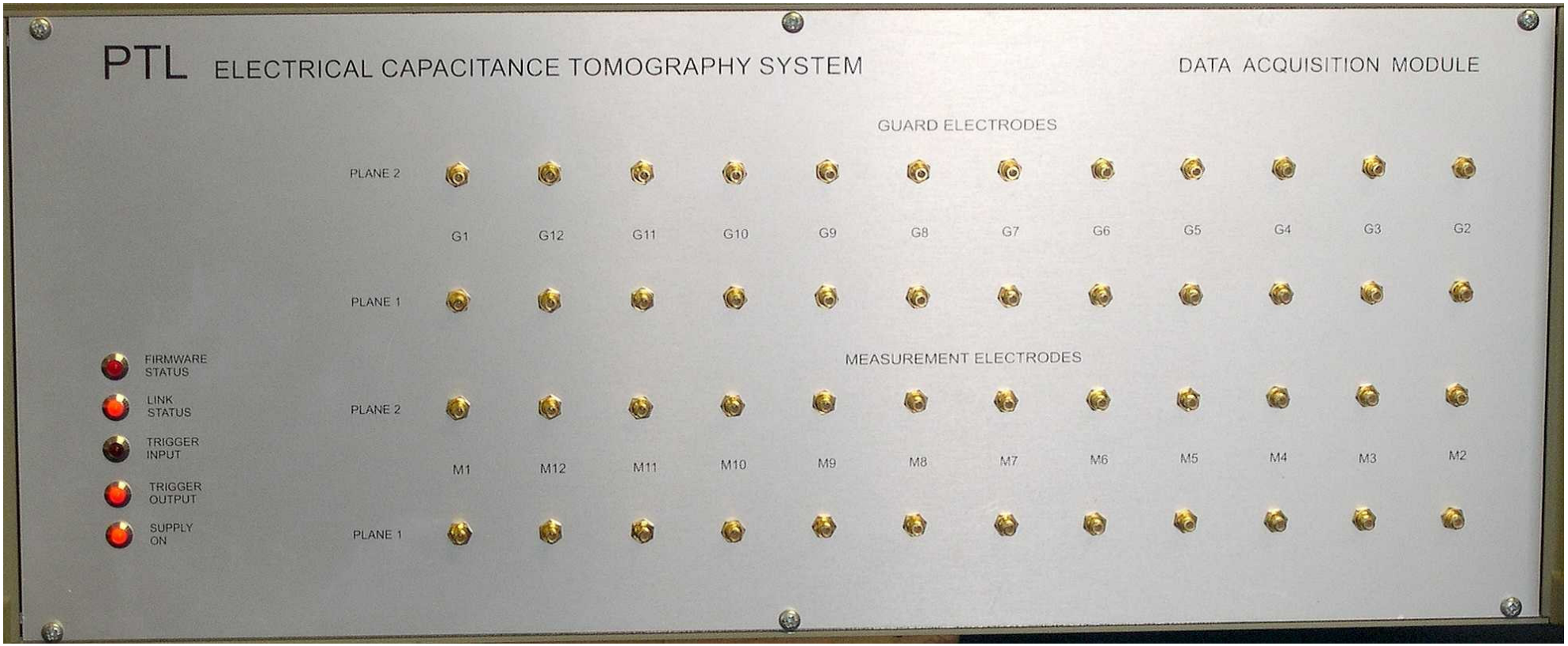

Figure 2.1.1 DAM200E CMU Front panel layout

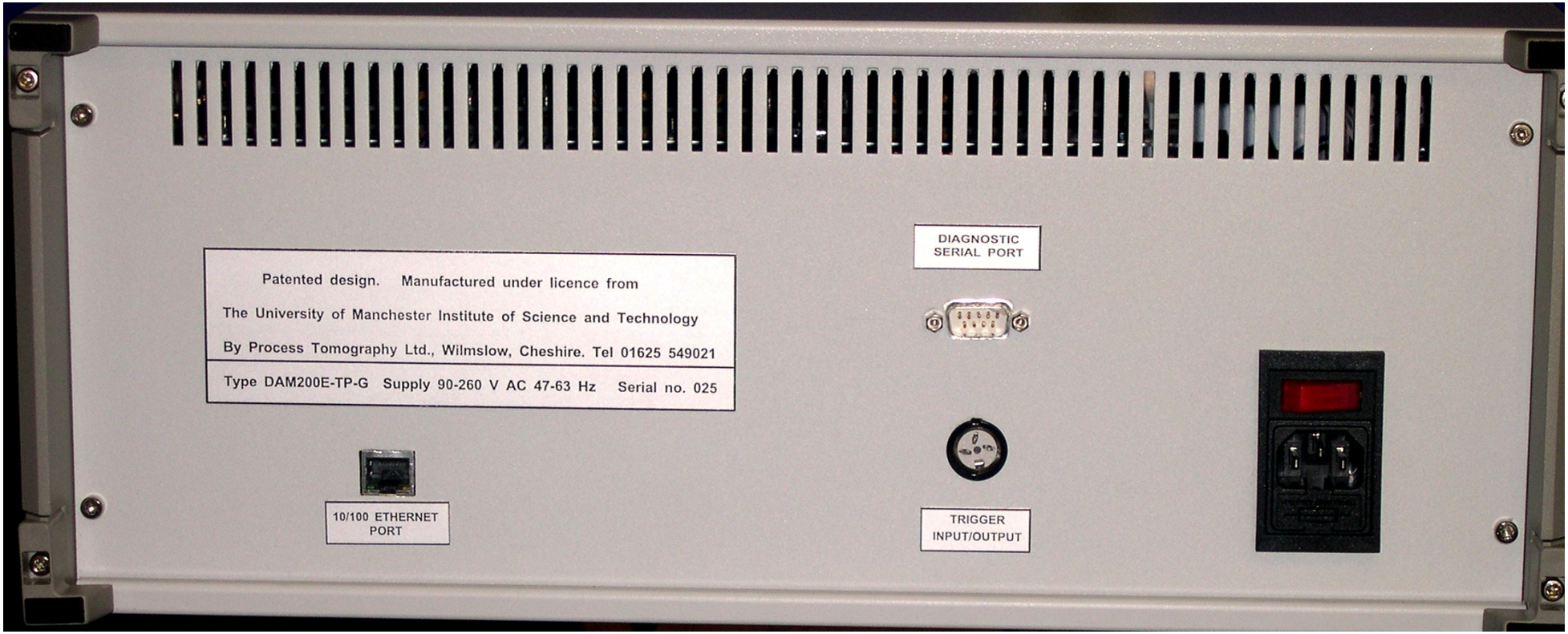

Figure 2.1.2. DAM200E CMU Rear panel layout

2.2 SETTING UP THE ECT SYSTEM

1. Assemble the **demonstration sensors** as described in **Appendix 2** (first time of use after unpacking only).

2. Connect the **mains lead s**upplied with the ECT system to the **power input connector** on the rear panel of the **DAM200E CMU**. Do not switch on the **CMU** yet.

3. Connect the coaxial leads from **one of the sensors** to the **Plane 1 Measurement Electrodes** input channel connectors (the **lower** row of connectors) on the front panel of the **CMU,** ensuring that each **numbered sensor lead** is connected correctly to the appropriate numbered **input channel connector** (**M1 to M12)** on the **DAM200E unit**. Note that the channel numbers start at 2 on the right hand end of the front panel and that channel 1 is next to channel 12 on the **CMU**. As the **demonstration sensors** do not contain **driven guard electrodes**, no connections should be made to the **Guard channels** on the DAM200E unit.

3. Connect the **crossed ethernet cable** supplied with the ECT system between the **CMU** (standard **LAN** ethernet socket on **rear panel** labelled "**10/100 Ethernet Port") a**nd the **ethernet port** on the **Control PC**.

Note that additional information about using the ECT system when the CMU and the control PC are connected to a l**ocal area network** can be obtained from PTL on request.

3. Connect up the remainder of the system as shown in figure 2.2.1. Do not make any connection to the **trigger input/output connector** or the **diagnostic serial port** on the rear panel.

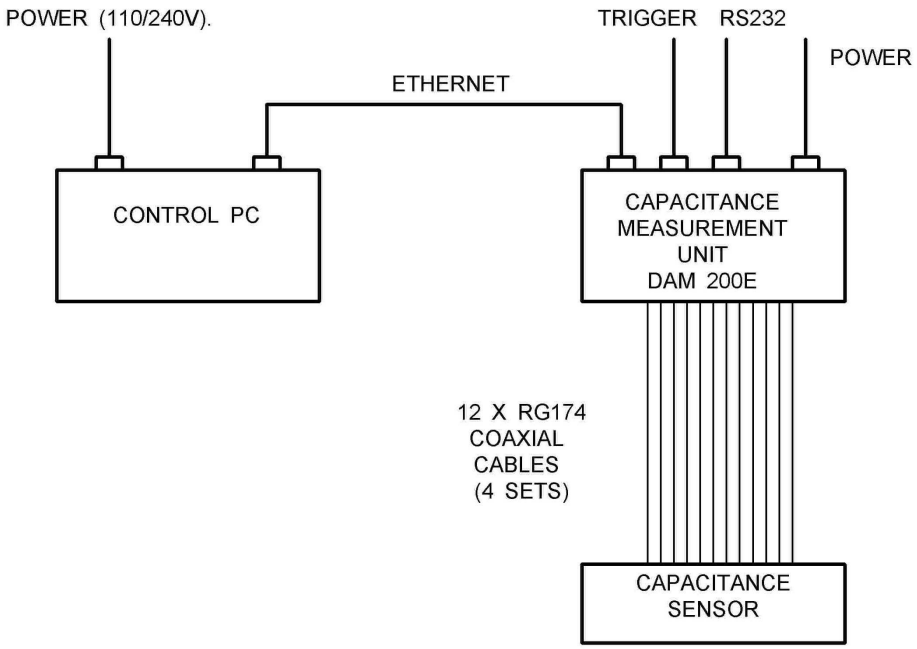

Figure 2.2.1 ECT system interconnection diagram

2.3 POWERING UP THE SYSTEM

1. Switch on the **PC** and the **DAM200E Capacitance Measurement Unit (mains switch** on **rear panel**). Both th**e Embedded PC** inside the **DAM200E** unit and the **Control PC** will start their boot-up sequences.

At the start of the **Embedded PC** boot sequence, all of the front panel **LED**s, (apart from the **Trigger Input LED**) will illuminate on the **DAM200E unit.** Approximately 10 seconds later, 2 **beeps** will sound from the **embedded PC** and after another 10 seconds, all of the **front panel LED**s, apart from the **Supply On LED**, will extinguish. After a further 2 seconds, when the **embedded PC** has completed its boot sequence, the internal software on the embedded PC will start to run and the **firmware status LED** on the front panel will start to **flash on and off at 1 second intervals**.

When the **control PC** has completed its start-up sequence, the **PC monitor** will display the **Windows Desktop.**

Once both computers have completed their start-up sequences and the **Firmware status LED** is flashing on the CMU, proceed to step 2 below.

2. Double-click on the **ECT software shortcut** on the **Desktop**. The **ECT software group window** shown in figure 2.3.1 will appear.

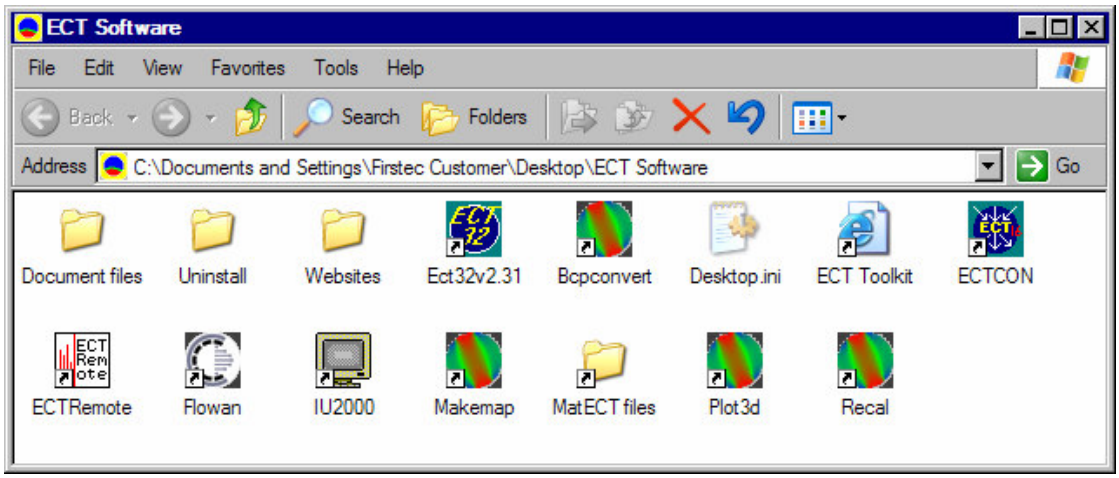

Figure 2.3.1 ECT Program Group window

1. Double click on the **ECT32v2** icon in the **ECT program group window.** The **Configuration** window, shown in figure 2.5.1 below, appears each time the **ECT32** software is run and allows some of the important software set up parameters to be defined and/or initialised.

Note that if this is the first time the **ECT32** software has been run on the PC, a **Registration Window** will appear. In this case, please follow the instructions given in **Appendix 7** in **Volume 2** of the **Operating Manual** to obtain the **User ID code** needed to fully activate the software.

However, note that the **ECT32 software** can be used in **Playback mode** only, without registering the software, by pressing the **Use in playback only mode** button in the **Registration Window**.

2.4 THE CONFIGURATION WINDOW

1. The **Configuration window** shown in figure 2.4.1 is the main set-up window for the **ECT32** system control software.

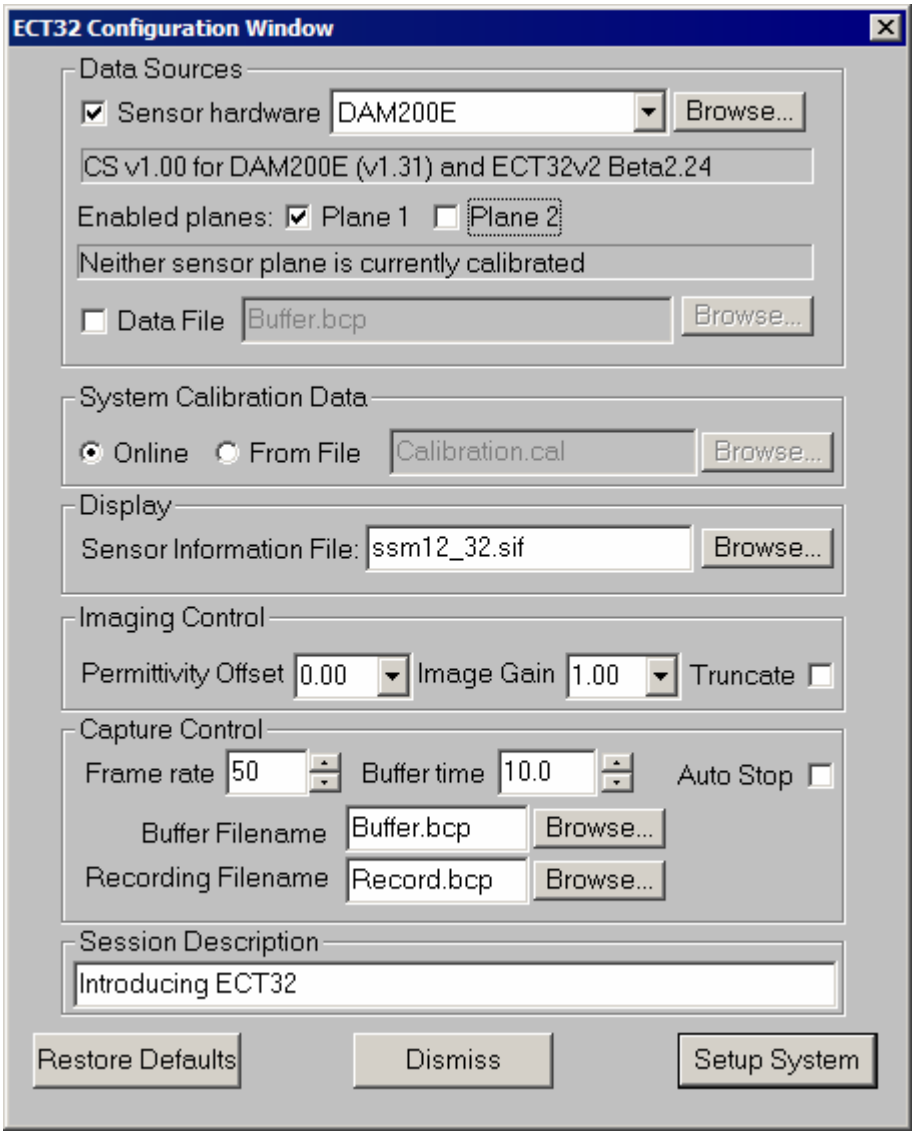

Figure 2.4.1 ECT32E Configuration Window

2. Left click the **Restore Defaults** button at the **bottom** of the **Configuration window,** then click in the **Plane 2 box** in the **Data Sources** parameter group to deselect plane 2.

3. Check the **Configuration window** parameters and, if necessary, modify any parameters which differ from those shown in **figure 2.4.1**. The most likely change needed will be to the **Sensor Information file** which should be set to **SSM12_32.sif** using the **Browse** button. This file is located in the **c:\ect32v2\configure** folder.

4. Left click the **Setup System** button at the **bottom** of the **Configuration** window. **The network connection window** shown in figure **2.4.2** will appear.

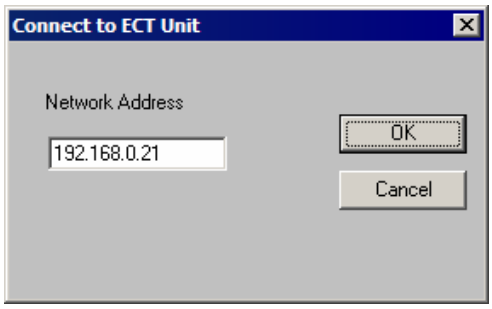

Figure 2.4.2 Network Connection window

5. If necessary, reset the correct network address for the **DAM200E CMU** and click on **OK**. The correct address is **192.168.0.XX**, where **XX** is the last 2 digits of the serial number of the DAM200E unit in use.

The **Link Status LED** on the **CMU** front panel will light and the **2-point ECT Calibration** window shown in figure 2.4.1 below, will appear.

2.5 SYSTEM CALIBRATION

The **demonstration sensor** is calibrated by following the instructions which appear in the calibration windows. The sensor is first filled with the **lower permittivity material** (in this case air) by standing the sensor vertically on end with the **electrodes** at the **top** of the tube. It is next filled with the **higher permittivity material** (polypropylene beads) by inverting the tube so that it is again vertical, but this time with the **electrodes** at the **bottom** of the tube. This is carried out as follows:

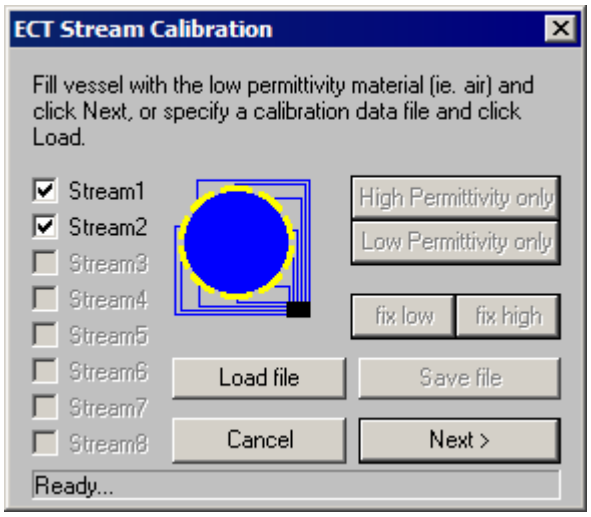

Figure 2.5.1 Low level calibration window

1. With the PC displaying the calibration window shown in **figure 2.5.1,** fill the **demonstration sensor** with the **lower permittivity material** (air) by inverting the sensor so that the electrodes are at the top of the sensor tube and click the **Next** button. After a short pause, followed by a beep, the screen changes to that shown in **figure 2.5.2.**

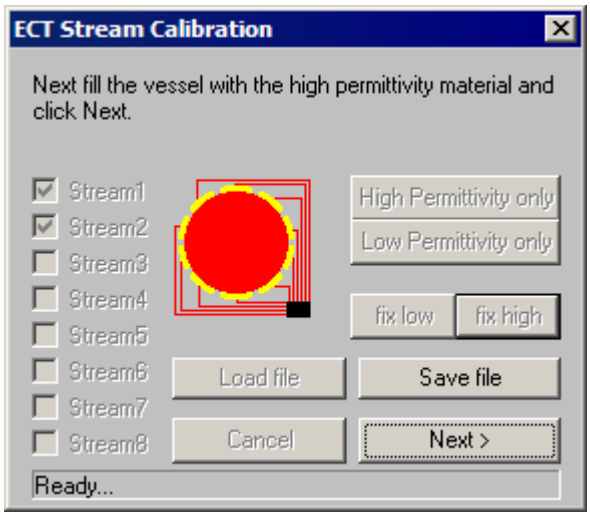

Figure 2.5.2 High level calibration window

2. Now fill the **demonstration sensor** with the **higher permittivity material** (plastic beads) by inverting the sensor tube so that the electrodes are at the bottom of the tube and again click the **Next** button. After a short pause, followed by a beep, the screen changes to that shown in **figure 2.5.3.**

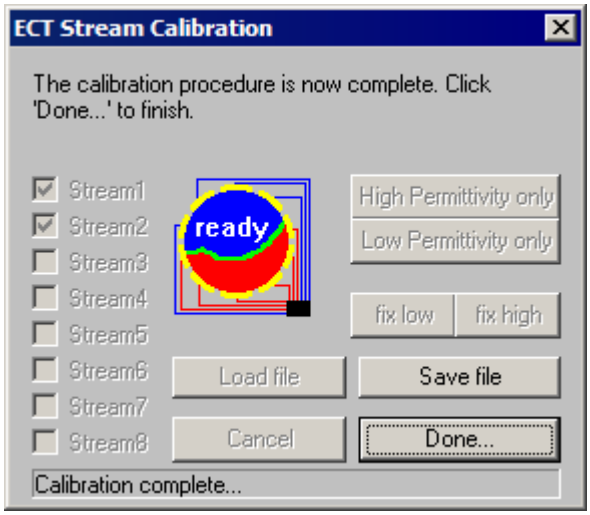

Figure 2.5.3 Final calibration window

3. Click on the **Save file** button and save the calibration data to a suitable file name in the **Working** folder. Note that the file extension **.cal** is added automatically to saved calibration file names.

4. Click on the **Done button** to complete the calibration process. The ECT system and sensor are now calibrated and ready to carry out **on-line measurements**, so the screen changes to the **main ECT32 window** shown in the next paragraph.

2.6 DATA CAPTURE

Once calibration has been completed, the main **ECT32 window** (the **ECT32 Desktop)** appears and a **live image** of the contents of the sensor contents is displayed as shown in **figure 2.6.1** at the **default frame rate (50 fps).** This image is likely to be that of a **full sensor**, as it follows immediately after sensor calibration with the **higher permittivity material**. This **data is being captured** on **a continuous basis**, to a **circular buffer file in memory.**

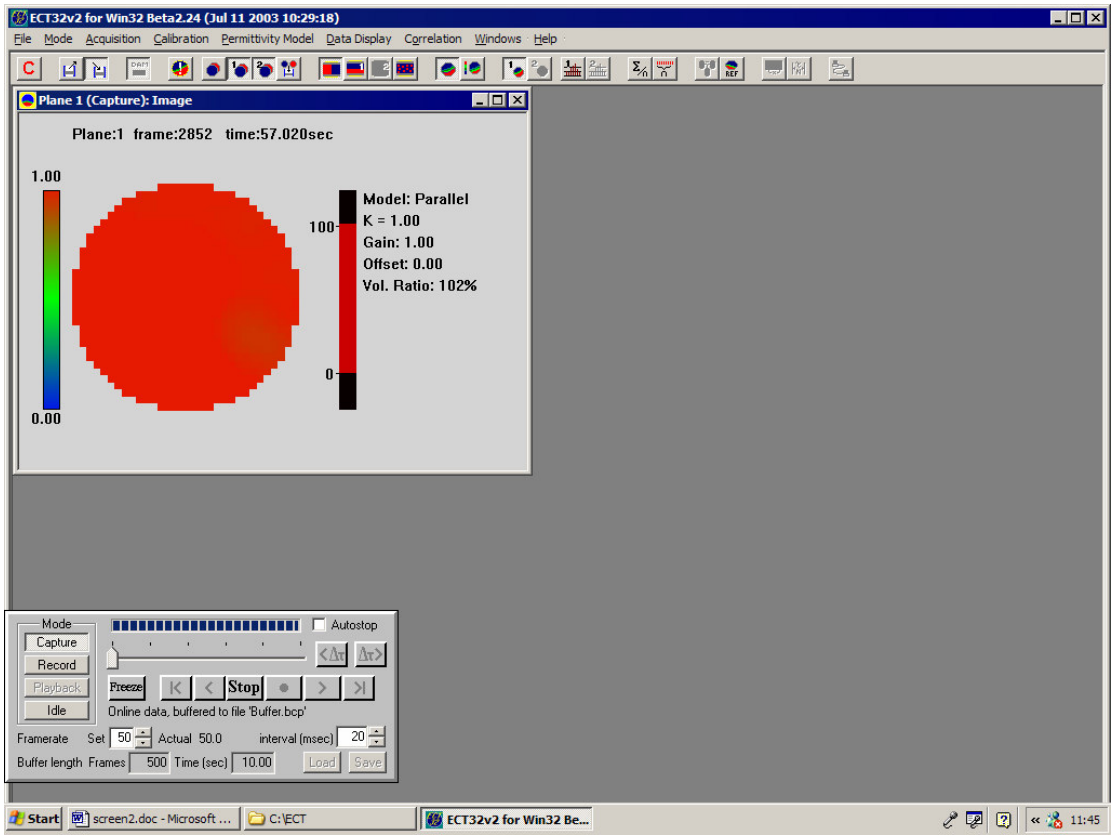

Figure 2.6.1 Main ECT32 window (ECT32 Desktop)

An **image** of the **full tube** is displayed in **red** using a **colour scale** which goes from **blue** (**filled with lower permittivity material**) via **green**, to **red** (**filled with higher permittivity material**) The user should experiment by tilting and/or twisting the **demonstration sensor** to see the images produced by a partially-filled sensor.

The data display format can be varied as follows:

1. Left click the **Plane 1 capacitances icon** (**icon 18**). This will open a new window, displaying the **normalised capacitances** as shown in **figure 2.6.2**

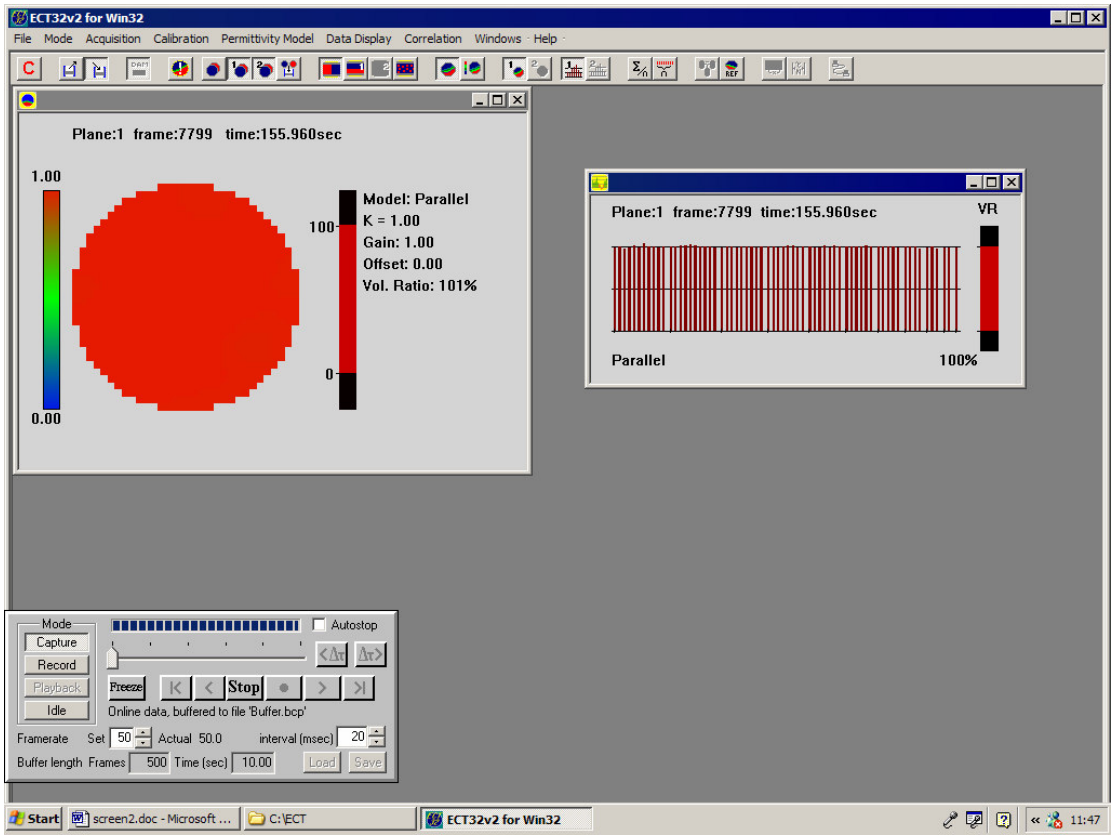

Figure 2.6.2 ECT Image and Normalised capacitances

These capacitances are displayed as sets of **vertical lines** (with a gap between each set) where each line represents the **normalised capacitance** on a nominal scale from 0 to 100%, with facilities for 30% over and under-range values. The first set of lines are the capacitances C_{12} to C_{1E} in order (where E is the total number of electrodes), the second set is C_{23} to C_{2E} and so on.

The **volume ratio** calculated from the normalised capacitances is displayed on a scale at the right hand edge of the capacitance window.

2. Move the **sensor** so that the image changes. Data is being **continuously captured** to a **rolling memory buffer,** whose size is determined by the figures set in the **Frames** and **Time** boxes in the **control panel**. The **buffer** is **continuously overwritten** as it is filled.

3. Click the **Stop button** in the **control panel** (shown in detail in **figure 2.7.1**). Data collection will cease and the system will automatically revert to **Playback mode.** Note that the **Playback button** is now depressed and that the number of frames captured and the **Time** in seconds are displayed in the **control panel**.

4. The **data** in the **memory buffer** is automatically saved to the **hard disk** each time that the system changes from **Capture mode** to **Playback mode**. The default file name is **buffer.cap.**

2.7 REPLAYING CAPTURED DATA

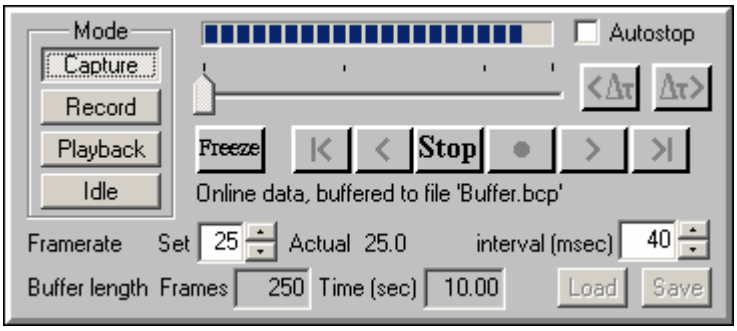

Figure 2.7.1 ECT32 Control Panel

1. Click the **forward play** [**>**] button on the **control panel** (second button from the right). The image data will be replayed and the **current image number** and the **time from the start of data collection** are displayed at the top of the image window and also on the right hand end of the **status bar** at the **bottom** of the window.

2. Click the **reverse play** [**<**] button (to left of **stop** button) on the **control panel.** The captured data will be replayed in **reverse order.**

3. Click the **Go to last frame [**>|**]** and **Go to first frame** [|<] buttons at the edges of the **control panel** in turn**.** Note that **t**hese set the **displayed image** to the **last** and **first** captured **frames** respectively.

4. Click the **increment one frame** button [**Δτ>**]. The image will advance to the next frame. Similarly, click the **decrement one frame** button [**<Δτ**]. The image will change to the previous frame.

5. Position the **mouse cursor** inside the **permittivity image** and left click the cursor. The **pixel under the cursor** is highlighted as a **white square** (the **pixel probe**) and the **normalised pixel permittivity** is displayed at the **bottom of the image.** A **sample permittivity image** is shown in figure 2.7.2 where the **pixel probe** indicates a **pixel value** of **0.99**. Move the mouse cursor outside the image and click again to turn off the pixel probe.

6. Note that the **Record button** has not been active so far. The function of this button is described later in chapter **25**.

7. **Exit** the **ECT32** software by clicking on the **X box** at the **top right hand corner** of the screen. The system will prompt with the message "**Do you really want to exit from ECT32?"** Respond by clicking the **Exit ECT32** button.

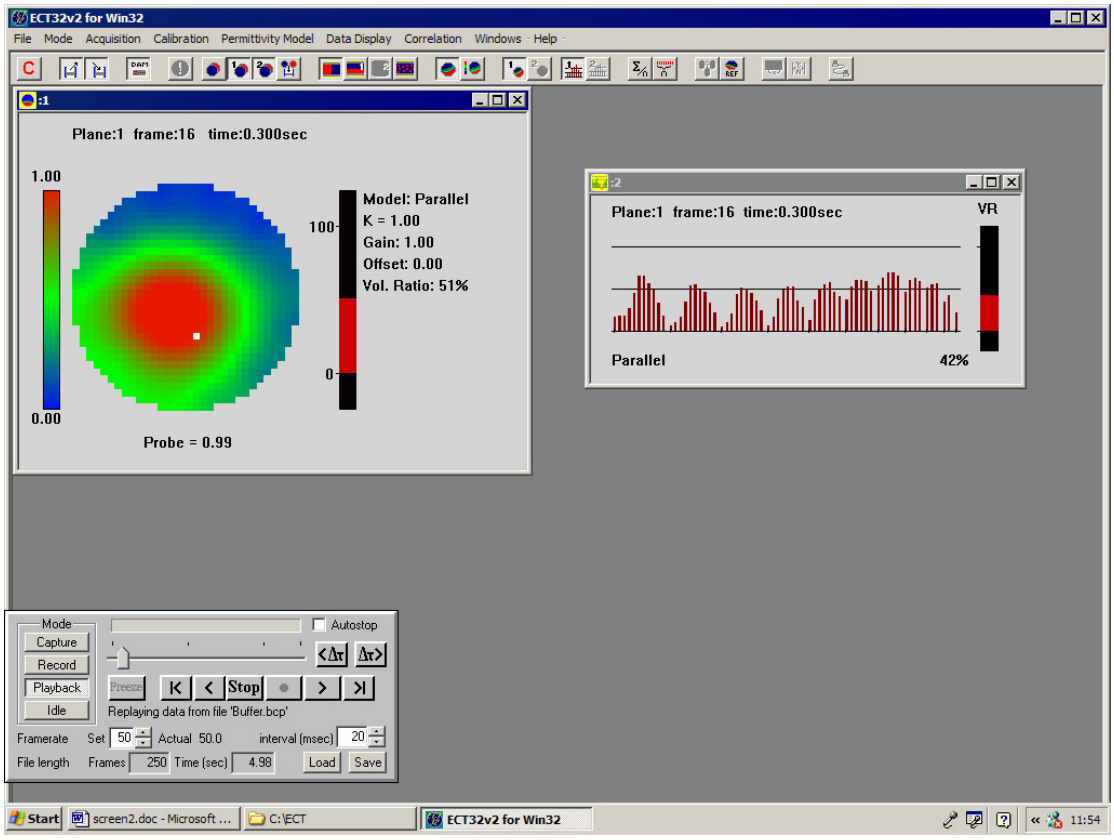

Figure 2.7.2 System in Playback Mode

2.8 TESTING THE SYSTEM USING A SENSOR CONNECTED TO PLANE 2

The sensor connected to plane 2 can be tested in a similar manner by repeating the steps in paragraph 2.4 but by connecting a sensor to **plane 2** and selecting **plane 2** rather than plane 1 in the **Configuration window**.

2.9 TESTING BOTH SENSOR PLANES SIMULTANEOUSLY

Similarly, with demonstration sensors connected to each measurement plane on the DAM200E unit, 2 measurement planes can be displayed simultaneously by repeating the steps in paragraph 2.4 but selecting both **Planes 1** and **Plane 2** in the **Configuration window**.

2.10 THE NEXT STEPS

This completes the **quick tour** of the **ECT32 software**. Detailed operating instructions, including a full description of the various windows and controls are given in **section 5**.

N.B In case of difficulty, please re-check the set up of the hardware and check that the software settings are correct as described above. If the problems persist, please read the detailed operating instructions given in **section 5**.

SECTION 2.

INTRODUCTION TO ELECTRICAL CAPACITANCE TOMOGRAPHY

In this section, consisting of a single chapter (3), the fundamental principles of Electrical Capacitance Tomography (ECT) are explained in a concise format. Further, more detailed information can be found later in this manual and also in the PTL software manuals and application notes which are included with each ECT system.

3. INTRODUCTION TO ELECTRICAL CAPACITANCE TOMOGRAPHY (ECT)

3.1 OVERVIEW OF ECT

ECT is used to obtain information about the spatial distribution of a mixture of dielectric materials inside a vessel, by measuring the electrical capacitances between sets of electrodes placed around its periphery and converting these measurements into an image showing the distribution of permittivity as a pixel-based plot or image. The images produced by ECT systems are approximate and of relatively low resolution, but they can be generated at relatively high speeds. Although it is possible to image vessels of any cross section, most of the work to-date has been carried out on circular vessels.

ECT can be used with any arbitrary mixture of different non-conducting dielectric materials such as plastics, hydrocarbons, sand or glass. However, an important application of ECT is viewing and measuring the spatial distribution of a mixture of two different dielectric materials (**a two-phase mixture**), as in this case, the **concentration distribution** of the two components over the cross-section of the vessel can be obtained from the the **permittivity distribution**.

The permittivity image resolution achievable depends on the number of independent capacitance measurements, but is generally low. However, images can be generated at high frame rates, typically 100fps. Successful applications of ECT include imaging 2-phase liquid/gas mixtures in oil pipelines and solids/gas mixtures in fluidised beds and pneumatic conveying systems. Where the mixture is flowing along the vessel, measurements of the concentration distributions at two axial planes permit the velocity profile and the overall flow rate to be found in some cases.

A typical ECT permittivity image format uses a square grid of 32 x 32 pixels to display the distribution of the normalised composite permittivity of each pixel. For a circular sensor, 812 of the available 1024 pixels are used to approximate the cross-section of the sensor. The values of each pixel represent the normalised value of the effective permittivity of that pixel. In the case of a mixture of two dielectric materials, these permittivity values are related to the fraction of the higher permittivity material present (the volume ratio (or voidage)) at that pixel location.

The overall volume ratio, which defines the ratio of the two materials present, averaged over the volume of the sensor, can also be obtained. The overall volume ratio of the materials inside the sensor at any moment in time is defined to be the percentage of the volume of the sensor occupied by the higher permittivity material. The volume of the sensor is the product of the cross-sectional area of the sensor and the length of the sensor measurement electrodes.

In all of the following we shall be referring to the relative permittivity (or dielectric constant) of materials. The relative permittivity of a material is its absolute permittivity divided by the permittivity of free space (or air). Hence the relative permittivity of air is 1 and typical values for other materials in solid or liquid format are polystyrene (2.5), glass (6.0) and mineral oil (2.3).

In this manual, we have used three different terms to describe the same concept, as they are all in common use. These are volume ratio, voidage and concentration, which we define to be the fraction of the higher permittivity material present in the mixture. These terms are inter-changeable in the following text. A typical application of ECT is for the real-time monitoring of the motion of fluids, including multi-phase flows, in process engineering plants. In general ECT can be used to monitor any process where the fluid to be observed has low electrical conductivity and a varying permittivity.

3.2. ECT MEASUREMENT SYSTEM CONFIGURATION

An ECT system consists of a capacitance sensor, measurement circuitry and a control computer. For imaging a single vessel type with a fixed cross-section and with a fixed electrode configuration, the measurement circuitry can be integrated into the sensor and the measurement circuits can be connected directly to the sensor electrodes. This simplifies the measurement of inter-electrode capacitances and is potentially a good design solution for standardised industrial sensors.

However, most current applications for ECT are in the research sector, where it is preferable to have a standard capacitance measuring unit which can be used with a wide range of sensors. In this case, screened cables connect the sensor to the measurement circuitry, which must be able to measure very small inter-electrode capacitances, of the order of 10^{-15} F (1 fF), in the presence of much larger capacitances to earth of the order of 200,000 fF (mainly due to the screened cables). A diagram of a very simple ECT system of this type is shown in figure **3.2.1**.

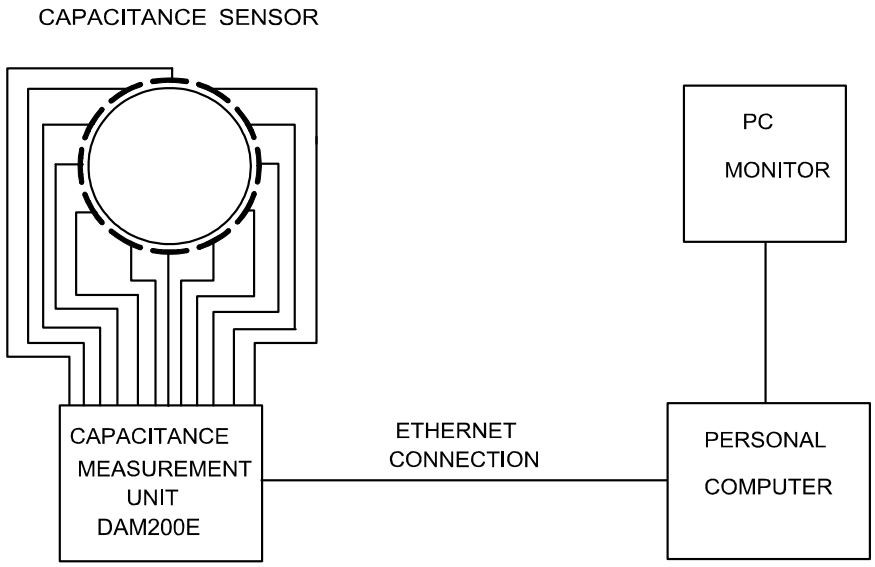

Figure 3.2.1 Basic PTL300E ECT System

If the vessel wall is non-conducting, electrodes can be located inside, within or outside the wall as shown in figure 3.2.2 However, if the tube wall is a conductor, internal electrodes must be used. The convention we use to identify electrodes is to number them anticlockwise, starting at the electrode at or just before 3 o'clock.

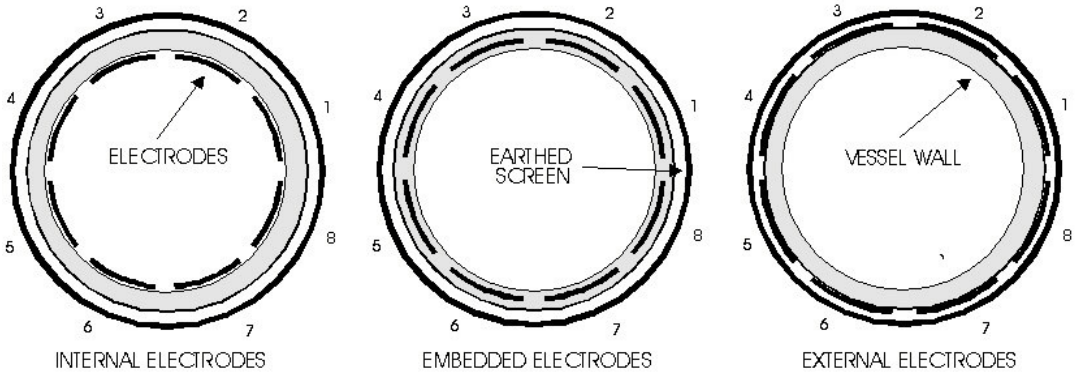

Figure 3.2.2 Circular sensor electrode configurations

The number of sensor electrodes that can be used depends on the range of values of inter-electrode capacitances and the upper and lower measurement limits of the capacitance measurement circuit. The capacitance values when the sensor contains air are referred to as “standing capacitances” and their relative values are shown in figure 3.2.3 for a 12-electrode circular sensor with internal electrodes.

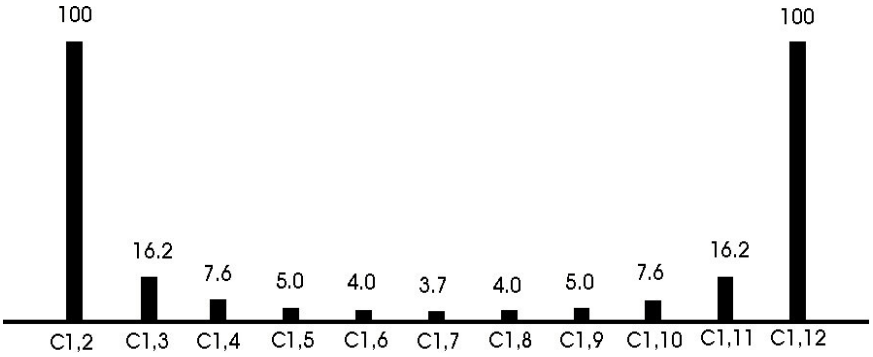

Figure 3.2.3. Inter-electrode capacitances

Sequential electrodes are referred to as adjacent electrodes, and have the largest standing capacitances, while diagonally opposing electrodes (opposite electrodes) have the smallest capacitances. Because of the wide range of these capacitances, they are usually normalised to lie within a standard range of values, as described in paragraph 3.9. As the number of electrodes increases, the electrode surface area per unit axial length decreases and the inter-electrode capacitances also decrease. When the smallest of these capacitances (for opposite electrodes), reaches the lowest value that can be measured reliably by the capacitance circuitry, the number of electrodes, and hence the image resolution, can only be increased further by increasing the axial lengths of the electrodes. However, these lengths cannot be increased indefinitely because the standing capacitances between pairs of adjacent electrodes will also increase and the measurement circuitry will saturate or overload once the highest capacitance measurement threshold is exceeded.

3.3. CAPACITANCE MEASUREMENT PROTOCOLS

Many different ECT measurement protocols are possible (Reinecke, 1994), as capacitances can be measured between many combinations of groups of electrodes (which effectively become new "virtual electrodes"). Most work to-date with circular vessels has used the simplest arrangement (which we refer to as protocol 1) where capacitances are measured between single pairs of electrodes. The measurement sequence for protocol 1 involves applying an alternating voltage from a low-impedance supply to one (source) electrode. The remaining (detector) electrodes are all held at zero (virtual ground) potential and the currents which flow into these detector electrodes (and which are proportional to the inter-electrode capacitances) are measured. A second electrode is then selected as the source electrode and the sequence is repeated until all possible electrode pair capacitances have been measured. This generates M independent inter-electrode capacitance measurements, where:

$$M = E.(E - 1)/2 \qquad (3.3.1)$$

and E is the number of electrodes located around the circumference. For example for E = 12, M = 66. As the measurements for a single frame of data are made sequentially, the capacitance data within the frame will be collected at different times and there will be some skewing of the data. Interpolation techniques can be used to de-skew this data if this effect is likely to produce significant errors.

Other possible protocols involve grouping electrodes and exciting them in pairs (protocol 2) and triplets (protocol 3) etc. The formula for the number of independent measurements for grouped electrodes is :

$$M = (E).(E - (2P - 1)) / 2 \qquad (3.3.2)$$

where P (the protocol number) is the number of electrodes which are grouped together. The advantage of using these more complex protocols is that they can generate a larger number of independent measurements for a given electrode size and capacitance measurement sensitivity than the simple single-pair protocol 1. Improved image resolution is therefore achievable, although at the expense of the maximum image frame rate, which falls as the protocol number or number of electrodes increases.

3.4. CAPACITANCE SENSOR ELECTRODE DESIGN

ECT can be used with vessels of any cross-section, but most work to-date has used circular geometries. For a sensor with internal electrodes, the components of capacitance due to the electric field inside the sensor will always increase in proportion to the material permittivity when a higher permittivity material is introduced inside the sensor. However for sensors with external electrodes, the permittivity of the wall causes non-linear changes in capacitance, which may increase or decrease depending on the wall thickness and the permittivities of the sensor wall and contents. In general, ECT sensors with external electrodes are easier to design and fabricate than internal electrode sensors and they are also non-invasive.

Axial resolution and overall measurement sensitivity can be improved by the use of driven axial guard electrodes, located either side of the measurement electrodes, as shown in the flexible laminate design of figure 3.4.1.

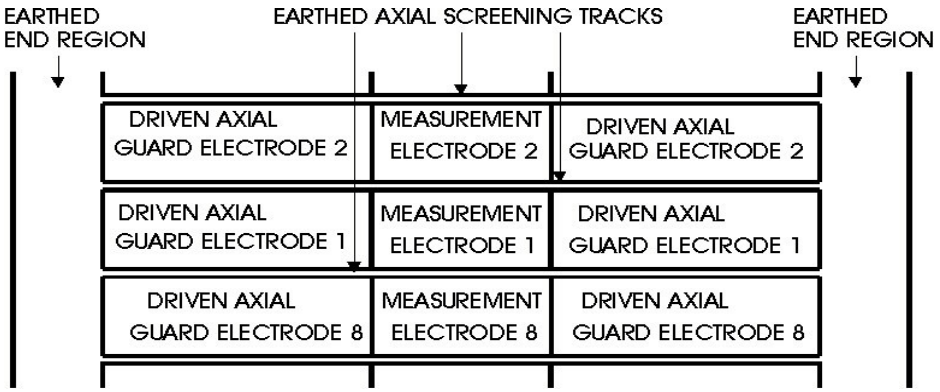

Figure 3.4.1 Partial PCB layout for an 8-electrode single-plane sensor

The driven axial guard electrodes are excited at the same electrical potentials as the associated measurement electrode and prevent the electric field from being diverted to earth at the ends of the measurement electrodes. For large diameter vessels, axial guard electrodes are normally an essential requirement to ensure that the capacitances between opposing electrodes are measurable.

With the current state of capacitance measurement technology, it is possible to measure capacitance changes between 2 unearthed electrodes of 0.1 fF in the presence of stray capacitance to earth of 200pF at a rate of 2000 measurements per second. This sets a practical lower design limit on the capacitance between any pair of electrodes of around 5fF, which equates to measurement electrodes of minimum axial length 3.5cm for an 8 electrode sensor or 5 cm for a 12 electrode sensor. These dimensions assume that effective driven axial guards are used. For this condition to be met, the sum of the lengths of the axial guard and the measurement electrodes must equal or exceed the sensor diameter.

3.5. CAPACITANCE SENSOR FABRICATION

The required electrode pattern can be designed using CAD software and the electrodes fabricated using photolithographic techniques from a flexible copper-coated laminate, which is then wrapped around the outside of an insulating tube to form the sensor. Part of a design for an 8-electrode single plane sensor with driven axial guards is illustrated in figure 3.4.1, which shows earthed screening tracks between the sets of electrodes (to reduce the adjacent electrode capacitances) together with earthed areas at the ends of the sensor (to allow the cable screens to be terminated). Coaxial leads (with a maximum length of 2m to minimise capacitance to ground) are connected to the electrodes and an earthed screen is located around the sensor to exclude any external signals. Discharge resistors (typically 1 MOhm) must be connected between each electrode and the cable screen to ensure that no static charge can build up on the electrodes and connecting leads, otherwise damage may occur when the sensor is connected to the capacitance measurement circuit. These basic techniques can be used to construct static or sliding sensors with internal or external electrodes. More complex fabrication techniques are needed for sensors for operation at elevated temperatures and pressures.

3.6 ECT SYSTEM OPERATION

ECT systems can be operated in many different ways but in this introductory section, we will describe the simplest method, which involves using the simplest capacitance measurement protocol together with a simple and approximate image reconstruction algorithm, known as Linear Back-Projection (LBP). The sequence of actions required to measure the permittivity distribution of a mixture of 2 dielectric fluids inside an ECT sensor using the LBP algorithm is as follows:

1. The properties of the capacitance sensor are measured or calculated initially to produce a sensor **sensitivity matrix** for the case when the sensor is empty. This matrix is a composed of a set of sub-matrices (or maps) whose elements correspond to the individual pixels in a rectangular grid which is used to define the sensor cross-section.

2. The sensor is normally calibrated at each end of the range of permittivities to be measured by filling the sensor with the lower permittivity material initially and measuring all of the individual inter-electrode capacitances. This operation is then repeated using the higher permittivity material. The data obtained during the calibration procedure is used to set up the measurement parameters for each measuring channel and is stored in a calibration data file.

3. Once the system has been calibrated, the capacitances between all unique pairs of sensor electrodes are measured continuously at high speed, giving E(E-1)/2 unique values per measurement or image frame, where E is the number of sensor electrodes.

4. The measured capacitance values are normalised to the values measured during the calibration process.

5. An image reconstruction algorithm, together with an appropriate sensor permittivity-concentration model is used to compute the cross sectional distribution of the permittivity of the material inside the pipe. Images can be constructed from the capacitance measurements either at the time of measurement (on-line) or from stored or captured data (off-line). The algorithm supplied as standard in the PTL300E system is the so-called linear back-projection (LBP) algorithm. This is a fast but approximate algorithm which uses the capacitance measurements, together with the sensitivity map to produce the image. Other alternative algorithms can be used with the stored data to produce more accurate images.

The various stages in this measurement process are described in more detail in the following chapters.

3.7 THE SENSITIVITY MATRIX

The sensitivity matrix describes how the measured capacitance between any combination of electrodes changes when a change is made to the dielectric constant of a single pixel inside the sensor. This can be better understood by considering the case where one electrode is connected to a positive potential V and all of the other electrodes are connected to earth.

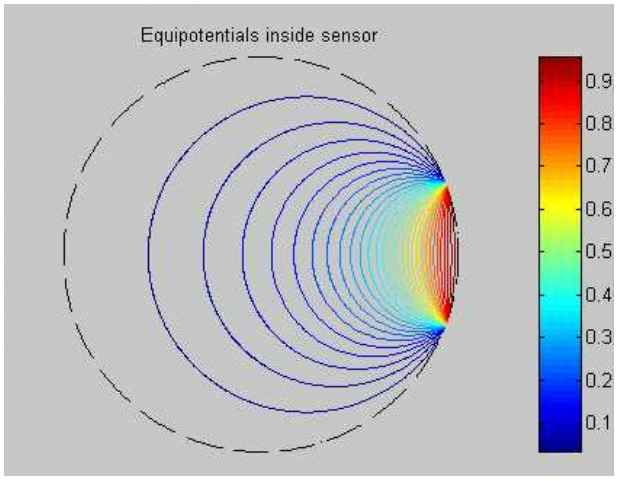

Figure 3.7.1 Equipotential lines inside ECT sensor

The electric field distribution for this situation is shown in figure 3.7.1 (the figure shows the equipotential lines) and is relatively uneven, the field being strongest near to the excited electrode and weakening with increasing distance from this electrode. The corresponding electric field lines are shown in the figure below.

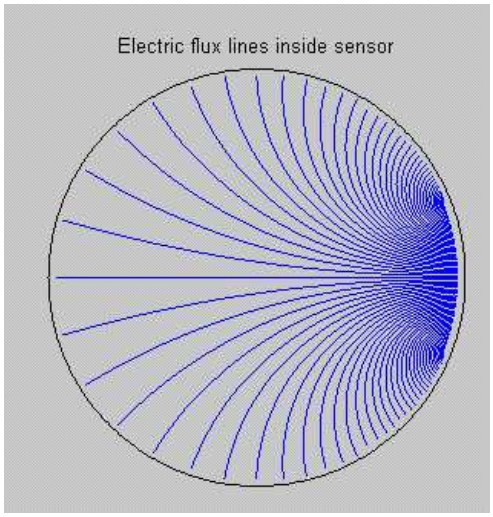

Figure 3.7.2 Electric field distribution inside ECT sensor

The effect of this uneven field distribution is that the change in capacitance measured between any two electrodes caused by an object with a given permittivity will vary depending on the location of the object. When used with a circular cross section sensor, the ECT system is most sensitive when an object is placed near the walls of the vessel and is least sensitive at the centre of the vessel. Allowance is made for this effect from knowledge of the variation of sensitivity with position for each pixel. This information is stored in the sensitivity map file. When the ECT system constructs images, it reads the sensitivity map and compensates the image pixels accordingly.

The sensitivity matrix must be calculated (or measured) for each individual sensor as a separate exercise prior to using the sensor with an ECT system. One method for calculating the sensitivity coefficient S of a pixel for an electrode-pair (i-j) is based on the use of equation 6.

$$S = \int_A \mathbf{E_i} . \mathbf{E_j} . dA \qquad (3.7.3)$$

where $\mathbf{E_i}$ is the electric field inside the sensor when one electrode of the pair i is excited as a source electrode, $\mathbf{E_j}$ is the electric field when electrode j is excited as a source electrode and the dot product of the two electric field vectors $\mathbf{E_i}$ and $\mathbf{E_j}$ is integrated over the area A of the pixel. The set of sensitivity coefficients for each electrode-pair is known as the sensitivity map for that pair.

For circular sensors with either internal or external electrodes, it is possible to derive an analytical expression for the electric fields where the sensor is either empty or filled with a material having uniform permittivity. In this case, the sensitivity coefficients (and also the electrode capacitances) can be calculated accurately by analytical means. For more complex geometries, numerical methods can be used to calculate the sensitivity coefficients. It is normally only necessary to calculate a few primary sensitivity maps for the unique geometrical electrode pairings, as all of the other maps can be derived from these by reflection or rotation. A set of primary maps for an 8-electrode sensor operating under protocol 1 is shown in figure 3.7.3.

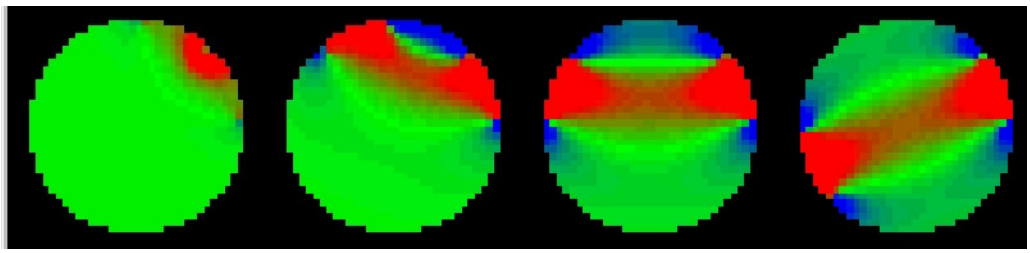

Figure 3.7.3 Primary Sensitivity Maps for an 8-electrode sensor

The maps show the relative pixel sensitivities on a compressed colour scale, where blue represents negative sensitivity, green represents zero sensitivity and red represents positive sensitivity regions.

3.8 ECT SYSTEM CALIBRATION

In the normal method of operation, an ECT system is calibrated by filling the sensor with the two reference materials in turn and by measuring the resultant inter-electrode capacitance values at these two extreme values of relative permittivity. This situation is shown diagramatically in figure 3.8.1 which illustrates how the measured inter-electrode capacitances change between the higher and lower values of permittivity used for calibration, for two materials of relative permittivity K_L and K_H. For simplicity, it has been assumed that the variation is linear.

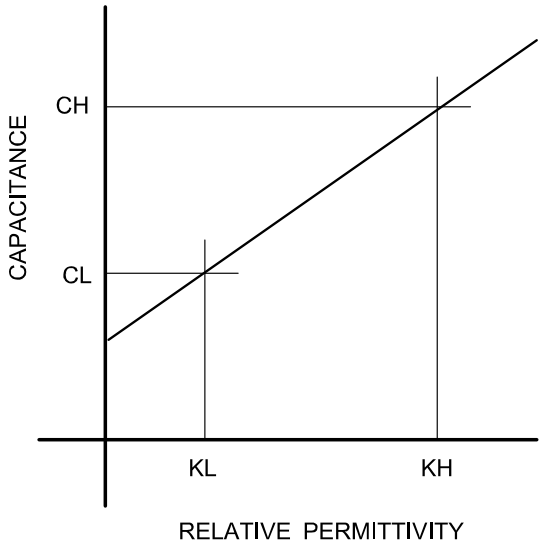

Figure 3.8.1 Principle of ECT System Calibration

This method of calibration defines the two nominal end points of the measurement range for most types of ECT measurement.

All subsequent capacitance values C_M are then normalised to have values C_N between zero (when the sensor is filled with the lower permittivity material) and 1 (when filled with the higher permittivity material) as described in the next paragraph.

3.9 CAPACITANCE MEASUREMENT AND NORMALISATION

Once the ECT system has been calibrated, the ECT system is ready to capture image data. When data capture is initiated, the capacitances between all unique pairs of sensor electrodes are measured continuously at high speed. These capacitance values are stored, initially in binary format in the control PC memory and are then available to construct an image of the permittivity distribution inside the sensor.

In PTL ECT systems, use is made of normalised parameters to represent the inter-electrode capacitance measurements and also the displayed values of pixel permittivity. This is carried out using the reference data in the calibration file which is generated during the calibration process.

This process is carried out as follows:

The inter-electrode capacitances measured at the lower permittivity calibration point (C_L) are assigned values of 0 while the inter-electrode capacitances measured at the higher permittivity calibration point (C_H) are assigned values of 1. This relationship is shown in graphical format in figure 3.9.1.

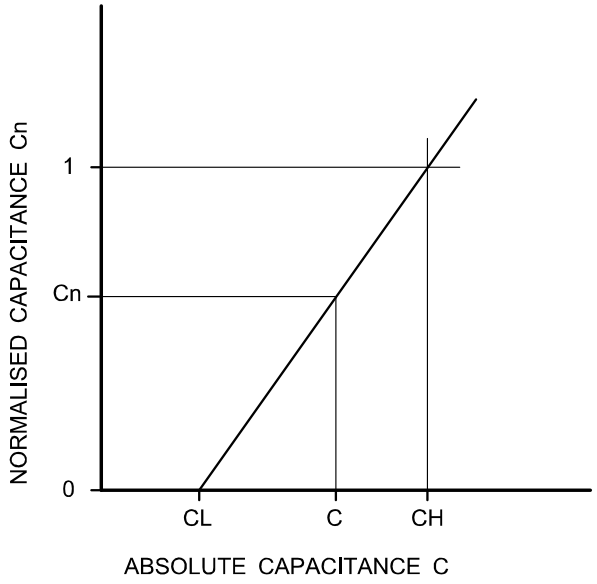

Figure 3.9.1 Capacitance normalisation

and is defined by the equation:

$$\mathbf{C_n = (C - C_L) / (C_H - C_L)} \qquad (3.9.1)$$

where **Cn** is the set of normalised inter-electrode capacitances and **C** are the set of absolute capacitances measured with the sensor containing a material of arbitrary permittivity, $\mathbf{C_H}$ are the set of capacitances measured at the higher permittivity calibration point and $\mathbf{C_L}$ are the set of capacitances measured at the lower permittivity calibration point.

3.10 NORMALISATION OF PIXEL PERMITTIVITY VALUES

The pixel values in the permittivity image are similarly normalised, so that they have the value 0 for the lower permittivity material and 1 when the sensor is filled with the higher permittivity material using equation 3.10.1.

$$\mathbf{K_n = (K - K_L) / (K_H - K_L)} \qquad (3.10.1)$$

where $\mathbf{K_n}$ is the set of normalised permittivities (pixel values) when the sensor is filled with a material of permittivity **K**, $\mathbf{K_H}$ is the effective permittivity of the material used to calibrate the sensor at the higher permittivity calibration point and $\mathbf{K_L}$ is the permittivity of the material used to calibrate the sensor at the lower permittivity calibration point.

The relationship between absolute and normalised permittivities is shown in figure 3.10.1.

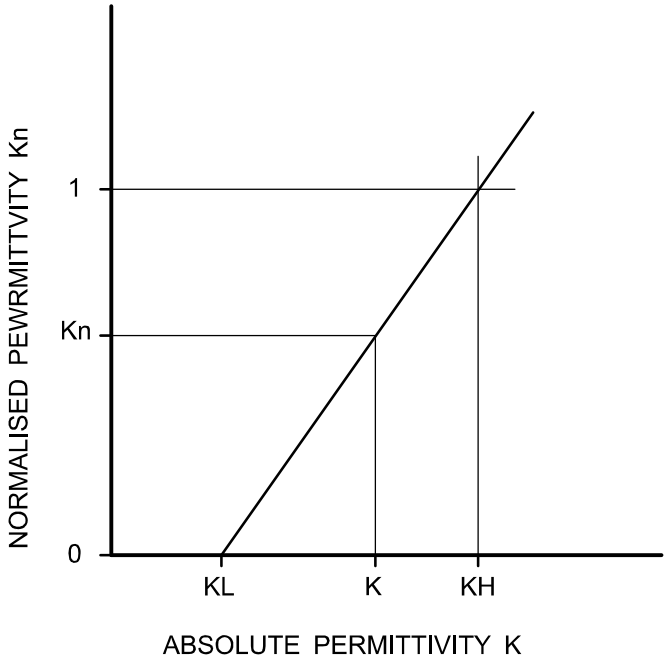

Figure 3.10.1 Normalisation of permittivity values

3.11 CAPACITANCE/PERMITTIVITY/CONCENTRATION MODELS

The relationship between the permittivity distribution and the capacitance measured between a pair of electrodes must be considered carefully if accurate permittivity/concentration images are to be obtained. If the two dielectric materials exist as discrete stratified permittivity layers between the two electrodes, then two component capacitances, each due to one of the dielectric materials, and effectively connected in parallel, will exist between the electrodes. The sum of these capacitances will therefore accurately reflect the relative proportions of the 2 materials present.

However, if the materials exist as alternating bands of permittivity between the electrodes, the capacitances measured between the electrodes will be constituted from component capacitances which are effectively connected in series. In this case, the reciprocal rule must be used to obtain the component permittivities and concentration from the measured capacitances. If there is a combination of these two basic material distributions, more complex relationships, such as the method described by Maxwell, must be used to define the permittivity/ concentration/ capacitance relationships. It is therefore very important to use the correct permittivity model (parallel/series/Maxwell etc) if accurate concentration values are to be obtained from the permittivity image. Further information on capacitance/ permittivity models (including Maxwell's method) is given in chapter 12 of this manual and also in the paper by Yang and Byars (see references in para 3.16).

3.12 LIMITS ON IMAGE RESOLUTION

The resolution of an ECT permittivity image is limited by the number of independent inter-electrode capacitance measurements that can be made and this relationship can be considered to be an example of spatial filtering, as shown in figure 3.12.1.

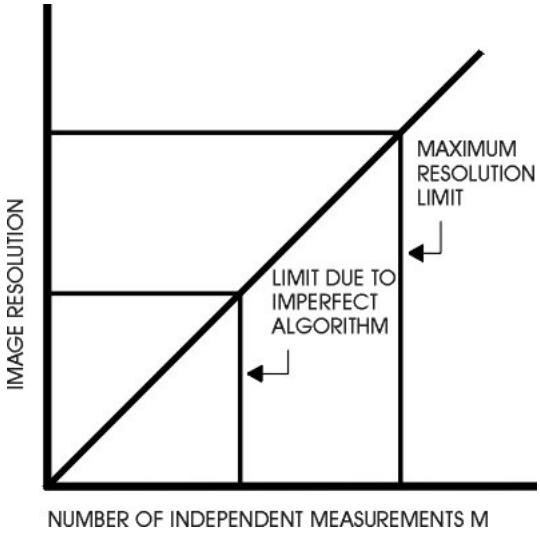

Figure 3.12.1 Resolution limits imposed by spatial filter.

The resolution limit is difficult to define mathematically, but a simple engineering estimate can be made by assuming that the number of independent measurements M corresponds to a similar number of discrete regions inside the sensor. If we assume that the angular resolution is equal to the number of electrodes E, then the radial resolution will equal M/E. For protocol 1 and a 12 electrode sensor, this gives a radial resolution limit of 5.5. For protocol 2 and 24 electrodes, this figure increases to 10.5.

It is not possible to obtain a unique solution for each image pixel when the number of pixels in the image exceeds the number of capacitance measurements. Furthermore, image distortion can occur because ECT is an inherently soft-field imaging method (the electric field is distorted by the material distribution inside the sensor). However, in many cases, the contrast between the permittivities of the materials inside the sensor is small, resulting in only limited image distortion. This allows approximate linear algorithms to be used to relate the capacitance measurements to the pixel values in the image and vice-versa. The method which has been used with greatest success to-date is known as Linear Back Projection (LBP).

3.13 IMAGE RECONSTRUCTION USING THE LBP ALGORITHM

The LBP algorithm is based on the solution of a set of forward and reverse (or inverse) linear transforms.

The forward transform is a matrix equation which relates the set of inter-electrode capacitance measurements **C** to the set of pixel permittivity values **K.** This transform assumes that the measured inter-electrode capacitances resulting from any arbitrary permittivity distribution **K** inside the sensor will be identical to those obtained by summing the component capacitance increases which occur when each pixel has its defined permittivity, with all other pixels values set to zero.

This forward transform is defined in equation 3.13.1, where bold characters represent matrices :

$$\mathbf{C = S.K} \qquad (3.13.1)$$

C is an (M x 1) dimensioned matrix containing the set of M inter-electrode pair capacitances (where M is typically 66 for a 12-electrode sensor or 28 for an 8-electrode sensor for protocol 1).

K is an (N x 1) dimensioned matrix (where N is 1024 for a 32 x 32 grid) containing the set of N pixel permittivity values which describe the permittivity distribution inside the sensor (the permittivity image).

S is the forward transform, usually known as the sensor Sensitivity Matrix. **S** has dimensions (M x N) and consists of M sets (or maps) of N (typically 1024) coefficients, (1 map for for each of the M capacitance-pairs), where the coefficients represent the relative change in capacitance of each capacitance pair when an identical change is made to the permittivity of each of the N (1024) pixels in turn.

In principle, once the set of inter-electrode capacitances **C** have been measured, the permittivity distribution **K** can be obtained from these measurements using an inverse transform **Q** as follows.

$$\mathbf{K = Q.C} \qquad (3.13.2)$$

Q is a matrix with dimensions (N x M) and, in principle, is simply the inverse of the matrix **S**. However, it is only possible to find the true inverse of a square matrix (where M = N). In physical terms, this is confirmation that it is not possible to obtain the individual values of a large number of pixels (eg 1024) from a smaller number of capacitance measurements (eg 66). As an exact inverse matrix does not exist, an approximate matrix must be used. The LBP algorithm uses the transpose of the sensitivity matrix, **S'** which has the dimensions (N x M) and this is justified by the following reasoning:

Although we have no means of knowing which pixels have contributed to the capacitance measured between any specific electrode-pair, we know from the sensitivity matrix **S** that certain pixels have more effect than others on this capacitance. Consequently, we allocate component values to each pixel proportional to the product of the electrode-pair capacitance and the pixel sensitivity coefficient for this electrode-pair. This process is repeated for each electrode-pair capacitance in turn and the component values obtained for each pixel are summed for the complete range of electrode-pairs.

This simple algorithm produces approximate, but very blurred permittivity images, and a typical image is shown in figure 3.1.4.2. The LBP algorithm acts as a spatial filter with a lower cut-off frequency than that of the fundamental filter (as shown in figure 3.12.1) and produces sub-optimal images from a given set of input data. Some methods for improving the accuracy of ECT images are described in later sections of this manual.

3.14 FORMAT OF PERMITTIVITY IMAGES

The permittivity distribution of a mixture of two fluids is often displayed as a series of normalised pixels located on either a (32 x 32) or (64 x 64) square pixel grid. If the sensor cross-section is circular, this circular contour must be projected onto the square grid containing typically 1024 pixels. Some of the pixels will lie outside the vessel circumference and the image is therefore formed from those pixels that lie inside the vessel. A typical arrangement which is commonly used is shown in figure 3.14.1, where the circular image is constructed using 812 of the available 1024 pixels.

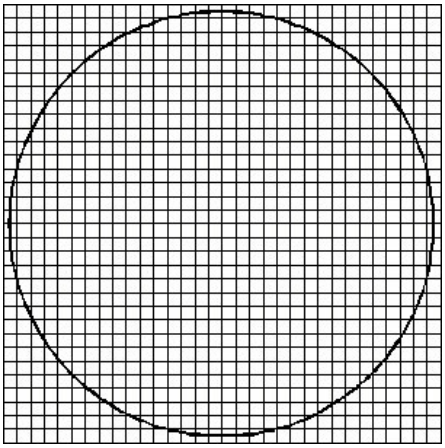

Figure 3.14.1 32 x 32 square pixel grid

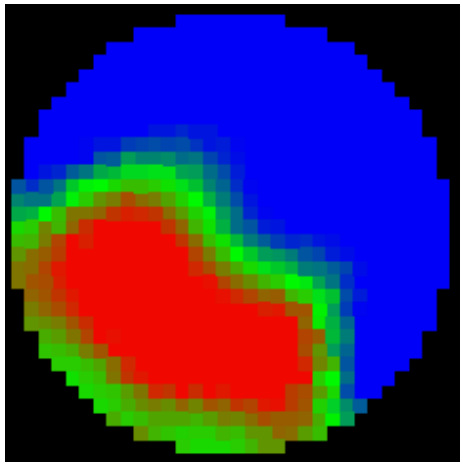

Figure 3.14.2
ECT image for contents of a circular sensor. Note that the colour scale progresses from zero (blue) through green to (1) red.

The permittivity distribution (image) is plotted using an appropriate colour scale to indicate the normalised pixel permittivity. A simple example is a graduated blue/green/red colour scale, where pixel values corresponding to the lower permittivity material used for calibration have the value zero and are shown in blue, while pixels corresponding to the higher permittivity material have the value 1 and are shown in red. A typical 32 x 32 ECT image, obtained using the methods described in paragraph 3.13, is shown in figure 3.14.2.

The normalised permittivity distribution corresponds to the fractional concentration distribution of the higher permittivity material.

3.15 SUMMARY

This completes the brief overview of basic ECT technology. Further and more detailed information is given in subsequent sections of this manual.

3.16 REFERENCES

A small selection of papers on electrical capacitance tomography is given below.

Huang S.M. et al., (1989), Tomographic imaging of two-component flow using capacitance sensors, J. Phys. E: Sci. Instrum. 22, pp 173-177.

Reinecke N. and Mewes D., (1994), Resolution enhancement for multi-electrode capacitance sensors, in Proc: Process Tomography, A strategy for Industrial Exploitation, Bergen Norway, pp50 - 61

Reinecke N. and Mewes D., (1996), Recent Developments and industrial/research applications of capacitance tomography, Meas. Sci. Technol. 7 pp 233-246

Yang W.Q. and Byars M., (1999) An improved normalisation approach for electrical capacitance tomography, in Proc : 1st World Congress on Industrial Proc. Tomography, Buxton, UK pp 215-218.

SECTION 3

This section contains information about Electrical Capacitance Tomography (ECT) which is specific to the **PTL300E ECT system.**

Chapter 4 gives a brief overview of the ECT system.

Chapter 5 discusses capacitance sensors.

Chapter 6 describes the capacitance measurement unit.

Chapter 7 discusses system calibration and normalisation

4. PTL300E ECT SYSTEM OVERVIEW

4.1 THE PTL300E ECT SYSTEM

The **PTL300E** is an **enhanced ECT system** controlled by Windows-based software running on an Intel-compatible PC. It can be used to monitor any process where the fluid to be observed has **low electrical conductivity** and a **varying permittivity**. A typical **application** is the **real-time monitoring** of the **motion of fluids**, including **multi-phase flows**, in process engineering plant. Specific applications where ECT has been successfully used to-date include the monitoring of powder conveying, flames, combustion and explosions, mineral processing, fluidised beds, wood rot, hydrate formation and catalyst structures, and for checking product uniformity.

PTL300E ECT systems consists of a **capacitance sensor** unit, a **Capacitance Measurement Unit** (CMU) and a **personal computer** equipped with **custom communications and control** software. A photograph of the complete ECT system is shown in figure 1.1 and a detailed specification is given in Appendix 1.

4.1 SYSTEM OPTIONS

Two versions of the **PTL300E** ECT system are available, suitable for use with sensors containing either one or two planes of measuring electrodes and one or two sets of driven guard electrodes.

The **single plane system (type PTL300E-SP-G)** consists of an industry-standard PC together with a **Capacitance Measurement Unit (CMU)** type **DAM200E-SP-G** and a **demonstration 12 element single-plane unguarded single-plane ECT sensor.** Capacitance sensors containing sets of between **2 and 12 measurement electrodes**, together with up to 2 sets of **driven axial guard electrodes,** can be used with the system.

The **twin-plane version (type PTL300E-TP-G)** is intended for imaging in two axial planes and is similar to the single plane system but uses a **dual-plane Data Acquisition Module type DAM200E-TP-G** and is supplied with an additional demonstration single-plane capacitance sensor. This version can be used to measure the velocity profile of the sensor contents under suitable flow conditions, by correlating the permittivity data between the two image planes of a suitable twin-plane capacitance sensor.

4.2 MEASUREMENT CAPABILITIES

PTL300E ECT systems are intended primarily for use with **mixtures of two materials having different dielectric constants (permittivities**). These are known as **two-phase mixtures** and for mixtures of this type, PTL300E ECT systems can provide approximate information about the relative proportions of the two materials inside the ECT sensor at any given time (**voidage)** as well as displaying their approximate **distribution** across the sensor plane.

PTL300E ECT systems can be used with **ECT sensors** containing either one or two sets of between 2 and 12 **measurement electrodes** and up to 2 sets of **driven guard electrodes and** capture capacitance data in accordance with **measurement protocol 1**.

The PTL300E-SP-G ECT system can be used to view the **contents** of closed pipes or vessels at one axial location while the **PTL300E-TP-G** system can be used to image at two separate axial locations simultaneously. If the **vessel walls** are **non-metallic** external sensor electrodes can be used. If the vessel walls are metallic, the **sensor electrodes** must be placed **inside the vessel walls. T**he materials to be imaged must be essentially **non-conducting dielectric materials** such as **oils, plastics, powders** or other similar materials**.**

Measured **inter-electrode capacitances can also be stored** in a **data file** on a continuous basis at speeds up to 300 frames per second, depending on the **number of electrodes** on the sensor. **Permittivity images** are displayed over a **cross section** made up from a selected number of **pixels** contained (typically) in a **32 X 32 square grid.** The **colour** of each individual pixel represents the **average value** of the **normalised permittivity** (in a range from 0 to 1) of the material in the cell.

The **ECT system** must be calibrated before it can be used. This involves **filling** the **ECT sensor** with two different **materials** having **permittivities** at the **lower** and **higher** ends of the **permittivity range** to be measured.

The equipment can be used in a number of different modes:

- In **Capture** mode, live images of materials can be displayed and captured at **data rates** selected by the user, while the **inter-electrode capacitance measurements** are streamed to a continuous **buffer file** which can then be saved to a data file following the cessation of data capture. This allows permittivity **images** to be **reconstructed and replayed** at a later date using other alternative software.

- In **Playback** mode, images can be replayed at the same or different rates, again selected by the user. Facilities are also provided for **single-stepping** through recorded images.

- In **Record** mode, capacitance data is streamed directly to a series of user-defined data files.

The **normalised permittivity** of individual **pixels** in the ECT **image** can be displayed either **On-line during data capture** or when the data is replayed. The values of the normalised inter-electrode capacitances can also be displayed in both Data **Capture** and **Playback** modes. The instantaneous **volume fraction** (or **concentration**) of the materials inside the sensor is displayed continuously on the image screen and a pixel probe allows the value of individual permittivity pixels to be displayed.

Alternative sets of **sensitivity maps** for different **dielectric materials** and/or **sensors** can be used and **diagnostic software** is provided which allows the measurement of **absolute** values of **inter-electrode capacitances** for sensor design and testing purposes.

Finally, the **recorded capacitance data** can be used for the **independent** calculation of **volume ratio** or for the calculation or display of images using other image reconstruction software.

4.3 PRINCIPLE OF OPERATION

The **PTL300E ECT system** produces one or more **cross-sectional images of the permittivity profile of the contents of a pipe or vessel** from **measurements of capacitance between combinations of sensor electrodes which surround the vessel**. The images are **approximate** and of **relatively low resolution**. Sensors of any cross-section can be imaged provided that a suitable sensitivity map for the sensor can be calculated.

Images are produced in the following way:

1. The properties of the sensor are measured or calculated initially to produce a **sensitivity map** of the sensor. This is a set of **numerical matrices** whose **elements** correspond to the individual **pixels** in a **rectangular grid** which is used to define the **sensor cross-section**.

2. The **sensor** is normally **calibrated** at **each end of the range of permittivities to be measured** by **filling** the sensor with the **lower permittivity material** initially and measuring all of the individual **inter-electrode capacitances**. This operation is then repeated using the **higher permittivity material**. The data obtained during the calibration procedure is used to set up the measurement parameters for each measuring channel and is stored in a **calibration data file**.

3. Once the system has been **calibrated**, the **capacitances** between **all unique pairs of sensor electrodes** are measured continuously at high speed, giving **E.(E-1)/2** unique values per **measurement or image frame**, where **E** is the number of sensor electrodes.

4. An **image reconstruction algorithm** is used to compute the **cross sectional distribution of the permittivity** of the **material inside the pipe**. Images can be constructed from the capacitance measurements either at the time of measurement (on-line) or from stored or captured data (off-line). The algorithm supplied as standard in the PTL300 system is the so-called **linear back-projection** (LBP) algorithm. This is a **fast** but **approximate** algorithm which uses the **capacitance measurements**, together with the **sensitivity map** to produce the image. Other alternative algorithms can be used with the stored data to produce more accurate images.

4.4 ECT PERMITTIVITY IMAGE FORMATS

ECT systems can be used to obtain **images of the distribution of permittivity** inside ECT sensors for **any arbitrary mixture of different dielectric materials**. However, an important application of ECT is viewing and measuring the spatial distribution of a **mixture of two different dielectric materials (a two-phase mixture).** For a **two-phase mixture**, ECT can be used to measure the **spatial distribution** of the **composite permittivity** of the two materials inside the sensor. From this permittivity distribution, it is possible to obtain the distribution of the **relative concentration** (**volume ratio**) of the two components over the cross-section of the vessel.

A typical ECT permittivity image format uses a **square grid of 32 x 32 pixels** to display the distribution of the **normalised composite permittivity of each pixel**. For a circular sensor, 812 pixels are used to approximate the cross-section of the sensor, as shown in figure 4.4.1.

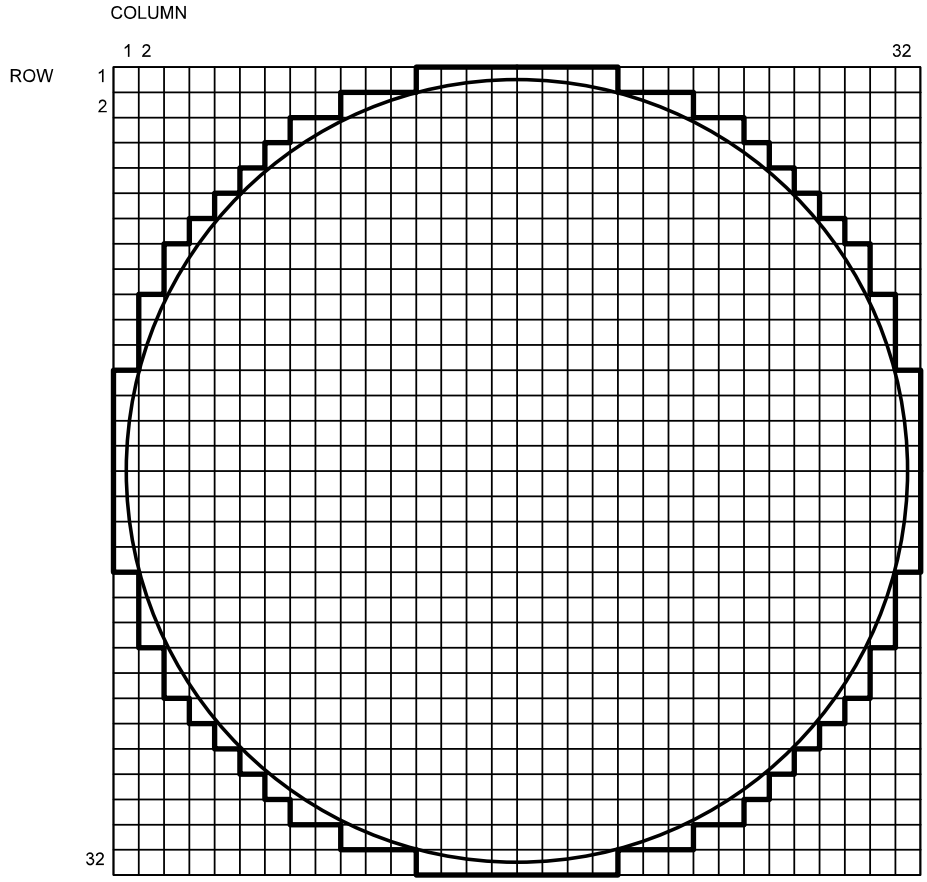

Figure 4.4.1. ECT Image Pixel format

The **values of each pixel** represent the **normalised value of the effective permittivity of that pixel**. In the case of a **mixture of two dielectric materials**, these **permittivity values** are related to the fraction of the higher permittivity material present (the **volume ratio** (or **voidage**)) **at that pixel location.**

The **overall volume ratio,** which defines the **ratio of the two materials present, averaged over the volume of the sensor**, can also be obtained. The **overall volume ratio** of the materials inside the sensor at any moment in time is defined to be **the percentage of the volume of the sensor occupied by the higher permittivity material**. The volume of the sensor is the product of the cross-sectional area of the sensor and the length of the sensor measurement electrodes.

In all of the following we shall be referring to the **relative permittivity** (or **dielectric constant**) of materials. The **relative permittivity** of a material is its **absolute permittivity** divided by the **permittivity of free space** (or air). Hence the relative permittivity of air is 1 and typical values for other materials in solid or liquid format are polystyrene (2.5), glass (6.0) and mineral oil (2.3).

In this manual, we have used three different terms to describe the same concept, as they are all in common use. These are **volume ratio**, **voidage** and **concentration**, which we define to be the fraction of the higher permittivity material present in the mixture. These terms are inter-changeable in the following test.

4.5 SOME TYPICAL PERMITTIVITY IMAGES

Figure 4.5.1 shows a sequence of images obtained from a number of applications, including the imaging of gas bubbles in oil, a fluidised bed experiment and a sensor imaging a flame. In all of the examples shown, the images are based on a normalised permittivity scale which progresses from zero (blue) through green, to a maximum value of 1 (red).

The first example shows a 15cm diameter clear plastic pipe containing a mixture of oil and gas. An external 12 element capacitance sensor is shown attached to the pipe. The ECT image shows a gas bubble passing through the sensor. The blue area of the image represents the gas bubble and the red area of the image represents the oil.

The second example shows a sequence of ECT images obtained using a fluidised bed consisting of a vertical pipe containing an epoxy powder. Air is blown vertically from the bottom of the bed, through a filter and the powder is fluidised by the air flow. An 8 element capacitance sensor with 2.5 cm long sensor electrodes was used to obtain the images. The image sequence shows the unfluidised initial state (red image) (A), partial fluidisation (green image) (B), excess fluidisation allowing the formation of an air hole (blue area) in the bed (C) and final state following the removal of the air supply (D).

The final example shows a 6 element capacitance sensor constructed inside an aluminium cylinder of internal diameter 10cm. The ECT image was obtained using a butane flame positioned approximately in the centre of the sensor.

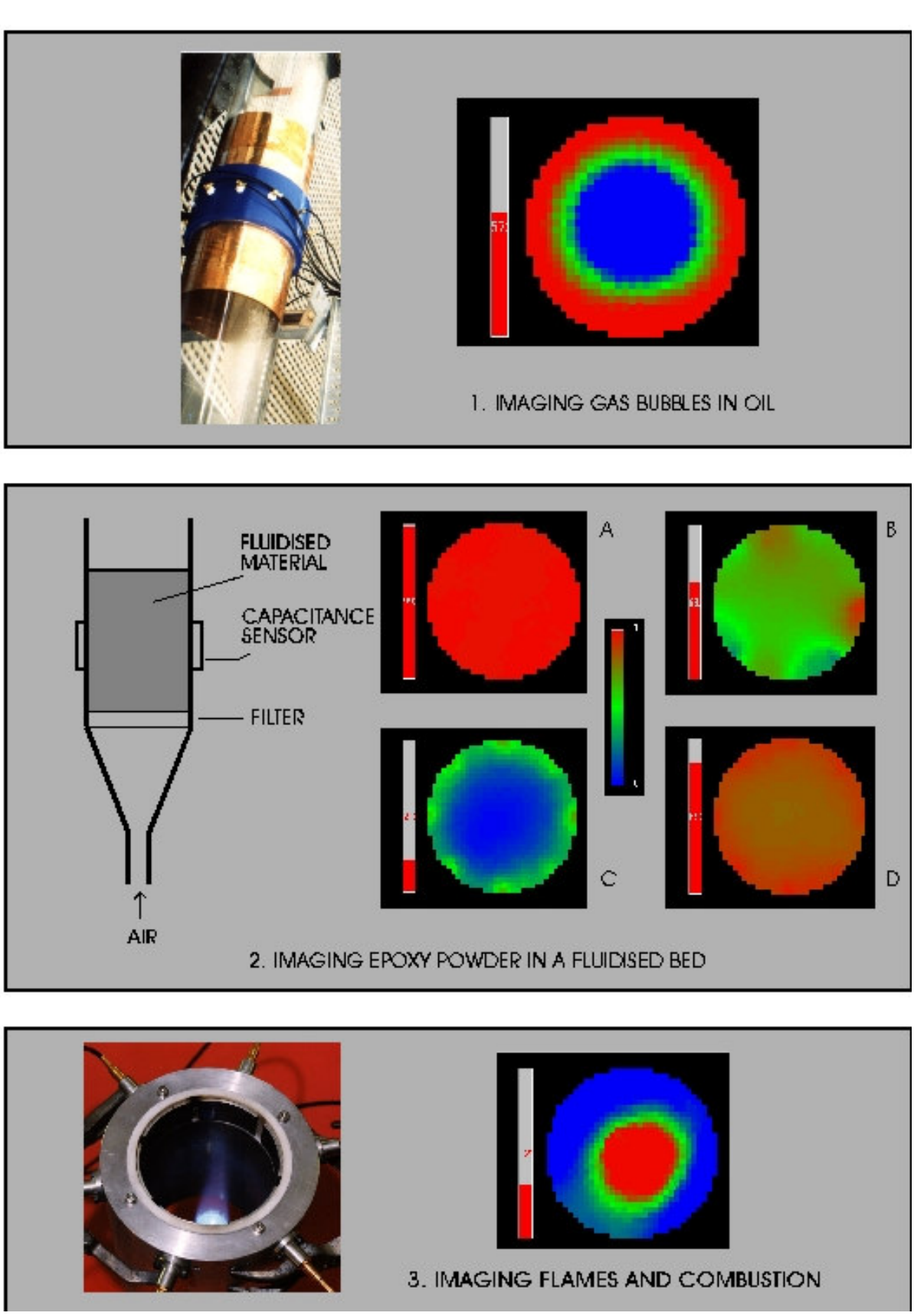

Figure 4.5.1 Examples of ECT images from some typical applications

4.6 CONDUCTIVITY EFFECTS

The PTL300E ECT system uses a relatively simple method to measure the capacitance impedances between pairs of sensor electrodes. Consequently, the capacitance measurement will also respond to any **conductive** component present between the electrodes. For normal applications, where the ECT sensor contains 'ideal' dielectric materials such as oil, glass or plastics, the **conductive component** is negligible and the capacitance measurement is reasonably accurate. However, when the **conductive component** of the **impedance between the electrodes** becomes comparable to the **capacitive component of impedance**, errors will occur.

The problem is most severe for sensors with **external** electrodes, as it is very difficult to obtain any accurate information from sensors with **external electrodes containing a fluid material which is not a perfect dielectric**, for the reasons given later in this section. In the following few paragraphs, we will consider the case of an ECT sensor constructed with **internal** electrodes, which are **in contact** with an **imperfect dielectric fluid,** which will be assumed to have **finite conductivity**.

In these circumstances, problems will occur when the **conductive** component of the impedance between pairs of electrodes becomes comparable with the **capacitive** component of impedance. This situation will occur first between the pairs of **opposite electrodes** in the ECT sensor (where the capacitance is lowest). For a typical ECT sensor, the capacitance between opposite electrodes at the lower permittivity calibration point is around 10 fF, which corresponds to a capacitive impedance of (1/2*PI*F*C) = 12.7 Mohm at 1.25 Mhz.

If the **conductive** impedance between the pair of opposite electrodes is comparable with, or less than this figure, the ECT system will respond to the **conductive** component as well as the **capacitive** component of impedance. As the conductivity of the material inside the sensor increases, the conductive impedance between the electrodes will fall and will become much lower than the capacitive component of impedance. In these circumstances, the ECT system will start to behave as an Electrical Resistance Tomography (ERT) system, responding predominantly to changes in the **conductivity** of the material rather than its **permittivity**.

In practice, the **effect of conductivity** is **just noticeable** with **pure distilled water**, becomes a **severe problem** with **tap water** and becomes the **dominant effect** for even **weak saline solutions**. In these circumstances, any images obtained from the ECT system will be based on the **conductive** properties of the medium rather than its dielectric properties. In fact the ECT system can be considered to be operating as an ERT system when the conductivity reaches these levels.

As the conductivity increases further, two further effects occur which drastically reduce the accuracy and effectiveness of the ECT system in its 'ERT' mode. The first of these is a saturation effect. As the resistance between the pairs of electrodes falls, the current which flows into the detector electrodes overloads or saturates the detector circuitry and no further changes in current are measurable unless steps are taken to reduce the measurement sensitivity.

The second effect occurs because the 'on' resistances of the electronic switches in the ECT system rather than the resistance of the medium start to limit both the voltage which can be applied between the sensor electrodes and also the currents which flow between them. So even if the measurement circuitry is desensitised to allow larger currents to be measured, there will be a loss of sensitivity because of the resistances of the electronic switches. In these circumstances it is preferable to use a constant-current-injection measurement technique (rather than the applied voltage method which is used in ECT systems) to obtain the ERT image and this is indeed the method which is used in commercial ERT measurement systems.

As mentioned earlier, the problem of conductive fluids is much more serious if **external** electrodes are used. This is because there is **relatively weak electrical coupling** through the **wall of the sensor** between the **electrodes** and the **sensor fluid** when compared with the **coupling across the fluid**. Consequently the conductive fluid tends to act as a **continuous and perfectly conducting object**. If the sensor is full, the fluid acts as a **circular conducting shield just inside the sensor wall** and simply **couples the electrodes together via the dielectric material of the sensor wall**. When this happens, the image obtained is simply that of the **outside surface of the fluid** only. Experience suggests that it is **not possible to image inside even slightly-conducting fluids using ECT sensors with external electrodes** (although it is just possible if distilled water is used).

5. ECT CAPACITANCE SENSORS

5.1 ELECTRODE LOCATION

Capacitance sensors for use with PTL300E ECT systems will normally be customised items for each individual application, and can take one of two basic forms. The simplest arrangement, for a single plane sensor, consists of a non-conducting section of pipe surrounded by an array of equally-spaced screened capacitance sensor electrodes. A demonstration 12-element sensor of this type is supplied with each ECT system and photographs showing its construction are shown in figure A2.1. An alternative arrangement is an insulated pipe liner, fitted with sensor electrodes which is inserted into the pipeline. A twin-plane sensor will contain two sets of measuring electrodes located at different axial planes, together with guard electrodes.

In general, ECT sensors can be constructed with electrodes located on either the **inner** or **outer** suface of non-conducting pipes (or embedded within the pipe wall). Electrodes are often located on the outer surface for convenience of construction and because in this arrangement, the electrodes are non-invasive. However, sensors with electrodes on the **outside** of the sensor wall can exhibit considerable non-linearity in their response to dielectric materials introduced inside the sensor. This effect is caused by the presence of the **sensor wall**, which introduces an **additional series coupling capacitance** into the measurement. If more accurate measurements are required, sensors with electrodes on the inside surface of the sensor wall should be used.

As the inter-electrode capacitances are typically fractions of a picoFarad, an **earthed screen** is required around the **electrodes** to eliminate the effects of extraneous signals, which would otherwise predominate and corrupt the measurements. The overall sensor assembly can be encased for operation in high-pressure systems and is connected to the **Data Acquisition Module** by **screened flexible coaxial leads.**

5.2 NUMBER OF ELECTRODES

PTL300E ECT systems can be used with capacitance sensors having between 2 and 12 measurement electrodes and a similar number of driven guard electrodes. Capacitance measurements (using protocol 1 only) are made between each electrode and every other electrode. For a sensor containing E measurement electrodes, there are E(E-1)/2 unique capacitance measurements. This corresponds to 66 individual measurements for a 12 electrode sensor.

The number of electrodes used will depend on the measurement priorities. There is a **trade-off** between the **axial** and **radial resolutions** of **ECT sensors**, the **capacitance measurement sensitivity** and the **maximum data capture rate**. **Shorter electrodes** will give **improved axial resolution** but at the expense of an **increase in system noise level**. This can be compensated by using **fewer electrodes** so that the **electrode area is maximised** and this in turn will give faster **maximum frame capture rates**.

PTL300E systems can capture data at more than 100 frames per second when 12 electrodes are in use. For a smaller number of electrodes, less time is needed to measure all of the inter-electrode capacitances and higher data capture rates can be achieved. For example, for an 8 electrode system, the number of individual capacitance measurements falls to 28 and the maximum image capture rate increases accordingly.

As a rule of thumb, faster frame capture rates require the use of a small number of electrodes and this also improves the axial resolution. However, if good angular resolution is required a larger number of longer measurement electrodes will be needed but the axial resolution and maximum frame capture rate will be reduced.

5.3 NEED FOR DRIVEN GUARD ELECTRODES

If the sensor electrodes are short compared with the diameter of the sensor, **axial guard electrodes** must be used in addition to the **measuring electrodes**, to prevent the **electric field** from spreading excessively at the ends of the **electrodes**. These **guard electrodes** are connected to guard driving circuitry on the data acquisition module.

As a guide, if the **length of measuring electrodes** is less than than approximately **twice the sensor diameter**, **axial guard electrodes**, driven with the same potentials as the measuring electrodes will be needed as shown in figure 5.3.1. The use of **driven guard electrodes** dramatically improves both the **axial resolution** and **signal-to-noise ratio** of **sensors with short electrodes**.

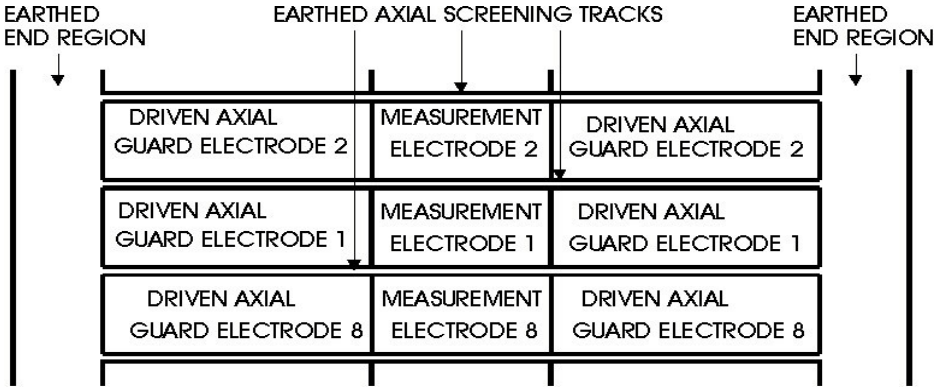

Figure 5.3.1 Driven guard electrode design for an 8-electrode sensor.

5.4 ELECTRODE NUMBERING CONVENTION

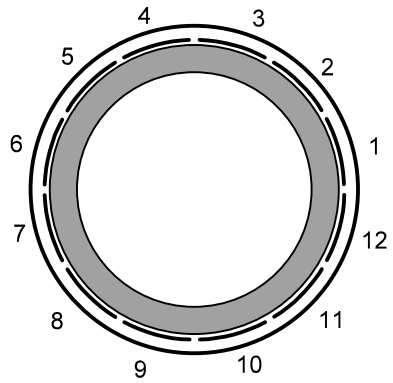

Figure 5.4.1 Electrode numbering convention

For all **PTL ECT sensors**, we use the convention that **electrodes are numbered anticlockwise** when the ca**pacitance sensor is viewed from the connector end** (or the end from which the captive coaxial leads emerge), starting in the first quadrant above the horizontal, as shown in figure 5.4.1.

The **location of each electrode on the boundary of the permittivity image** is determined by the **geometry** of the **sensor model** used to define the **sensor sensitivity map**. Standard sensitivity maps for circular sensors with 6,8 and 12 electrodes are provided with PTL300E ECT systems. For these maps and for sensors with 6 and 12 electrodes, the centre of electrode 1 lies on the horizontal axis (at 3 o clock) and the remaining electrodes are distributed at 30 or 60 degree intervals. For 8 electrode sensors, the centre of electrode 1 is at 22.5 degrees above the horizontal axis and the remaining electrodes are distributed at 45 degree intervals.

5.5 ELECTRODE EXCITATION

Channels 2 to 11 on the DAM200E unit can be selected to be either source or detector channels and the corresponding electrodes on the capacitance sensor will therefore also be excited as either source or detection electrodes. Channel 1 on the DAM200E sets electrode 1 to be either a source electrode or grounds it and channel 12 always sets electrode 12 to be a detector electrode. The driven guard electrodes follow the potentials of the corresponding measurement electrodes.

As it is necessary to maximise the surface area of each electrode to optimise the measurement sensitivity, it is tempting to cover the circumference of the sensor with electrodes with minimal spacing between adjacent electrodes. However, this can lead to problems, as the standing capacitance between adjacent electrodes will be very large and may saturate the capacitance measuring equipment. Consequently, thin earthed axial guard electrodes are normally located between adjacent electrodes to reduce this standing capacitance to manageable values. A typical electrode pattern of this type has already been shown in figure 5.3.1.

A consequence of this arrangement is that the electrical potential on every electrode is well-defined, which makes it relatively straightforward to calculate the **sensor sensitivity map** and also results in an **electrically-optimum** sensor design. An important point which must be understood is that, because of the **finite axial length of each sensor electrode,** the **permittivity image** will be the **average over the volume of the sensor occupied by each set of measurement electrodes.**

5.6 CAPACITANCE VALUES

The DAM200E CMU can measure inter-electrode capacitances in the range 0.1 to 2000fF. A good design rule is to design the sensor electrodes so that the capacitance per unit length between **adjacent** electrodes is minimised, with a target value for adjacent electrodes of the order of 500fF for 10 cm long electrodes with air inside the sensor. This allows for an increase in capacitance between adjacent electrodes by a factor of 4 when the sensor contains a dielectric material. This is normally sufficient for most materials which are likely to be imaged.

The capacitance between adjacent electrodes can be reduced by placing an earthed screening track between each electrode and by using an outer screen located at a set radial distance from the electrodes. With the outer screen located approximately 0.5 cm from the electrodes the capacitance between adjacent electrodes is approximately halved compared with the value in the absence of the screen, but there is little effect on the capacitance between non-adjacent electrodes. The inter-electrode capacitance can be further reduced by the addition of a radial screen between each sensor electrode, connected between the earthed screening track and the outer screen.

Having designed for minimum capacitance per unit length between adjacent electrodes, the absolute values of inter electrode capacitances can be adjusted by varying the axial length of the electrodes.
For most ECT sensors, the capacitance between any pair of electrodes will consist of two components, a **primary capacitance** component via the internal volume of the sensor which contains the dielectric

fluids and a **secondary capacitance** component due to coupling via external paths, for example, through the vessel walls and in the space between the electrodes and the external screen.

For sensors with internal electrodes, the primary capacitance components usually predominate and if the sensor is filled with a dielectric material, the capacitances between all electrodes will increase approximately by the dielectric constant of the material inside the sensor.

For sensors with external electrodes, the secondary capacitances can be of comparable magnitude or larger than the primary capacitances. Experience shows that when these sensors are filled with a dielectric material, only the capacitances between opposite electrodes increase by a factor equal to the dielectric constant of the material. The capacitance increases between other electrode combinations will be less, because of the effect of the secondary capacitances.

Typical measured capacitances between all electrode-pairs for a guarded 12-electrode sensor with and without a vessel wall are shown in figure 5.7.1

Sensor mounted on 63.5 mm o/d plexiglass tube with 3.2mm wall Capacitances (fF)

src											
1	405.70	35.42	13.86	9.01	6.82	6.15	7.12	9.10	13.87	33.40	392.58
2	420.26	29.96	14.16	9.04	6.95	6.72	7.52	9.61	14.83	32.89	
3	419.09	34.69	15.78	10.37	8.03	7.42	8.06	10.37	15.36		
4	398.79	33.04	15.09	9.58	7.13	6.54	7.22	8.97			
5	407.08	33.61	14.79	9.09	6.89	6.47	7.03				
6	421.19	34.30	14.58	9.39	6.89	6.21					
7	416.80	34.02	14.65	9.06	6.92						
8	403.11	34.51	14.34	9.40							
9	458.36	35.16	15.18								
10	414.63	35.52									
11	413.10										
Cinj	3.38	3.62	-1.15	3.59	-0.67	-7.66	1.72	-5.51	-7.84	5.48	-148.58

Sensor with no wall. Sensor i/d 63.5mm Capacitances (fF)

Src											
1	198.40	32.15	13.36	8.83	6.64	5.97	6.92	8.83	13.15	28.98	180.59
2	211.21	27.01	13.69	8.82	6.74	6.57	7.40	9.39	14.26	29.37	
3	217.75	31.50	15.27	10.10	7.91	7.33	7.99	10.11	14.91		
4	196.06	29.55	14.37	9.28	7.00	6.41	7.09	8.71			
5	210.26	29.68	14.22	8.94	6.83	6.36	7.03				
6	201.54	29.37	13.86	9.13	6.73	6.14					
7	199.19	29.10	13.81	8.74	6.79						
8	188.29	28.95	13.51	9.15							
9	242.86	29.05	14.28								
10	202.27	30.00									
11	195.56										
Cinj	3.71	3.98	-0.91	3.93	-0.44	-7.47	2.02	-5.33	-7.78	5.65	-148.25

Figure 5.7.1 Inter-electrode capacitances with and without a vessel wall.

In these figures, the first column shows the source electrode and the columns are for each detector electrode using the normal measurement sequence C12, C13 etc.

5.7 AVOIDANCE OF STATIC CHARGE PROBLEMS

It is important to prevent static charge building up on the sensor electrodes, as this may damage the CMOS input circuitry of the DAM200 unit when the charged electrodes are connected to the unit. For this reason, discharge resistors must be permanently connected between each sensor and driven guard electrode and earth. A suitable value for these resistors is 1 M ohm. If printed circuit electrodes are used, it is usually convenient to solder the discharge resistors in circuit at the location where the coaxial leads are connected to the electrodes and earth.

5.8 THE DEMONSTRATION SENSORS

The demonstration sensors supplied with PTL300E ECT systems are 12 element **unguarded** sensors containing a quantity of glass or plastic beads inside a 51mm diameter PVC tube. The sensor electrodes are formed from flexible copper-clad laminate and are 100 mm long with axial earthed guard tracks between electrodes and an earthed screen at each end of the sensor. The whole assembly is screened by an outer copper tube formed from copper sheet which is formed around the electrode assembly and spaced approximately 5mm from the electrodes. The sensor contains 12 x 1Mohm discharge resistors connected between the sensor electrodes and the earthed section of the flexible PCB.

An image sequence showing the construction of the demonstration sensor is shown in Appendix 2 and a photograph of the completed sensor is shown in figure 5.8.1.

Figure 5.8.1 Demonstration 12-electrode unguarded ECT sensor

The total tube length of the sensor is more than twice the active sensor length and includes a transparent viewing section. The sensor is half-filled with beads and it is therefore possible to either fill or empty the capacitance sensor section simply by inverting the tube assembly.

The sensor has 12 individually-numbered 1.25 metre leads terminated in SMB connectors and these must be connected to the corresponding numbered channels on the Data Acquisition Module.

Further information on the design of ECT sensors can be found in **PTL Application note AN3**, copies of which are available on request.

6. THE DAM200E CAPACITANCE MEASUREMENT UNIT

6.1 OVERVIEW

The inter-electrode capacitances are measured by the **Capacitance Measurement Unit (CMU)**, controlled by a standard Personal Computer (the **Control PC**) running proprietary PTL (**ECT32)** control software under the MS Windows operating system. The **CMU** contains an **embedded PC** running **PTL embedded software** under the **Linux** operating system and this embedded PC is linked to the control PC by a standard **10/100 ethernet** connection.

The CMU contains 1 [or more] set[s] of capacitance measuring circuitry, together with circuitry for driving any guard electrodes. The presence of the earthed screen around the sensor and the screened connecting leads means that a **stray-immune** method must be used for measuring the inter-electrode capacitances. The technique used in the DAM200 unit is a development of the charge transfer method, operating at a switching frequency of 1.25 MHz, which allows capacitance values down to 0.0001pF (0.1 femtoFarads) to be resolved. Details of the capacitance measurement circuitry are given in paragraph 6.2.

All adjustments of the **CMU** are made from within the system software. These include adjustment of the circuit gain for individual capacitance measurements, calibration of the system, and continuous automatic monitoring and compensation for zero drift in the capacitance measuring circuitry.

The ethernet connection between the **CMU** and the **host control computer** can be implemented either by the use of a **direct cross-over ethernet lead** between the 2 units or by connecting the **PC** and **CMU** to an **ethernet hub** using conventional (uncrossed) ethernet leads.

The **DAM200E CMU** can carry out **Protocol 1** capacitance measurement sequences in which **one measurement electrode** in **each electrode plane** and the equivalent **driven guard electrode** is set to be a source electrode, while the remaining (**detector**) electrodes are maintained at **virtual earth** potentials. Capacitance sensors having one (or two) planes of between 2 and 12 measurement electrodes and an optional set of driven guard electrodes can be used with the DAM200E CMU.

6.2 HARDWARE DETAILS

The CMU contains measurement circuitry for up to 2 planes of measurement electrodes and two sets of driven guard electrodes. Each plane of measurement electrodes is controlled and measured by an analogue measurement circuit board and an associated digital control board and the driven guard electrodes are controlled by circuitry on two further driven guard control boards. The CMU also contains an embedded PC with a digital interface and input/output triggering circuitry. A functional drawing of the CMU is shown in figure 6.2.1.

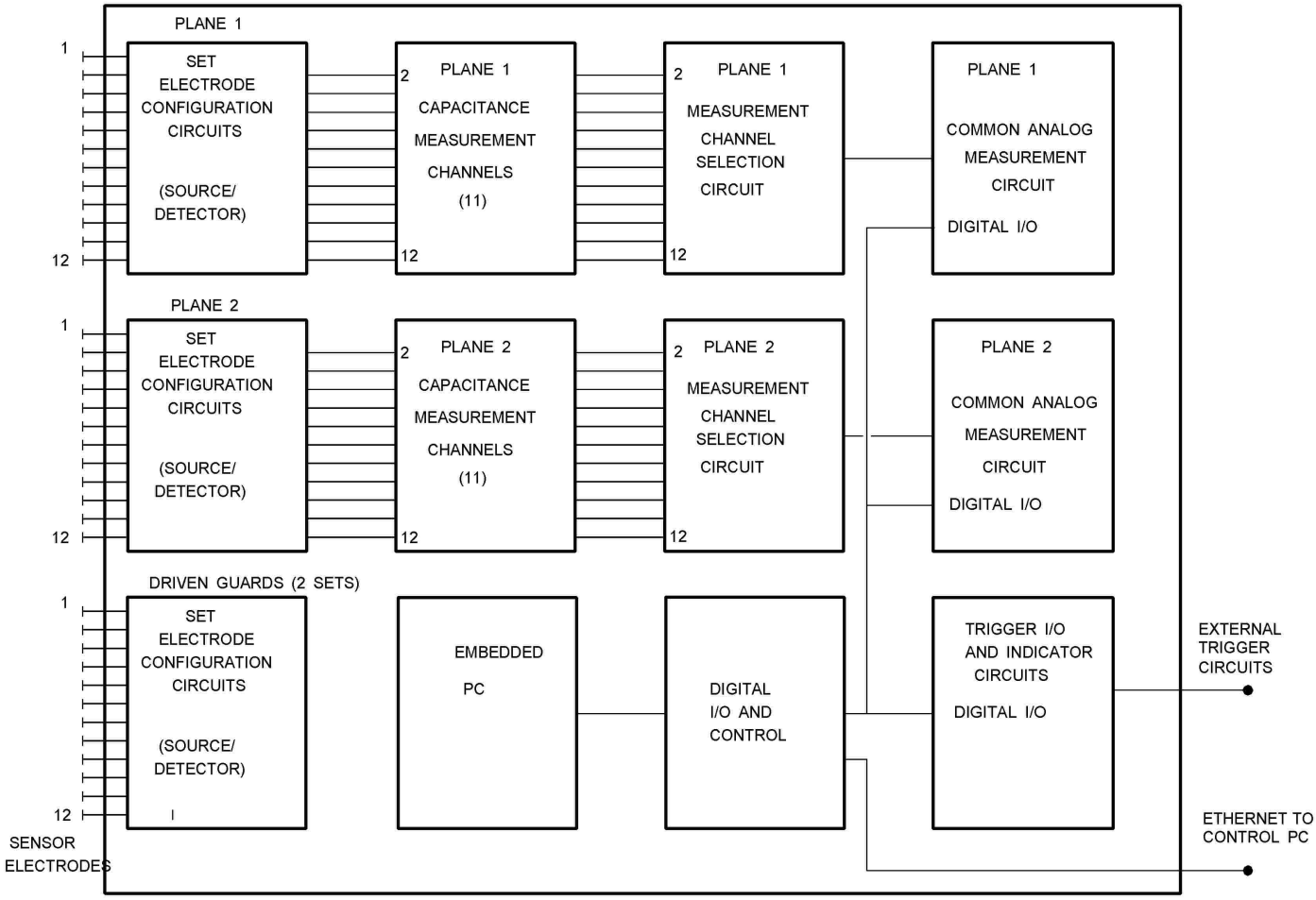

Figure 6.2.1 Component parts of the DAM200E-TP-G Capacitance Measurement Unit

Each **analogue** circuit board contains 12 capacitance measuring/control channels, an 11-way multiplexer circuit and a common analogue measuring circuit containing a DC bridge circuit and a 12-bit Analogue-to-Digital Converter (ADC) Each **digital** board contains the control and communications circuits for its associated analogue board. The **driven guard** boards provide an excitation signal to each driven guard electrode, identical to that applied to the equivalent measurement electrodes.

The CMU can measure capacitances in the range 0.1 - 2000fF (1fF = 10^{-15}F), and the inter-electrode capacitances of the capacitance sensor must therefore lie within this range when the sensor contains the dielectric materials to be imaged. The bridge circuit in the CMU is normally operated so that the 12-bit ADC (max output count 4095) operates between approximately 20% of full scale (900 counts) for all low-permittivity capacitance values (when the sensor is filled with the lower permittivity material) and 80% of full-scale (3200 counts) for all high permittivity capacitance values (when the sensor is filled with the higher permittivity material). This gives a measurement "headroom" of approximately 30% of the nominal measurement range above and below the nominal measurement range defined during the sensor calibration process. This headroom is needed to cope with soft field effects which can cause the measured capacitances to either exceed or fail to reach the values measured during calibration.

6.3. CAPACITANCE MEASUREMENT

6.3.1 Requirements For Capacitance Measurement System

The capacitance measuring system must be able to measure very small inter-electrode capacitances, of the order of 10^-15 Farads (1 fF), in the presence of much larger capacitances to earth of the order of 200,000 fF (mainly due to the screened connecting cables and the outer screen of the sensor). It must be able to measure the small capacitances between opposing electrodes (10fF) as well as the much larger capacitances between adjacent electrodes (500fF) and must be able to do this at high speeds. The measurement circuit must noise-free as far as possible, immune to any interfering signals and must be stable and exhibit low long-term drift.

6.3.2 Measurement principle

The technique for measuring the capacitances between electrode pairs in the **PTL300E DAM200E** measurement system uses a set of 11 charge/discharge capacitance/voltage converters and a common analogue measurement channel in the form of a programmable DC bridge. A simplified block diagram of the measurement circuitry for one measurement plane is shown in figure 6.3.1 below.

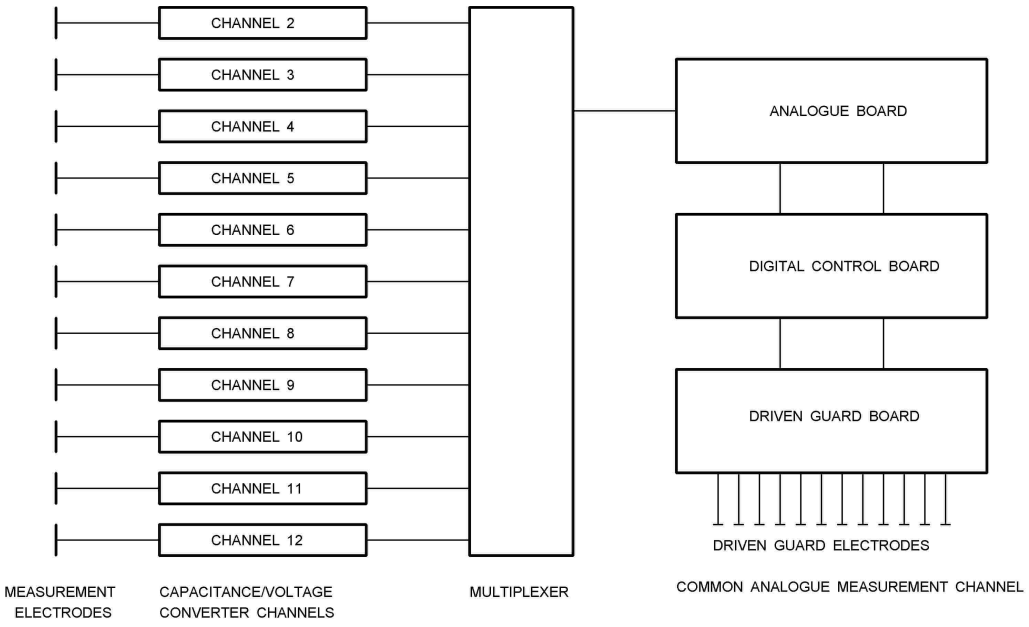

Figure 6.3.1 Capacitance measurement circuitry for a single plane of electrodes

The **operation** of the **DAM200E measurement circuitry** is described in detail in **Appendix 4** in **Volume 2** of this manual.

6.4 CAPACITANCE MEASUREMENT SEQUENCE

6.4.1 Protocol 1

The **DAM200E CMU** is designed to measure capacitances under protocol 1, where one measurement electrode in each electrode plane and the equivalent driven guard electrode are set to be source electrodes, while the remaining (detector) electrodes are maintained at virtual earth potentials. This results in the following sequence of capacitance measurements for a 12-electrode sensor:

	Source channel
C_{1-2}, C_{1-3}, C_{1-4}, C_{1-5}, C_{1-6}, C_{1-7}, C_{1-8}, C_{1-9}, C_{1-10}, C_{1-11}, C_{1-12},	1
C_{2-3}, C_{2-4}, C_{2-5}, C_{2-6}, C_{2-7}, C_{2-8}, C_{2-9}, C_{2-10}, C_{2-11}, C_{2-12}	2
C_{3-4}, C_{3-5}, C_{3-6}, C_{3-7}, C_{3-8}, C_{3-9}, C_{3-10}, C_{3-11}, C_{3-12}	3
C_{4-5}, C_{4-6}, C_{4-7}, C_{4-8}, C_{4-9}, C_{4-10}, C_{4-11}, C_{4-12}	4
C_{5-6}, C_{5-7}, C_{5-8}, C_{5-9}, C_{5-10}, C_{5-11}, C_{5-12}	5
C_{6-7}, C_{6-8}, C_{6-9}, C_{6-10}, C_{6-11}, C_{6-12}	6
C_{7-8}, C_{7-9}, C_{7-10}, C_{7-11}, C_{7-12}	7
C_{8-9}, C_{8-10}, C_{8-11}, C_{8-12}	8
C_{9-10}, C_{9-11}, C_{9-12}	9
C_{10-11}, C_{10-12}	10
C_{11-12}	11

where, for example, C_{1-2} means the capacitance measured between electrodes 1 and 2 with electrode 1 set to be a source electrode and electrode 2 set to be a detector electrode.

As the capacitances between pairs of electrodes are independent of the direction of measurement, reciprocal measurements (eg C_{2-1}) are not made in the interest of capturing frames of data at the highest possible capture rates.

The rate at which measurements can be made depends on the response time of the capacitance measurement circuits inside the CMU. The outputs of the electronic filters in the capacitance measurement channels must be allowed to reach their maximum values before the ADCs in each channel are read. For the filters in the DAM200E, a delay of approximately 380uS is needed after the source channel has been selected before the individual measurement channels can be read. Moreover, an additional delay of approximately 20 uS is required betweeen selecting the output of each successive capacitance measurement channel to the common measurement channel via the multiplexer.

6.4.2 Capacitance Measurement Control Sequence

The table in paragraph 6.4.1 defines the required measurement sequence to capture a full frame of capacitance data. The actual measurement sequence implemented in the CMU is as follows:

1.Set channel 1 to be a source channel. Wait approximately 380uS to allow the outputs of the electronic filters in the measurement channels to settle.

2. Measure the capacitances between electrode 1 and the remaining electrodes in numerical order with a delay of 20uS between each of these measurements.

3. Set channel 2 to be a source channel. Wait approximately 380uS to allow the outputs of the electronic filters in the measurement channels to settle.

4. Measure the capacitances between electrode 2 and the remaining electrodes in numerical order with a delay of 20uS between each of these measurements.

Repeat this sequence for each source electrode channel in turn up to channel 11.

The capacitance data within a frame will be skewed in time as a result of this sequential data capture scheme. If this is important, supplementary software is available which can be used to "de-skew" the capacitance data.

A finite time is taken to capture a full frame of data and the total time delay is seen to be 380 x 11 + 20 x 66 = 5500 uS, corresponding to a maximum possible frame rate of 182 fps for a 12-electrode sensor. In practice, because of additional delays within the PC digital interface and the ethernet link, the fastest rates that can be achieved in practice are around 105 fps for a 12-electrode sensor, but this capture rate can be achieved using either one or 2 measurement planes.

6.5 CIRCUIT DESIGN INFORMATION

Detailed information about the electronic measurement circuitry used in the DAM200E unit is given in Appendix 4.

7 ECT SYSTEM CALIBRATION AND NORMALISATION

Section 6 explained how the inter-electrode capacitances are measured. Although an ECT system can be operated on the basis of absolute capacitance measurements, most practical ECT systems use normalised capacitances. These are derived from the absolute capacitances by carrying out a series of measurements under controlled conditions and generating a calibration data file.

7.1 CALIBRATION PRINCIPLE

In the normal method of operation, an ECT system is calibrated by filling the sensor with the **two reference materials in turn** and measuring the **resultant inter-electrode capacitance values** at these **two extreme values of relative permittivity**.

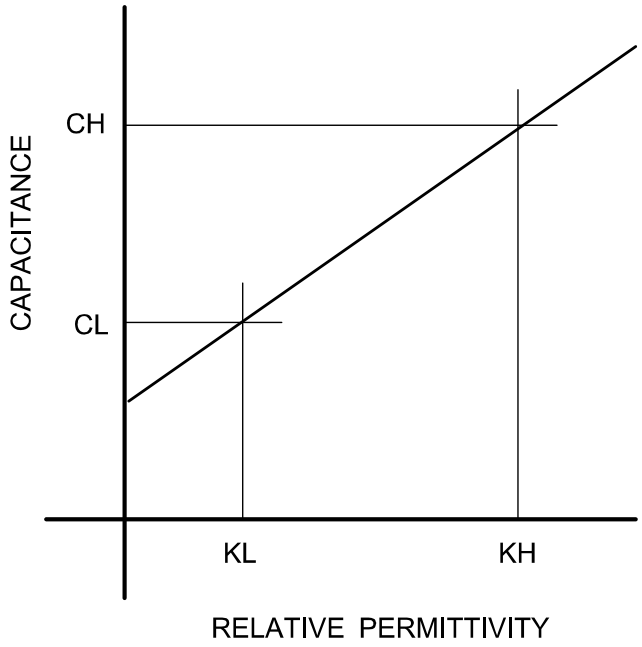

Figure 7.1.1 Relationship between capacitances and permittivity

This situation is shown diagramatically in figure 7.1.1, which illustrates how the **measured inter-electrode capacitances** change between the **higher** and **lower values of permittivity** used for calibration, for two materials of relative permittivity K_L and K_H. For simplicity, it has been assumed that the variation is linear.

This method of calibration defines the **two end points** of the **measurement range** for most types of ECT measurement.

The data generated during the calibration process is held in a calibration file. A valid calibration file must be available before the ECT system can be used to capture valid data.

7.2 CALIBRATION FILE GENERATION

Calibration involves carrying out a sequence of measurements to determine the inter-electrode capacitances between all combination of electrodes when the sensor is filled in turn with dielectric materials at the lower and upper ends of the permittivity range to be measured. This information is stored as sets of 3 integer counts, M1, M2 ansd M3 which determine the offset voltage used to balance the bridge measurement circuit, the gain of the measurement circuit and the output count of the ADC.

Once these parameters have been measured and stored in a calibration file, this data can be used to set the parameters in the common analogue measurement channel to measure the inter-electrode capacitances when the sensor contains an arbitrary distribution of the two materials used to calibrate the sensor.

The calibration process is described in detail in Appendix 4 and the basic principle is described blow

7.2.1 Charge Injection Capacitances measurement

The capacitance measurement circuits will indicate a small value of capacitance between pairs of sensor electrodes even when no excitation voltage is applied to either electrode. This is caused by capacitive coupling of the clock waveforms used to control the CMOS switches in the measurement circuit, which causes small quantities of charge to appear at the switch outputs. These spurious capacitances are known as charge injection capacitances and can be measured by operating the ECT system with no source electrode excited.

The first stage of the calibration is therefore to measure the charge injection capacitances for each capacitance to voltage measurement channel and to record the M1, M2 and M3 parameters for each of these measurement channels. These parameters are then converted into absolute capacitances (C_0) as described in Appendix 4.

7.2.2 Lower Permittivity Capacitances measurement

The next step is to measure the set of inter-electrode capacitances C_L when the sensor is filled with the lower permittivity material. This is carried out as follows:

The sensor is filled with the lower permittivity material and the values of inter-electrode capacitances are measured as described in Appendix 4. The corresponding M1, M2 and M3 values are again recorded and converted to absolute capacitances C_L. The true value of the inter-electrode capacitances at the low permittivity calibration point are then calculated by subtracting the appropriate charge injection capacitances C_0 from the measured values C_L.

7.2.3 Higher Permittivity Capacitances measurement

The procedure described in para 7.22 is then repeated with the sensor filled with the higher permittivity material and the absolute values of capacitance C_H are again calculated and corrected.

7.2.4 Capacitance normalisation

The measured sets of calibration capacitances C_L and C_H are then used to normalise the subsequent measured capacitances as described in section 7.3.

7.2.5 Sample Calibration Data

A typical set of raw data held in the calibration data file is shown in Appendix 3 together with an explanation of the data format. The first set of data is the low-level permittivity calibration data, the second set is the high-level permittivity calibration data and the final set is the DC zero calibration data. For further information on the data format and information about interpretation of this data, please refer to Appendix 3.

7.2.6 Measurement of a range of calibration files.

True calibration can only be carried out when it is possible to fill the sensor with the lower and higher permittivity materials respectively. The ECT32 software allows partial recalibration, at either the lower or higher permittivity points only, and this faclity is very useful for dealing with minor zero or full drift problems. However, it is a sensible precaution to measure a range of calibration files for a particular sensor under different conditions of room temperature etc before attempting to capture ECT data which will be used for subsequent analysis or processing. These calibration files can then be stored and the optimum file for the current measurement conditions can then be selected for use during data capture without the need for further full recalibration of the sensor.

7.3 CAPACITANCE MEASUREMENTS AND NORMALISATION

In PTL ECT systems, use is made of **normalised parameters** to represent both **the inter-electrode capacitance measurements** and also the displayed values of **pixel permittivity**.

Following the calibration process, the range of capacitance measurements for each electrode combination is known. Consequently the measurement system gains and offsets can be adjusted to **normalise** the capacitance measurements to lie between the values 0 and 1, where **0 corresponds to the values measured at the lower permittivity calibration point** and **1 corresponds to the values measured at the upper permittivity calibration point,** for each inter-electrode capacitance measurement.

When data capture starts, the **capacitances** between **all unique pairs of sensor electrodes** are measured continuously and these **capacitance values** are stored as **normalised values** for each frame of data in a binary data file. The normalised capacitance measurements can be displayed as vertical lines in the ECT32 software by displaying the appropriate capacitance windows.

7.3.1 Normalisation Of Inter-Electrode Capacitances

The absolute **inter-electrode capacitances** are normalised as follows: The values measured at the **lower permittivity** calibration point ($\mathbf{C_L}$) are assigned values of 0 while the **inter-electrode capacitances** measured at the **higher permittivity** calibration point ($\mathbf{C_H}$) are assigned values of 1. This relationship is shown in graphical format in figure 7.3.1 and is defined by the equation:

$$C_N = (C - C_L) / (C_H - C_L) \qquad (7.3.1)$$

where $\mathbf{C_n}$ is the set of normalised inter-electrode capacitances and $\mathbf{C}$ are the set of absolute capacitances measured with the sensor containing a material of arbitrary permittivity, $\mathbf{C_H}$ are the set of absolute capacitances measured at the higher permittivity calibration point and $\mathbf{C_L}$ are the set of absolute capacitances measured at the lower permittivity calibration point.

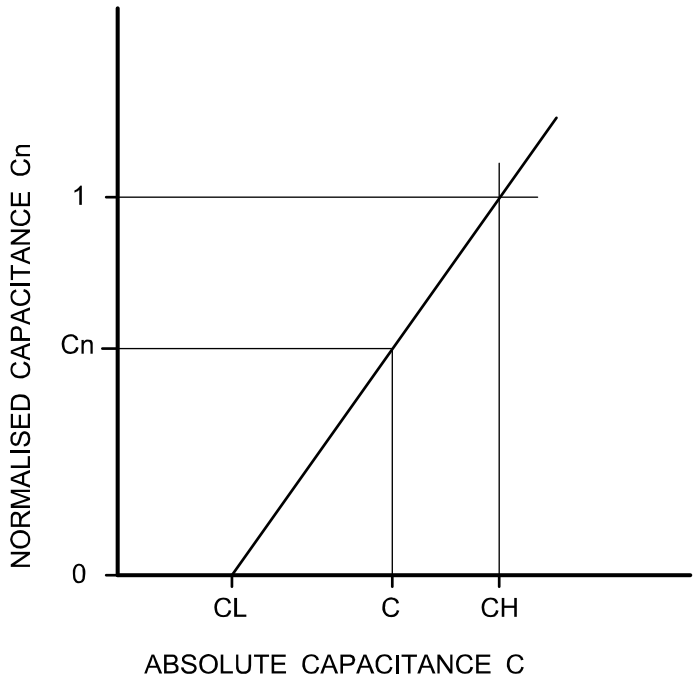

Figure 7.3.1 Normalisation of inter-electrode capacitances

The absolute capacitances C_M can be calculated from the normalised capacitances as follows:

$$C = C_N \,.\, (C_H - C_L) + C_L \qquad (7.3.2)$$

7.4 NORMALISATION OF PIXEL PERMITTIVITY VALUES

The **relative permittivity** values of each **pixel** are calculated from the **normalised capacitance** values and are themselves normalised in a similar manner to the inter-electrode capacitances. Specifically:

The **permittivity values** for each **pixel** in the ECT image for **the lower permittivity calibration point (K_L)** are assigned values of 0, while the **pixel permittivities** in the image at the **higher calibration point (K_H)** are assigned values of 1. This relationship is shown in graphical format in figure **7.4.1** and is defined by the equation:

$$K_n = (K - K_L) / (K_H - K_L) \qquad (7.4.1)$$

where $\mathbf{K_n}$ is the set of normalised permittivities (pixel values) when the sensor is filled with a material of permittivity $\mathbf{K}$, $\mathbf{K_H}$ is the effective permittivity of the material used to calibrate the sensor at the higher permittivity calibration point and $\mathbf{K_L}$ is the permittivity of the material used to calibrate the sensor at the lower permittivity calibration point.

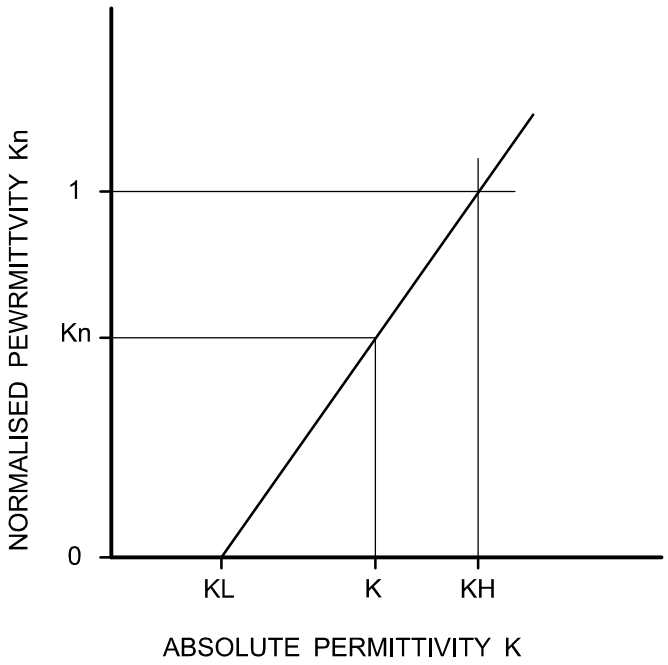

Figure 7.4.1 Normalisation of pixel permittivity values

SECTION 4

CALCULATION OF PERMITTIVITY AND CONCENTRATION DISTRIBUTIONS

This section explains how permittivity and concentration images are obtained from the normalised capacitance measurements.

8 IMAGE RECONSTRUCTION OVERVIEW

8.1 OBJECTIVES OF ECT

ECT systems can be used to obtain **images of the distribution of permittivity** inside ECT sensors for **a**ny arbitrary **mixture of different dielectric materials**. However, the **PTL300E ECT system** is intended primarily for use with **mixtures of two materials** having **different dielectric constants (permittivities**). These are known as **two-phase mixtures** and for mixtures of this type, the ECT system can provide approximate information about the **relative proportions (voidage)** of the two materials inside the ECT sensor at any given time**,** as well as displaying their **approximate distribution** across the sensor plane. The main task in an ECT system is therefore to convert the m**easured capacitance values** into a **permittivity image**. For a mixture of 2 dielectric materials, the **concentration distribution** is related to the **permittivity distribution**, so once the capacitance measurements have been made, the task reduces to calculating the permittivity distribution from these measurements.

8.2 ECT SYSTEM OPERATION

The basic method of operation of PTL ECT systems is as follows:

1. The properties of the sensor are measured or calculated to produce a **sensitivity matrix** of the sensor. This is a set of **sub-matrices** whose **elements** correspond to the individual **pixels** in a **rectangular grid** which is used to define the **sensor cross-section**. The sub-matrices are known as **sensitivity maps**.

2. The **sensor** is normally **calibrated** at **each end of the range of permittivities to be measured** by **filling** the sensor with the **lower permittivity material** initially and measuring all of the individual **inter-electrode capacitances**. This operation is then repeated using the **higher permittivity material**. The data obtained during the calibration procedure is used to set up the measurement parameters for each measuring channel and is stored in a **calibration data file**.

3. Once the system has been **calibrated**, the **capacitances** between **all unique pairs of sensor electrodes** are measured continuously at high speed, giving **E(E-1)/2** unique values per **measurement or image frame**, where **E** is the number of sensor electrodes. These capacitance measurements are then converted to **normalised** values.

4. A **sensor concentration/permittivity model**, which defines the relationship between the concentration distribution across the sensor and the resultant inter-electrode capacitance measurements is chosen and the normalised capacitance measurements are modified according to this sensor model.

5. An **image reconstruction algorithm** is used to compute the **cross sectional distribution of the permittivity** of the **material inside the pipe**. Images can be constructed from the capacitance measurements either at the time of measurement (on-line) or from stored or captured data (off-line). The standard algorithm supplied with the PTL300E system is the so-called **Linear Back-Projection** (LBP) algorithm. This is a **fast** but **approximate** algorithm which uses the **capacitance measurements**, together with the **sensitivity map** to produce the image. Other alternative algorithms can be used with the stored data to produce more accurate images.

8.3 IMAGE RECONSTRUCTION PROBLEMS

There are several problems which make it difficult to calculate accurate permittivity distributions inside the sensor from the normalised measured inter-electrode capacitances. Some of these are listed below:

1. **The limited number of unique inter-electrode capacitance measurements** available severely limits the **image resolution** that can be achieved.

2. The **soft field effect**, which causes the **electric field lines** inside the sensor to be distorted by the **sensor contents**, means that simple image reconstruction algorithms may produce distorted images.

3. The relationship between the **measured capacitances** and the **permittivity distribution** inside the sensor depends on how the constituent materials are distributed inside the sensor. A suitable **sensor capacitance/permittivity/concentration model** must be chosen if accurate concentration figures are to be obtained.

4. Accurate information about the capacitance sensor (the sensor **sensitivity matrix**) must be known before permittivity images can be calculated.

8.4 LINEAR AND NON-LINEAR IMAGE RECONSTRUCTION METHODS

Most **ECT sensors** are inherently **non-linear devices**, partly because of the **soft field effect** and also because, in many cases, the **electrodes are located outside the walls of insulating vessels** so that the sensor can be **non-invasive.** In these cases, the electric field lines between the sensor electrodes are distorted by the vessel wall. Moreover, the capacitive coupling from the electrodes to the material inside the sensor will be weakened if the permittivity of the sensor contents is higher than that of the vessel wall.

Fortunately, in many cases, the permittivity contrasts between the materials in the mixture are relatively small (<3), resulting in correspondingly small distortions in the electric field. In these cases, linear methods, such as the LBP algorithm, already described briefly in paragraph 3.13, can be used with good effect to calculate the permittivity image. Improved accuracy can be achieved by using iterative versions of this algorithm. Further information about iterative algorithms is given in chapter 13 of this manual and also in **PTL Application Note AN4**. Even when the permittivity contrasts are higher, linear methods can still be used along with with iteration to obtain reasonable images.

However, when the permittivity contrasts are large (>10), **non-linear image reconstruction methods** must be used if accurate images are to be obtained. This is particularly the case when one of the dielectric materials is water, which has a very high relative permittivity (dielectric constant) of 80 (for pure distilled water). Non-linear image reconstruction methods are outside the scope of this manual at present

8.5. ECT IMAGE FORMATS, PERMITTIVITY DEFINITIONS AND VOIDAGE

A typical ECT permittivity image format uses a **square grid of 32 x 32 pixels** to display the distribution of the **normalised composite permittivity of each pixel**. For a circular sensor, 812 pixels are used to approximate the cross-section of the sensor. The **values of each pixel** represent the **normalised value of the effective permittivity of that pixel**. In the case of a **mixture of two dielectric materials**, these **permittivity values** are related to the fraction of the higher permittivity material present (the **volume ratio** (or **voidage**)) **at that pixel location.**

In principle, for an ideal ECT sensor with **internal electrodes** and containing a **dielectric material of uniform permittivity**, there will be a **linear relationship** between the **normalised inter-electrode capacitances** and the resulting **normalised pixel permittivity values**. For example, if the sensor contains a uniform material of **normalised permittivity $K_n = P$**, the **normalised inter-electrode capacitances** will all have the value **P,** resulting in an **image where each pixel also has the value P**.

The **overall volume ratio,** which defines the **ratio of the two materials present, averaged over the volume of the sensor**, can also be obtained. The **overall volume ratio** of the materials inside the sensor at any moment in time is defined to be **the percentage of the volume of the sensor occupied by the higher permittivity material**. The volume of the sensor is the product of the cross-sectional area of the sensor and the length of the sensor measurement electrodes.

In all of the following we shall be referring to the **relative permittivity** (or **dielectric constant**) of materials. The **relative permittivity** of a material is its **absolute permittivity** divided by the **permittivity of free space** (or air). Hence the relative permittivity of air is 1 and typical values for other materials in solid or liquid format are polystyrene (2.5), glass (6.0) and mineral oil (2.3).

In this manual, we have used three different terms to describe the same concept, as they are all in common use. These are **volume ratio**, **voidage** and **concentration**, which we define to be the fraction of the higher permittivity material present in the mixture. These terms are inter-changeable in the following text.

Section 4 of this manual describes in detail the steps needed to obtain a permittivity image from the inter-electrode capacitances measured by the CMU, based on the use of the **Linear Back Projection (LBP)** algorithm and derivatives of this algorithm.

9 THE LINEAR BACK PROJECTION (LBP) ALGORITHM

ECT is an example of what Mathematicians call an "**Inverse Problem**". Whereas we can measure the **inter-electrode capacitances** of an ECT sensor, what we actually want to know is the corresponding **permittivity distribution** inside the sensor, which can be considered to be the **inverse** of the actual measurement.

9.1 The Forward Problem

When the sensor inter-electrode capacitances are measured, the resulting values of capacitance are a direct result of the permittivity distribution inside the sensor. For a given sensor, containing E measurement electrodes in each measurement plane, there will be m unique inter-electrode capacitance measurements where:

m = E . (E-1) / 2 and E is the number of electrodes. For example, if E = 12 then there are m = 66 possible capacitance measurements.

We can represent the set of capacitance measurements corresponding to one image frame as an array (or matrix) **C** containing m measured normalised capacitance values.

If we similarly define the permittivity distribution as a set of n normalised square permittivity pixels, they can be represented as an n - element array or matrix **K.** For example. if the permittivity distribution is based on a 32 x 32 pixel grid, then n = 32 x 32 = 1024 pixels.

If we now assume that the relationship between the measured capacitances and the permittivity distribution inside the sensor is substantially linear (which may or may not be the case in practice), we can use the **electrical superposition theorem** to define the relationship between these two matrix parameters. Writing the **superposition theorem** in a form relevant to this situtation, it states that the capacitance measured between any electrode pair for a given permittivity distribution **K** will be equal to the sum of the capacitances which would exist between the same electrode pair if each pixel in the permittivity distribution acted independently, with all other pixels set to zero normalised permittivity.

That is, we can find the capacitance between one pair of electrodes for a given permittivity distribution **K** by setting up a set of n pixel distributions, where successive pixels, starting with the first pixel, are set to their **K** value with all of the other pixels set to **K** = 0. We then measure the elemental inter-electrode capacitances for each case where one pixel is non-zero and add up all of these elemental capacitance values for each non-zero pixel distribution to obtain the value of capacitance **C** for the overall permittivity distribution **K**.

This can be represented mathematically as a matrix equation:

$$\mathbf{C} = \mathbf{S}.\mathbf{K} \qquad (9.1)$$

where: **C** is a matrix containing the set of m measured normalised inter-electrode capacitances
K is a matrix containing the set of n normalised permittivity values
S is a matrix which relates **C** and **S** and is known as the sensor sensitivity matrix (or forward transform) and has the dimensions (m x n).

In practice, most ECT sensors containing low-permittivity materials are sufficiently linear for this approximation to be valid and equation 9.1 is substantially accurate in these cases.

So if we know the permittivity distribution **K** inside the ECT sensor, we can calculate the capacitances that would be measured between each electrode-pair using equation 1, provided that we also know the values of the elements in the matrix **S**.

These values can be found by any of a variety of different methods and the process of obtaining these values (solving for the **sensitivity matrix S**) is known as solving the **"Forward Problem"** in Inverse Problem terminology.

9.2 The Inverse Problem

In principle, once the sensitivity matrix **S** is known, it is a mathematically simple process to obtain the permittivity distribution **K** from the capacitance measurements **C** by inverting matrix equation 9.1. That is:

$$\mathbf{K} = \mathbf{S}^{-1}.\mathbf{C} \qquad (9.2)$$

The solution of this equation is known as solving the **Inverse Problem** by mathematicians and $\mathbf{S}^{-1}$ is known as the **Inverse Transform**.

Unfortunately, it is only possible to obtain the inverse of a square matrix, where (in this case) the number of inter-electrode capacitance measurements m equals the number of pixels n in the permittivity distribution. However, we have already seen that for even a relatively low-resolution image, n is typically 1024 whereas, for a 12-electrode sensor, there will only be m=66 capacitance measurements. Consequently it is not possible to use a true inverse of the sensitivity matrix to solve the inverse problem and some other suitable transform must be found.

In the LBP algorithm, the **transpose** of the **sensitivity matrix** (obtained by swapping the rows and columns of the sensitivity matrix) is used as the **inverse transform**. This n x m element matrix has the correct dimensions to satisfy equation 9.2 but is at best, a poor approximation to a true inverse transform. However, the use of this transform can be justified on physical grounds and as will be seen, although its use produces very blurred images, these can be improved by the subsequent use of more sophisticated algorithms.

So the **inverse problem** can now be defined as follows:

$$\mathbf{K} = \mathbf{C}.\mathbf{S}^{T} \qquad (9.3)$$

where: **K** is the permittivitty distribution to be found
C is the set of measured inter-electrode capacitances
$\mathbf{S}^{T}$ is the transpose of the sensitivity matrix

The LBP algorithm is simple and fast. However, the images produced by this algorithm are blurred because, unlike the case of X-rays, where a single ray path between source and detector will pass through only one set of pixels, the electric field between two capacitance electrodes spreads out and intercepts many pixels. The effect of this is to give a spurious and unwanted level of background permittivity to each pixel. This can be removed by some form of filtering or thresholding if required. Alternatively, an iterative technique as described in chapter 13 and PTL application note **AN4** can be used to improve the image accuracy.

It is clear that the **sensitivity matrix** and its **transpose** are the keys to using the LBP algorithm and the next chapter discusses these matrices in further detail.

10 THE SENSITIVITY MATRIX

The **sensor sensitivity matrix** contains information about how the measured capacitance between any combination of electrodes changes when a change is made to the permittivity of a single pixel inside the sensor.

10.1 THE ELECTRIC FIELD DISTRIBUTION INSIDE THE SENSOR

The variation in sensitivity inside the sensor can be better understood by considering the case where one electrode of the sensor (at 3 o clock in the figure below), is connected to a positive potential V and all of the other electrodes are connected to earth (or virtual earth).

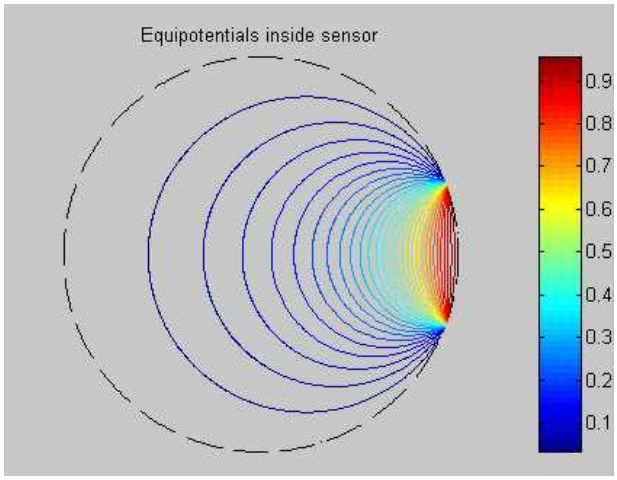

Figure 10.1.1 Equipotential lines inside ECT sensor

The electric field distribution for this situation is shown in figure 10.1.1 (the figure shows the equipotential lines) and is relatively uneven, the field being strongest near to the excited electrode (where the equipotential lines are closest together) and weakening with increasing distance from this electrode. The corresponding electric field lines are shown in the figure below.

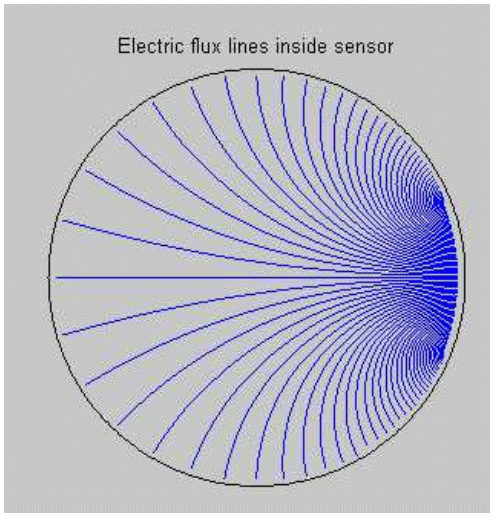

Figure 10.1.2 Electric field distribution inside ECT sensor

A second example, calculated and plotted using different software for an excited electrode located at 11 o clock is shown below.

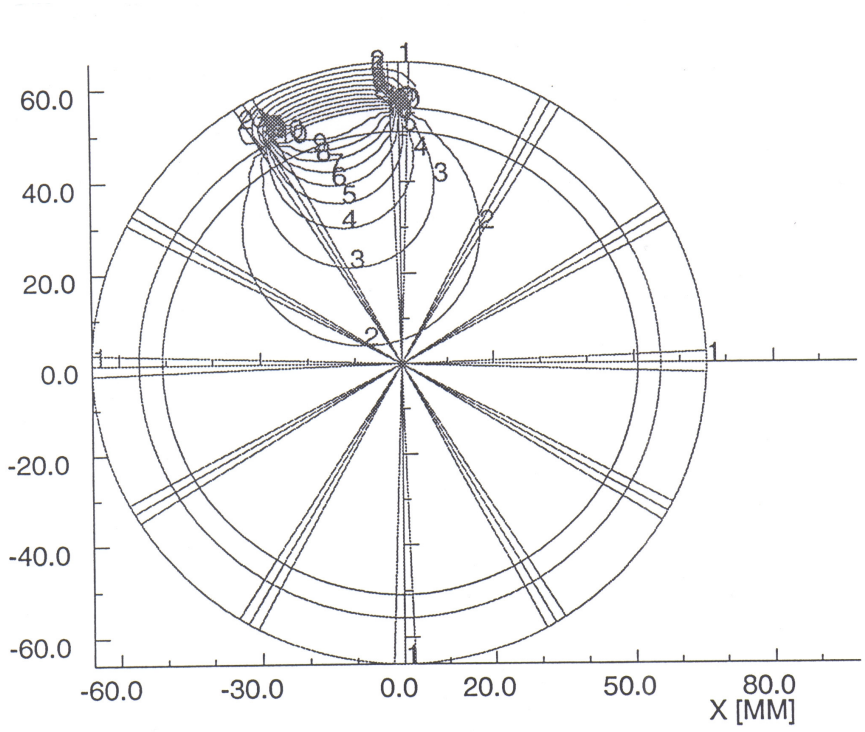

Figure 10.1.3 Equipotentials for an electrode located around 11 o clock

The effect of these uneven electric field distributions is that the change in capacitance measured between any two electrodes caused by an object with a given permittivity will vary depending on the location of the object inside the sensor. For example, when used with a circular cross section sensor, the ECT system is most sensitive when an object is placed near the walls of the vessel and is least sensitive at the centre of the vessel.

Allowance is made for this effect in the LBP algorithm because the variation of sensitivity with position for each pixel is stored in the sensitivity map file. When the ECT system constructs images, it reads the sensitivity map and calculate the image pixels accordingly.

10.2 CALCULATION OF THE SENSITIVITY MATRIX

The sensitivity matrix must be calculated (or measured) for each individual sensor as a separate exercise prior to using the sensor with an ECT system. Two methods for doing this are described below. In general, the first method is preferred as experience has shown that it gives better results and is relatively fast due to easier computation.

10.2.1 Calculation directly from electric fields

The first method for calculating the sensitivity coefficient S of a pixel for an electrode-pair (i-j) is based on the use of equation 10.1.

$$S = \int_A \mathbf{E_i} . \mathbf{E_j} \, . \, dA \qquad (10.1)$$

where $\mathbf{E_i}$ is the electric field inside the sensor when one electrode of the pair i is excited as a source electrode, $\mathbf{E_j}$ is the electric field when electrode j is excited as a source electrode and the dot product of the two electric field vectors $\mathbf{E_i}$ and $\mathbf{E_j}$ is integrated over the area A of the pixel. The set of sensitivity coefficients for **each electrode-pair** is known as the **sensitivity map** for that pair. Hence the **sensitivity matrix** can be considered to be formed from **m sensitivity maps**, one for **each inter-electrode capacitance pair**.

For empty circular sensors with either internal or external electrodes, it is possible to derive an **analytical series expression** for the electric fields and in this case, the sensitivity coefficients (and also the electrode capacitances) can be calculated accurately. For more complex geometries, numerical methods can be used to calculate the sensitivity coefficients. As circular ECT sensors have a high degree of symmetry, it is normally only necessary to calculate a few primary sensitivity maps for the set of unique geometrical electrode pairings, as all of the maps for the remaining electrode pairings can be derived from these primary maps by reflection or rotation (see paragraph 10.8 and Appendix 11 for further information about this).

10.2.2 Calculation from capacitances

A second method for calculating sensitivity matrices is based on calculating the inter-electrode capacitances when each pixel in turn contains the higher permittivity material, with all other pixel permittivities set to zero. That is:

$$Sij(n) = Cij(n) - Cij(LOW) \,/\, (Cij(HIGH) - Cij(LOW)) \qquad (10.2)$$

where: Sij(n) is the sensitivity coefficient for the nth pixel for the capacitance pair i-j

Cij(n) is the capacitance measured between the ith and jth electrodes when pixel n contains the higher permittivity material and all of the other pixels contain the lower permittivity material.

Cij(LOW) is the capacitance measured between the ith and jth electrodes when the sensor contains the lower permittivity material only.

Cij(HIGH) is the capacitance measured between the ith and jth electrodes when the sensor contains the higher permittivity material only.

Calculation of the inter-electrode capacitances requires knowledge of both the electric potential distribution V(x,y) and the permittivity distribution K(x,y) inside the sensor.

The electric potential distribution Vi(x,y) inside the sensor is calculated with electrode i as the source electrode (at a potential +Vs) and all of the other electrodes set to be detector electrodes (at 0V potential). Finite element methods are normally used to calculate Vi(x,y) for a given sensor geometry.

The permittivity distribution K(x,y) can be defined quite simply, as K is set to equal the lower value of permittivity for all pixels except the kth pixel, for which the coefficients are to be calculated, in which case it is set to the high permittivity value.

Once the electric potential distribution Vi(x,y) is known, the inter-electrode capacitances Cij(k) can be calculated using equation 10.3 below:

$$Cij(k) = -(1/V_S)\int_{-R}^{R}\int_{-R}^{R} K(x,y).\ \nabla Vi(x,y).\ dx\ dy \qquad (10.3)$$

where R is the internal radius of the circular vessel

Having calculated each of the inter-electrode capacitances, the sensitivity coefficients may then be calculated using equation (10.2).

10.3 NORMALISATION OF SENSITIVITY MATRICES

Whichever method is used, the sensitivity coefficients have to be normalised so that when equations 9.1 and 9.3 are used, the pixel values have the value 1 when the normalised capacitances have the value 1 and vice-versa.

10.4 TYPICAL SET OF PRIMARY SENSITITIVITY MAPS

A set of primary maps for an 8-electrode sensor operating under protocol 1 and calculated using the method described in paragraph 10.2.1 is shown in figure **10.4.1**.

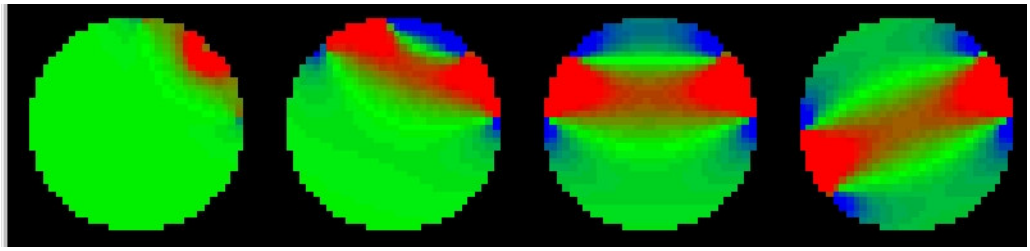

Figure 10.4.1 Primary Sensitivity Maps for an 8-electrode sensor

The maps show the relative pixel sensitivities on a compressed colour scale, where blue pixels represent areas of negative sensitivity, where the capacitance for the electrode pair will decrease when the permittivity of the pixel increases, green pixels represents areas of zero sensitivity and red pixels represents positive sensitivity regions, where the capacitance increases when the pixel permittivity increases.

10.5 SYMMETRY PROPERTIES OF SENSITIVITY MAPS

In principle, we need to calculate the sensitivity map for each electrode pair. Fortunately we only need to calculate the set of primary sensitivity maps, as shown, for example, in figure 10.4, because ECT sensors often have a high degree of symmetry. For example, of the 66 possible capacitance measurements for a 12 element sensor, there are only 6 unique inter-electrode-pair capacitances if the sensor is empty and is symmetrical. These are the capacitances C12, C13, C14, C15, C16, C17. That is the capacitances measured between adjacent electrodes, between next but one electrodes and so on, up to that between diametrically opposed electrodes. All of the other sensitivity maps may be deduced from the maps for these electrode pairs from the symmetry properties of the sensor.

The equivalence between the remaining capacitance measurements and the 6 values for which the sensitivity coefficients are actually calculated or measured is shown in table 10.1. This shows the 6 coefficients S12 - S17 calculated in the plane theta = 0 and the equivalent coefficients for the planes theta from 30 to 330 degrees.

Table 10.5.1

Equivalence Of Sensitivity Coefficients For A 12 Electrode Sensor

THETA 0 Degrees	30	60	90	120	150	180	210	240	270	300	330
S1,2	S2,3	S3,4	S4,5	S5,6	S6,7	S7,8	S8,9	S9,10	S10,11	S11,12	S1,12
S1,3	S2,4	S3,5	S4,6	S5,7	S6,8	S7,9	S8,10	S9,11	S10,12	S1,11	S2,12
S1,4	S2,5	S3,6	S4,7	S5,8	S6,9	S7,10	S8,11	S9,12	S1,10	S2,11	S3,12
S1,5	S2,6	S3,7	S4,8	S5,9	S6,10	S7,11	S8,12	S1,9	S2,10	S3,11	S4,12
S1,6	S2,7	S3,8	S4,9	S5,10	S6,11	S7,12	S1,8	S2,9	S3,10	S4,11	S5,12
S1,7	S2,8	S3,9	S4,10	S5,11	S6,12						

10.6 USE OF MODIFIED SENSITIVITY MATRICES FOR HIGH PERMITTIVITY MATERIALS

In certain cases (for example, when the sensor contains a high permittivity fluid such as water), it may be necessary to use a modified sensitivity matrix rather than the standard matrix. This will be necessary when sensors with **electrodes outside the wall of the vessel** are used to image **high permittivity materials**. This is because an undesirable effect occurs when the fluid to be imaged has a relative permittivity exceeding a value around 10. This occurs for example when water (permittivity = 80) is the fluid to be imaged. The effect is to cause the capacitance measured between adjacent electrodes to decrease rather than to increase when the higher permittivity material is present. This problem can also occur with lower permittivity materials for sensors with thick walls

One solution to this problem is to ignore the capacitances measured between all pairs of adjacent electrodes. This can be achieved by modifying the sensitivity map so that the sensitivity coeficients for adjacent electrodes S[i-(i+1)] are set to zero. A better method is to correct for the sensor C/K characteristics as described in PTL application note AN 10.

10.7 PTL STANDARD GENERIC SENSITIVITY MAPS

In principle, a unique sensitivity map should be calculated for each individual ECT sensor. In practice, good results are obtained using standard generic maps for particular sensor geometries. Two sets of standard generic sensitivity map files for circular sensors are provided for use with the PTL ECT systems. The **standard sensitivity maps** are suitable for imaging most materials having a relative permittivity less than 10 (but not water). The **Water sensitivity maps** are modified versions of the standard maps with the coefficients for adjacent electrodes set to zero. These modified maps give improved images for high permittivity materials such as water.

10.8 CALCULATION OF CUSTOM SENSITIVITY MATRICES

Sensitivity matrices for specific circular sensors can be calculated using custom PTL **Makemap** software which is now supplied with each ECT system. Further information about the use of this software can be found in **Appendix 11**. All ECT sensors designed and supplied by PTL are now supplied with a custom sensitivity map.

11 CALCULATION OF PERMITTIVITY IMAGES

Once the sensitivity map of the sensor is known, sets of captured capacitance data can be converted into permittivity distribution images using a suitable image reconstuction algorithm. The simplest algorithm, the LBP algorithm, has already been described in chapter 9 and images are obtained directly using equation 9.3. Some sample ECT permittivity images are shown below.

11.1 SAMPLE ECT IMAGES

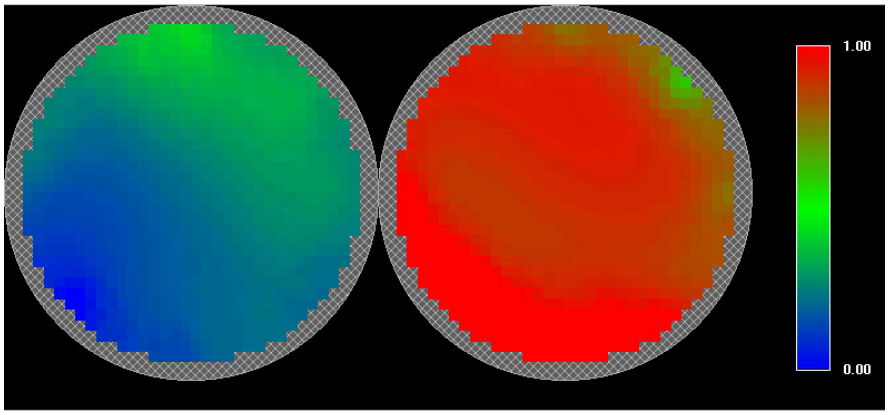

Figure 11.1.1 ECT Images for a fluidised bed

Figure 11.1.1 shows two image at closely-spaced measurement planes for a vertical fluidised bed. The first frame shows an area of low fliuid concentration while the second image shows an area of high concentration.

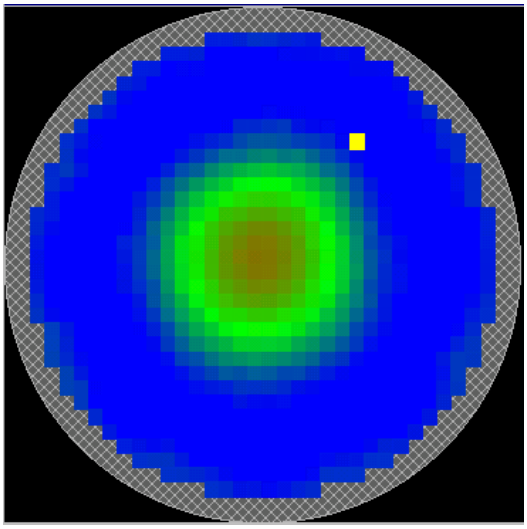

Figure 11.1.2 ECT image of a cylindical dielectric rod

Figure 11.1.2 shows a typical ECT image for a circular dielectric rod.

11.2 IMAGE RESOLUTION

The resolution of an ECT permittivity image is ultimately limited by the number of independent inter-electrode capacitance measurements that are available to the image reconstruction algorithm. The relationship between image resolution and the number of capacitance measurements can be considered to be an example of spatial filtering, as shown in figure 11.2.1 below.

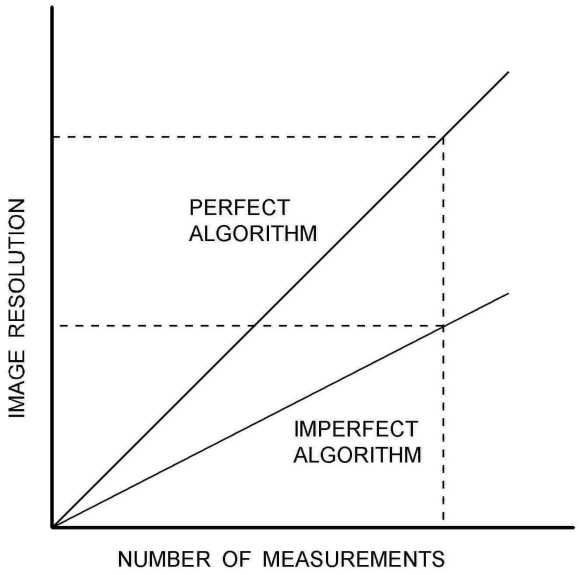

Figure 11.2.1 Resolution limits imposed by spatial filtering.

In this figure, the upper line represents relationship between the image resolution that would be achieved using a "perfect" image reconstruction algorithm for a given number of available capacitance measurements. The lower line shows the same relationship for a less-effective algorithm, as any real algorithm will be less effective than the hypothetical perfect algorithm.

The upper resolution limit for a perfect algorithm is difficult to define mathematically, but a simple engineering estimate can be made by assuming that the number of independent measurements M corresponds to a similar number of discrete regions inside the sensor. If we assume that the angular resolution is equal to the number of electrodes E, then the radial resolution will equal (M / E). For protocol 1 and a 12 electrode sensor, this gives a radial resolution limit of 5.5. For protocol 2 and 24 electrodes, this figure increases to 10.5.

The LBP algorithm is an example of an imperfect algorithm because, although the forward transform (the sensitivity matrix) can be reasonably accurate, the inverse transform used in this algorithm is relatively inaccurate. Consequently, the quality of image obtained using the LBP algorithm is relatively poor. Fortunately, these LBP images can be improved, either by further image processing or by the use of more sophisticated algorithms.

12 VOIDAGE CALCULATION

12.1 NOTE ON ABSOLUTE AND RELATIVE VOIDAGES

We define **voidage** to be the **percentage** of the **higher permittivity material** inside the sensor when the sensor contains a **mixture of 2 dielectric materials**. Other terms which have the same meaning as voidage in this contect are "**Concentration"** and **"Volume Ratio**". Voidage can refere to the total contents of the sensor (the overall voidage), or to an individual pixel or groups of pixels.

All **voidage** values obtained from PTL ECT systems are based on the assumption that the **voidage is 100%** when the sensor is filled with the **higher permittivity material** and is **zero** when the sensor is filled with the **lower permittivity material**. Consequently, the **voidage values obtained from an ECT system** are **Relative Voidages**.

If the two materials used for calibration are **liquids**, then the **voidages** obtained from the ECT system will correspond nominally to the actual **absolute voidages**.

However, in many cases, one of the reference materials (the lower permittivity material) will be **air**. Air has a dielectric constant (relative permittivity) of 1, which is, by definition, the lowest possible value of dielectric constant which can exist for any real material. If the **second reference material** is in **granular or powder form**, the **upper calibration point** will be formed by a **mixture of air and the granular material**.

This will result in a **lower permittivity** for the **upper calibration point** than would be obtained by simply assuming the relative permittivity of the dielectric material in its solid form. For example for a mixture of glass beads and air, the measured permittivity of the mixture is around 3, whereas the permittivity of solid glass is approximately 6.

In this case, the **absolute voidage** for both the individual pixels and the sensor as a whole is obtained by multiplying the indicated **relative voidage** by the **actual voidage** at the upper calibration point.

For example, if the indicated **relative voidage** of a pixel is **p** and the **absolute voidage** when the sensor is full of the higher permittivity material is **f**, then **the absolute voidage of the pixel, VR,** will be given by:

$$\mathbf{VR = p.f} \qquad (12.1)$$

It should be noted that the **permittivity** or **volume ratio distribution** can only be obtained from the **inter-electrode capacitance measurements** if:

1. There are no more than 2 materials present inside the sensor.

2. The sensor has been correctly calibrated using these two materials.

12.2 CALCULATION OF VOIDAGE OF SENSOR CONTENTS

Having obtained the **permittivity distribution** across the sensor, the next step is to derive the **overall volume ratio (voidage),** of the mixture of the two dielectric materials inside the sensor, and also the **distribution** of this **voidage** across the sensor. The overall voidage can be obtained either from the **measurements of the normalised capacitances** between the sensor electrodes or from the **permittivity distribution of the mixture**, derived from these measurements. The **voidage distribution** can only be obtained from the **permittivity distribution**.

12.2.1 CALCULATION OF OVERALL VOIDAGE

In principle, the **overall voidage** of the contents of the ECT sensor can be calculated from either the **normalised pixel values** in the reconstructed **ECT image** or from the **normalised capacitance measurements** directly.

In the case of calculation from **image pixels**, this is done by **summing** the **values of the individual pixels in the ECT image** for the required image frame and dividing this figure by the number of pixels.

Putting this in mathematical terms,

$$VR = (1/N) \sum_{i=1}^{N} K(i) \qquad (12.2.1)$$

where VR is the voidage, N is the total number of pixels and K(i) is the normalised permittivity of the ith pixel.

In the case of calculation from the **normalised inter-electrode capacitances**, the **voidage** is obtained by **summing all of the normalised capacitance values for one image frame** and dividing these by the number of capacitance measurements. Again, putting this in mathematical terms,

$$VR = (1/M) \sum_{m=1}^{M} C(m) \qquad (12.2.2)$$

where M is the total number of electrode-pair measurements and C_m are the individual electrode-pair normalised capacitances.

There are a number of possible methods which can be used to calculate the voidage and the choice of the optimum method depends on the electrical model used to describe the physical distribution of the two materials inside the sensor. For some applications**,** such as liquid or dense-phase mixtures, a simple **parallel capacitance model** can be used to obtain the **voidage distribution** directly from the **permittivity distribution of the mixture**. In this case, the **voidage** is numerically equal to the **normalised pixel values**. Other methods for calculating voidage are described in the following paragraphs and in PTL application note **AN2**.

12.3 CORRECTION FOR SENSOR CAPACITANCE/PERMITTIVITY MODELS

The equations in paragraph 12.2 are based on the assumption that the voidage is directly proportional to the normalised permittivity inside the sensor. This assumption may be valid under some circumstances and invalid in others. This is explored in detail in this chapter.

There are a number of possible methods which can be used to calculate the **voidage** of a 2-phase dielectric mixture and the choice of the optimum method depends on the electrical model used to describe the physical distribution of the two materials inside the sensor. For some applications**,** such as liquid or dense-phase mixtures, a simple **parallel capacitance** model can be used to obtain the voidage distribution directly from the permittivity distribution of the mixture. However, in other applications, such as fluidised beds with high levels of fluidisation, the use of a model based on **capacitances in series** produces better accuracy and sensitivity.

A further model which combines the parallel and series models and which was developed by **Maxwell** in the 19th century is a useful compromise in many practical applications. The need for these sensor models is discussed in this chapter. Further information can be found in **PTL Application Note AN2**.

The reason why these models are needed can be understood by considering the case of simple parallel plate capacitance cell containing two different dielectric materials as discussed in paragraph 12.4.

12.4 EFFECTIVE PERMITTIVITY OF A MIXTURE OF TWO DIELECTRIC MATERIALS

Permittivity images are calculated from the normalised capacitances using equation 9.3. However, before this is carried out, a sensor capacitance/permittivity model must be chosen and the normalised capacitances modified according to this model.

At first sight it is not obvious why different sensor models are needed. However a quick study of figure 12.4.1 gives an insight into the problem. We have shown a parallel plate capacitor (or capacitance cell) consisting of 2 horizontal electrodes 1 and 2. The first figure (a) shows the cell empty (filled with air, k= 1) and the second figure (b) shows the cell filled with a material of relative permittivity k.

Figures c and d show the cell half-filled with the dielectric material but with 2 very different distributions of the dielectric.

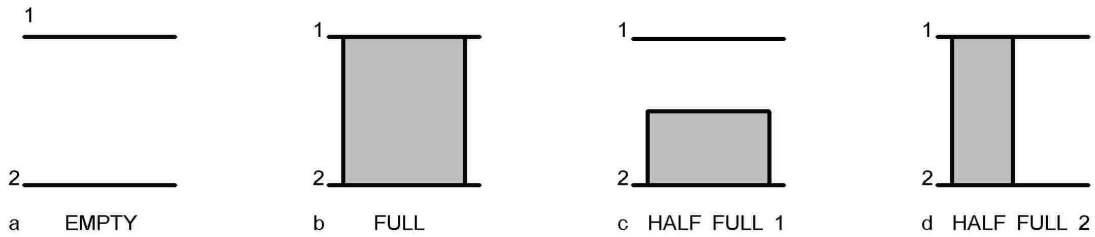

Figure 12.4.1 Capacitance/permittivity distribution models

If we assume that we can treat these cells as perfect parallel plate capacitors, we will measure the following values of relative capacitance for cells a to d:

a: (empty) 1

b: (full) k

c: (half-full horizontally) 2k/(k + 1),

d: (half-full vertically) 1/2(1 + k)

When the cell is filled with the dielectric material, the capacitance increases by a factor of k. However, when the cell is partially-full, the way the capacitance increases depends on the distribution of the dielectric material inside the sensor.

Where the distribution is layered vertically, as shown in figure d, the capacitance of the cell increases linearly with the proportion of dielectric material present. The effect is to create 2 elemental capacitances which are in parallel with each other. The capacitance of 2 parallel capacitors is found simply by adding up the 2 individual capacitances. That is:

$$C = C1 + C2 \qquad (12.4.1)$$

However, if the distribution is layered horizontally, as shown in figure c, The capacitance increases in a non-linear manner. There are now effectively 2 capacitors in series formed by the air and dielectric regions. The capacitance of 2 capacitors in series is found by the reciprocal rule ie:

$$1/C = 1/C1 + 1/C2 \qquad (12.4.2)$$

Hence we have 2 fundamentally different methods of calculating how the capacitances will increase when the sensor is half-filled with a dielectric material. We refer to these 2 models as the **parallel** and **series capacitance models.**

It is worth noting that, at the end points (where the sensor is either empty or full, both methods give the same values (0 and 1) for the normalised capacitances. However, whereas the **parallel** model gives a straight line relationship between these 2 points, which means that in this case, the concentration is linearly related to the capacitances, the **series** model gives a series of **non-linear curves**, depending on the permittivity of the dielectric material in the sensor.

12.5 SERIES MODEL CORRECTION

Whereas for the parallel model, there is a straight-line relationship betyween the measured capacitances and the voidage, the results obtained using the series model are shown below for a range of permittivities K. The graph plots the indicated voidage (calculated from the measured capacitances) against the actual voidage (calculated on the basis of the proportion of dielectric material present inside the sensor). The deviation from a linear relationship increases with the permittivity of the material in the sensor.

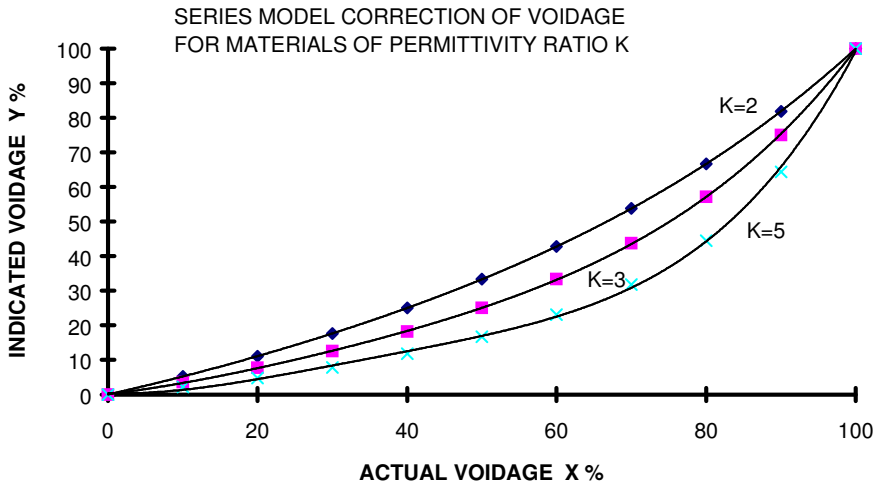

Figure 12.5.1

The effect of this relationship is that the voidages calculated using the simple linear (parallel) model will always under-estimate the true voidage if the material distribution effectively forms parallel paths between pairs of electrodes.

This problem can be corrected by modifying the measured normalised capacitances by a correction factor defined in equation 11.2 below:

$$C_{n2} = C_n.(K_H/K_{L)} / (1 + C_n(1 - K_L/K_H)) \qquad (12.5.1)$$

Where C_{n2} is the corrected normalised capacitance, C_n is the measured normalised capacitance and K_L and K_H are the relative permittivities of the 2 materials in the sensor

It should be noted that when $K_L = K_H$, $C_{n2} = C_{n1}$ and no correction is made to the measured capacitance values. Equation 11.2 can therefore be applied universally, corresponding to the parallel model when K = KH/KL = 1 and corresponding to the serioes model when K > 1.

The **parallel capacitance model** tends to be valid for densely packed materials, such as liquids, or powdered/granular materials in **dense-phase** processes. In this case, no modification of the measured capacitances is required and K is set to 1.

However, where the concentration values are low, as is the situation in lean-phase conveying or particles, the **series model** must be used to obtain accurate voidage values.

12.6. OTHER PERMITTIVITY MODELS

There are a number of other models which can be used to calculate the relationship between the voidage and the effective permittivity of the material inside the sensor.

12.6.1 Maxwell Model

This model is a compromise between the series and parallel models. It yields a slightly different correction factor which, in practice is applicable to mixtures of two materials where both the **parallel** and **series** models apply in diffferent regions of the mixture.

$$C_{n2} = K_{en}.(2 + k)/(3 + C_n.(k - 1) \qquad (12.6.1)$$

where $k = K_H / K_L$

12.6.2 Yang/Szuster Model

A variation on the series model, which does not rely on knowing the ratio of the permittivities of the materials used at calibration, has been developed independently by Dr W.Yang of UMIST in the UK and K. Szuster in Poland. This method effectively deduces the permittivity ratio from the calibration data.

The correction factor which results from this model is given in equation 12.6.2.

$$C_{n2} = C_n. (C_H/C_m) \qquad (12.6.2)$$

where:
C_H is the absolute value of the capacitance measured during calibration for the higher permittivity material.

C_m is the absolute value of the measured capacitance.

13 AN ITERATIVE METHOD FOR IMPROVING IMAGE QUALITY

The iterative image reconstruction method is based on the use of equations 9.1 and 9.3. The idea is to use these two equations alternately to correct the sets of capacitance and pixel values in turn and hence produce a more accurate image from the capacitance measurements. The details are as follows:

1. Measure a set of (typically 66) normalised capacitances $\mathbf{C_1}$ for one image frame.

2. Correct the set of normalised measured capacitances $\mathbf{C_1}$ using the series model correction formula (or some other correction formula, see paragraphs 12.6/7).

3. Calculate the set of (typically1024) pixel permittivities $\mathbf{K_1}$ corresponding to $\mathbf{C_1}$ using equation (9.3) ie.

$$\mathbf{K_1 = S^T.C_1} \qquad (13.1)$$

Note that the matrix $\mathbf{S^T}$ must be normalised as follows: As $\mathbf{K_1}$ is a set of 1024 pixels and $\mathbf{C_1}$ is a set of (eg 66) capacitance readings, then $\mathbf{S^T}$ must be normalised by dividing each of the elements (permittivity coefficients) in $\mathbf{S^T}$ which contribute to each specific pixel value in $\mathbf{K_1}$ by the sum of all of the values of permittivity coefficients in $\mathbf{S^T}$ which contribute to the specific pixel location (a sum of eg 66 permittivity coefficients).

4. Truncate the individual pixel values **k** so that they lie within the range $\mathbf{0 < k < 1}$ and save and display the image.

5. Use these new values of permittivity to back-calculate a new set of inter-electrode capacitances $\mathbf{C_2}$ using equation (1) ie:

$$\mathbf{C_2 = S.\ K_1} \qquad (13.2)$$

Note that in this case, the matrix **S** must be normalised as follows: As $\mathbf{C_2}$ is a set of eg 66 inter-electrode capacitance measurements and $\mathbf{K_1}$ is a set of 1024 pixel values, then **S** must be normalised by dividing each of the elements (capacitance coefficients) in **S** which contribute to each specific inter-electrode capacitance measurement by the sum of all of the capacitance coefficients in **S** which contribute to this capacitance measurement (a sum of 1024 capacitance coefficients).

6. Calculate a set of error capacitances $\mathbf{\Delta C}$ where:

$$\mathbf{\Delta C = (C_2 - C_1)} \qquad (13.3)$$

7. Truncate $\mathbf{\Delta C}$ to limit the maximum values of $\mathbf{\Delta C}$ so that they lie within the range $(-0.05 < \mathbf{\Delta C} < 0.05)$ or some other pre-defined limits. This is necessary to prevent the feedback loop from becoming unstable.

8. Multiply $\mathbf{\Delta C}$ by a gain factor (typically 1.5) which **is** determined by empirical means.

9. Use equation (13.1) and the error capacitances **ΔC** to calculate a set of error pixel values **ΔK**. ie:

$$\mathbf{\Delta K = S^T . \Delta C} \qquad (13.4)$$

10. Use the set of error pixels to generate a new set of pixel values $\mathbf{K_2}$ where:

$$\mathbf{K_2 = (K_1 - \Delta K)} \qquad (13.5)$$

11. Truncate these pixel values to lie within the range $0 < \mathbf{k} < 1$ and save and display the image.

12. Repeat steps 5 to 11 using the new set of **K** values $\mathbf{K_2}$ (instead of $\mathbf{K_1}$) in equation (13.2). In equation 13.3, generate the error capacitances by subtracting the **original** measured capacitances from the current set.

11. Repeat step 12 as many times as necessary to obtain an accurate image.

An illustration of the image improvement which can be obtained is shown in the following figure 13.1.1. The image data is for a 60mm OD plexiglass tube with 5mm walls, placed approximately centrally inside an 8 electrode ECT sensor having an internal diameter of 100mm. The figure shows the improvements in the image as the number of iterations is steadily increased.

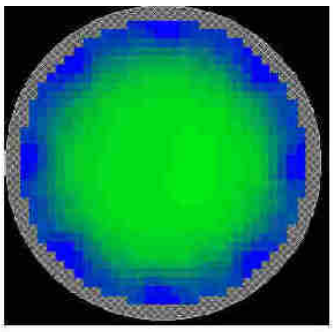

LBP IMAGE

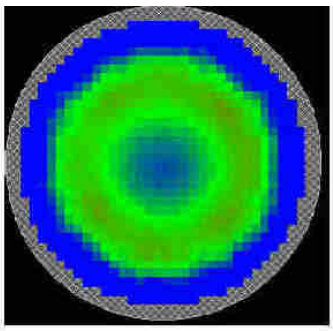

10 ITERATIONS

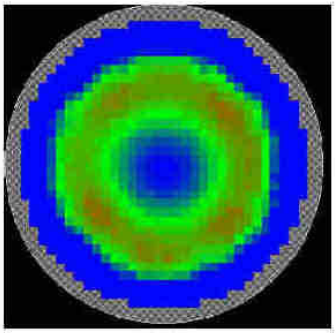

20 ITERATIONS

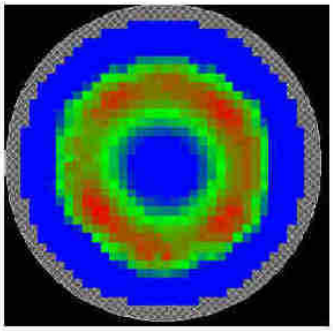

50 ITERATIONS

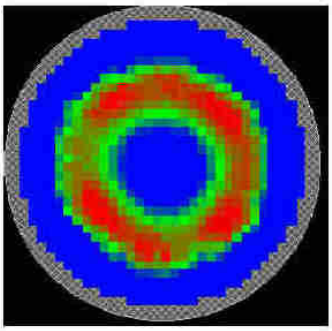

100 ITERATIONS

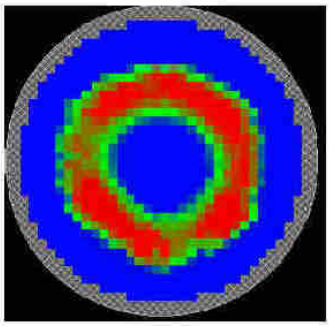

200 ITERATIONS

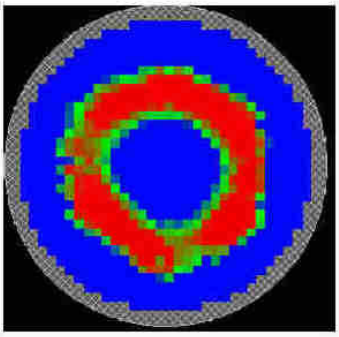

500 ITERATIONS

TUBE IMAGE SHOWING IMPROVEMENTS WITH INCREASING NUMBER OF ITERATIONS

Figure 13.1.1

14. IMAGE RECONSTRUCTION ACCURACY TESTS

Tests were carried out using a 12-electrode sensor with **internal** electrodes to determine the accuracy of image reconstruction based on the calculation of voidage. Tests were carried out using sensitivity matrices calculated using the PTL **Makemap** software, the **iterative algorithm** and a range of **permittivity models** The detailed results are shown in this chapter but can be summarised as follows:

For the case of a dielectric rod in air (ie **a higher permittivity object** inside a **lower permittivity space**) the **series permittivity model** gives the most accurate values of voidage when the permittivity ratio of the materials used for sensor calibration is used.

For the case of a cylindrical void containing air inside a sensor filled with glass beads (ie a **lower permittivity object** inside a **higher permittivity space**) the **Maxwell permittivity model** gives the most accurate values of voidage when the permittivity ratio of the materials used for sensor calibration is used.

Details of the individual tests are given in paragraphs 14.1 and 14.2.

14.1 PLASTIC ROD CONTAINING GLASS BEADS IN AIR

The following results were obtained by calibrating a 12-electrode sensor, of internal diameter 128mm, with air and glass beads (effective K = 3). A thin plastic tube of external diameter 40mm filled with glass beads was then introduced into the sensor. The true voidage is (40/128)^2 = 9.8%.

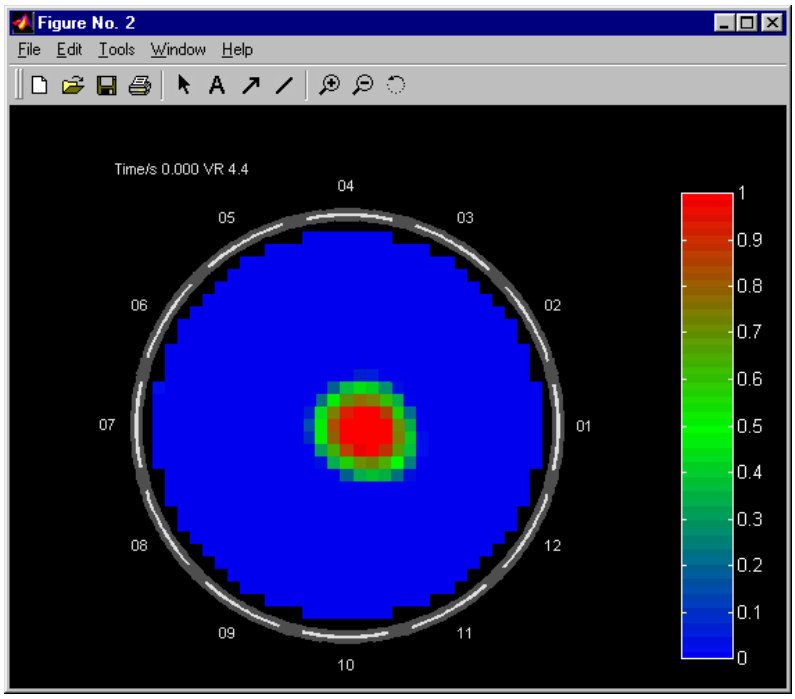

Figure 14.1.1 Parallel model, (K = 1), N=100, VR = 4.4%

Figure 14.1.1 shows the image obtained using the **parallel permittivity model** for 100 iterations and a permittivity ratio of 1. The voidage (VR) obtained is 4.8%, which is less than the known value (9.8%).

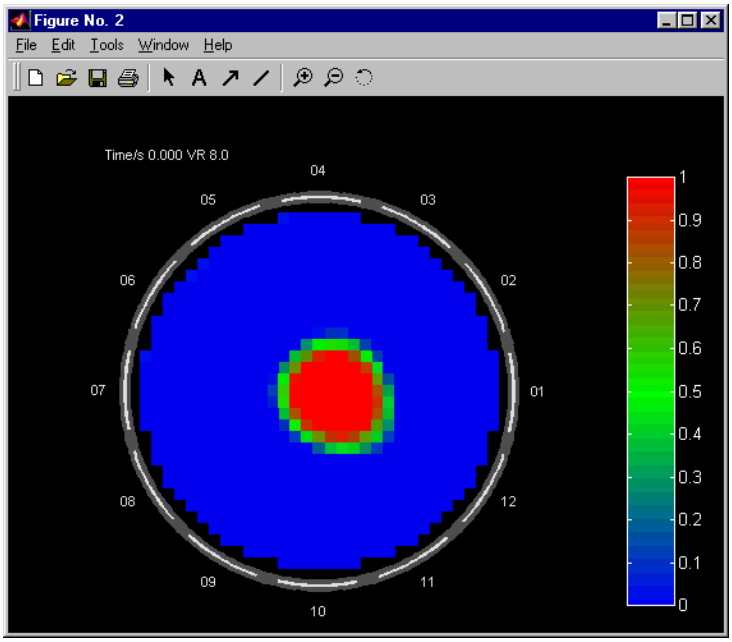

Figure 14.1.2 Series model, K = 2, N=100, VR = 8.0%

Figure 14.1.2 shows the same data but this time using the **series model** for a permittivity ratio of 2. The voidage (VR) has increased but is still less than the known value.

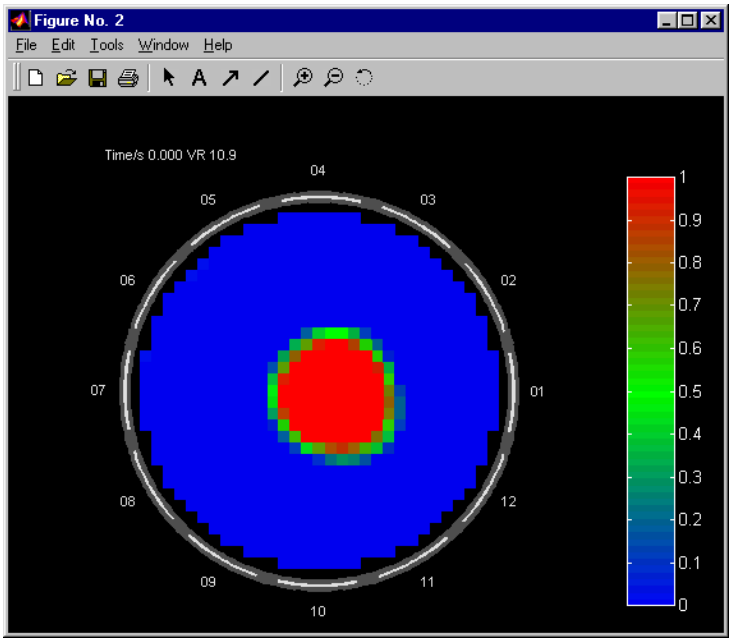

Figure 14.1.3 Series model, K = 3, N=100, VR = 10.9%

Figure 14.1.3 shows the same data but this time for the correct permittivity ratio of 3. The calculated voidage (VR) is 10.9% and now exceeds the known value. If the Maxwell model is used to construct the image, the VR is found to be 7.05% using the same data as used in figure 14.1.3.

14.2 CYLINDRICAL AIR VOID INSIDE GLASS BEADS

For a second set of tests, the sensor was filled with glass beads and the same plastic tube, this time empty, was inserted inside the sensor. The known voidage is 90.2%.

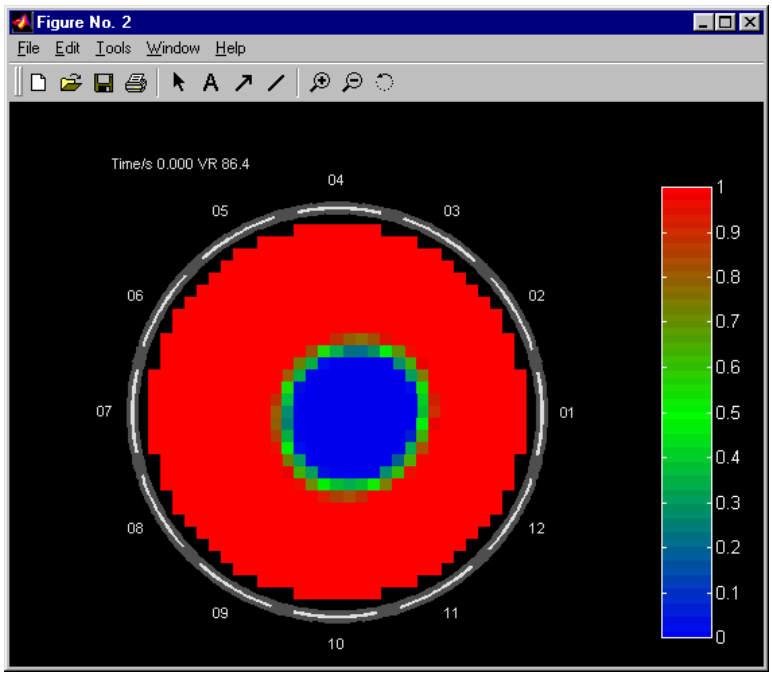

Figure 14.2.1 Parallel model, (K = 1), N=100, VR = 86.4%

Figure 14.2.1 shows the image constructed using the **parallel permittivity model** (K = 1). The calculated voidage (86.4%) is lower than the known voidage (90.2%).

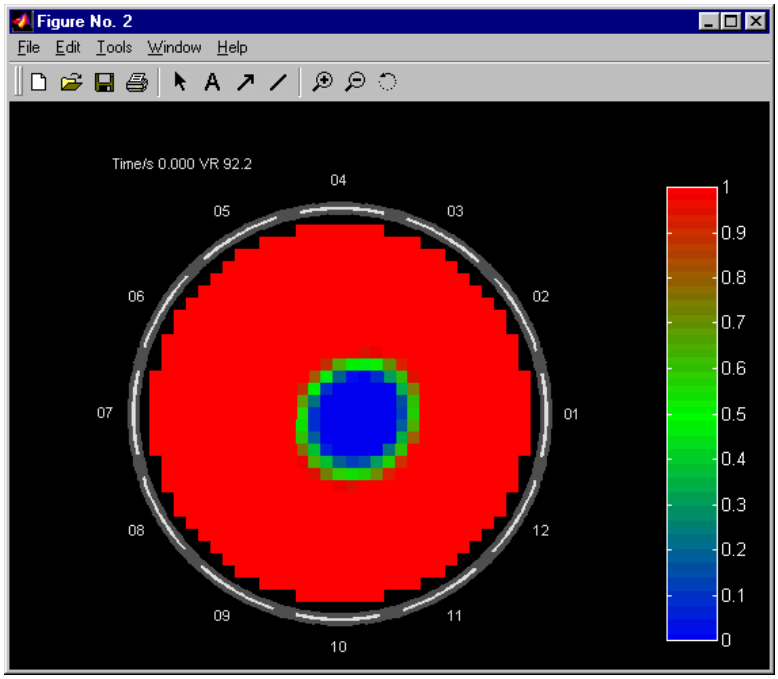

Figure 14.2.2 Series model, K = 2, N=100, VR = 92.2%

Figure 14.2.2 shows the same data calculated using the **series model** and a permittivity ratio of 2. The calculated voidage now exceeds the known voidage.

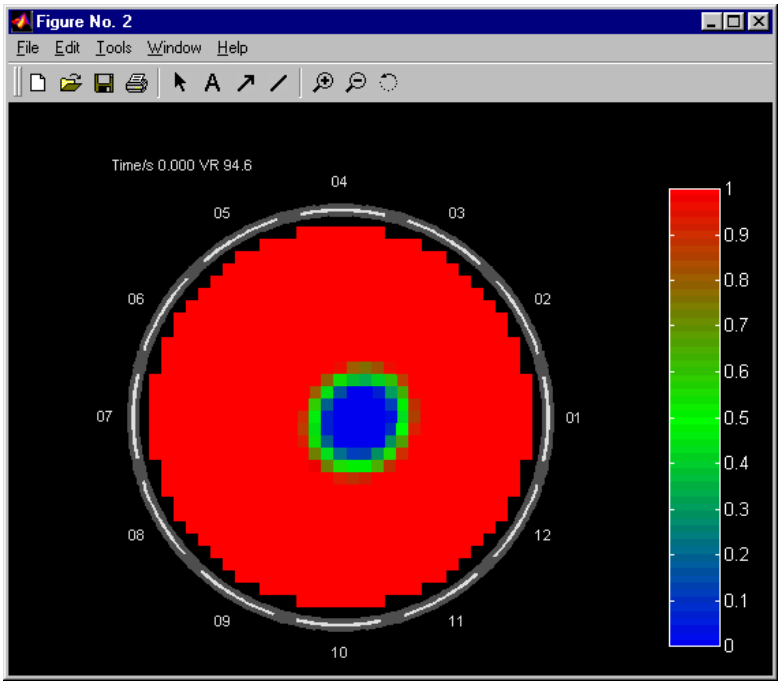

Figure 14.2.3 Series model, K = 3, N=100, VR = 94.6%

Figure 14.2.3 shows the results recalculated for the correct permittivtiy ratio of 3. The results show an even higher voidage (94.6%).

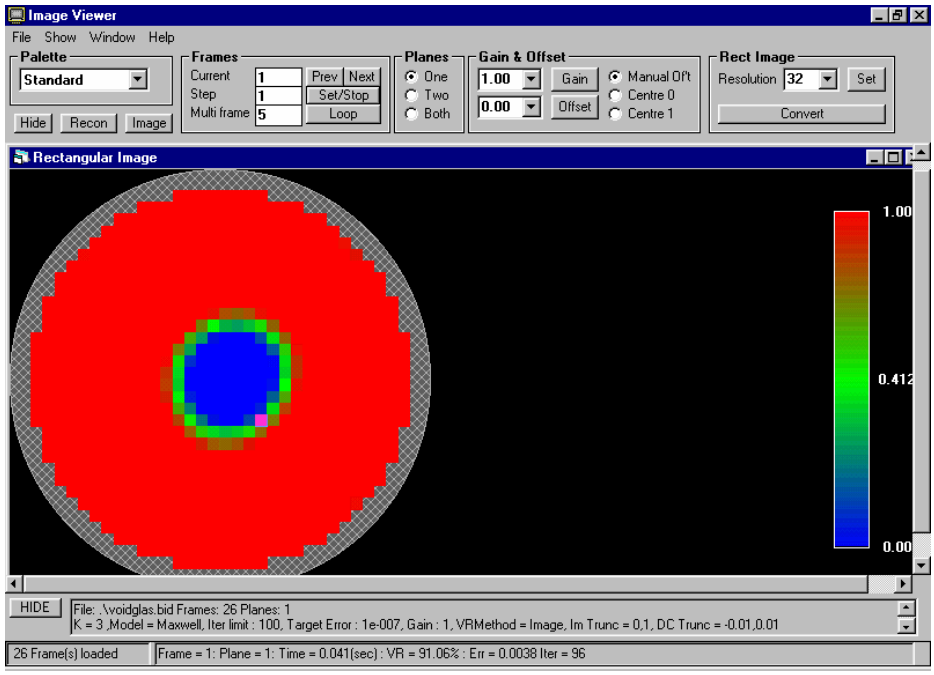

Figure 14.2.4 Maxwell model, K = 3, N=100, VR = 91.1%

For comparison, figure 14.2.4 shows the same data recalculated using the Maxwell permittivity model. The results are now close to the true voidage.

15 GENERATION OF ENHANCED IMAGES WITHOUT ITERATION

It is possible to calculate **enhanced inverse transforms (tranformation matrices)** which give better quality images than those produced by LBP, (which uses the simple transpose of the sensitivity matrix as the inverse transform).

A number of different **transformation matrices** can be used, but two methods which give useful improvements over back-projection are based on methods originally described by **Tikhonov** and **Landweber.** In principle, the **Landweber** method should give similar results to the iterative algorithm when **pixel truncation is disabled.** Both the **Landweber** and **Tikhonov transformation matrices** can be obtained from the **sensitivity matrix** for the sensor. This process is termed **regularisation** by Mathematicians.

15.1 The Tikhonov Transform

We are indebted to Dr Andrew Reader of UMIST (DIAS) for the following explanation of the **Tikhonov transform**:

In the **LBP** method, the forward and inverse transforms are defined by the two matrix equations:

$$\mathbf{C = S.K} \qquad (15.1)$$

$$\mathbf{K = S^T.C} \qquad (15.2)$$

where:

S is the sensor sensitivity matrix, $\mathbf{S^T}$ is the transpose sensitivity matrix and the **forward transform** (equation 15.1) is assumed to be **accurate**, but the i**nverse transform** (equation 15.2) is known to be **inaccurate**.

Let **K** be the actual (physical) permittivity distribution and $\mathbf{K_{BP}}$ be the (erroneous) distribution calculated from the capacitance measurements **C** using equation (15.2).

Then $\mathbf{K_{BP} = S^T.C}$ (15.3)

Substituting for **C** using equation 15.2 we obtain:

$$\mathbf{K_{BP} = S^T.S.K} \qquad (15.4)$$

Hence $\mathbf{K = K_{BP}.(S^T.S)^{-1}}$ (15.5)

and substituting for $\mathbf{K_{BP}}$ from equation (10.1.4) we obtain:

$$\mathbf{K = S^T.C.(S^T.S)^{-1}} \qquad (15.6)$$

giving $$\mathbf{K} = \frac{\mathbf{S^T.C}}{\mathbf{S^T.S}} \qquad (15.7)$$

That is, the true permittivity distribution **K** is obtained by using the inverse transform $\frac{\mathbf{S^T}}{\mathbf{S^T.S}}$ instead of the simple transpose matrix $\mathbf{S^T}$.

However, the matrix $\mathbf{S^T.S}$ has squared sensitivity coefficients along its primary diagonal and if these coefficients are small, their squared values will be very small. There is a clear danger that dividing the matrix $\mathbf{S^T}$ by this denominator matrix $\mathbf{S^T.S}$ will result in some divisions by very small numbers or even by zero. To prevent this from happening the Tikhonov transform introduces an additional constant term **t** to the diagonal elements of the denominator matrix by adding a further scaled identity matrix t.**I** to the denominator.

That is equation (15.7) becomes:

$$\mathbf{K} = \frac{\mathbf{S^T.C}}{\mathbf{S^T.S} + t.\mathbf{I}} \qquad (15.8)$$

where t is a scalar constant (the Tikhonov constant) and **I** is the identity matrix (a matrix with ones along the primary diagonal and zeroes elsewhere).

As can be seen, equation 15.8 is similar to the LBP inverse transform except that the transpose matrix S^T is replaced by the new transform $\mathbf{Q^T}$ where:

$$\mathbf{Q^T} = \frac{\mathbf{S^T.C}}{\mathbf{S^T.S} + t.\mathbf{I}} \qquad (15.9)$$

This transform is readily computed from the sensor sensitivity matrix.

The Tikhonov transform can also be written in the alternative from shown in equation 15.10 below:

$$\mathbf{Q_T = S^T . (S . S^T + t . I)^{-1}} \qquad (15.10)$$

In physical terms, what the Tikhonov transform does is correct the effect of the erroneous matrix $\mathbf{S^T}$ (which causes low-pass spatial filtering of the permittivity distribution, removing all of the fine detail) by the use of a complementary transform (which has the effect of passing the data through an amplified high-pass filter). However, there is a limit to how much gain can be used without simply amplifying the noise in the low-pass-filtered capacitance measurements. The identity matrix and scaling factor effectively limit the gain which is applied to the correcting transform. Larger values of t will have a large moderating effect while small values of t will have minimal effect. The choice of t is therefore critical to avoid spurious artefacts in the reconstructed image. Typical safe values for **T** are in the range 0.1 to 100. Low values of **T** yield very noisy higher-definition images while higher values of **T** produce images similar to those produced by LBP.

To use the Tikhonov transform, all that is required is to replace the inverse transform used in the inverse problem equation (the transpose sensitivity matrix) by the Tikhonov transform.

15.2 The Landweber Transform

The **transformation matrix Q_L** used in **Landweber's** method can be derived from the **sensor sensitivity matrix S** by defining a **transform parameter L** and an **iteration parameter N** (which defines the number of iterations).

Q_L is defined in equation 7.1 as follows:

$$Q_L = V \,.\, F\,(W, t, N)\,.\, U' \qquad (15.13)$$

where:

V, W and **U** are the matrices obtained by applying the **Single Value Decomposition** (**SVD**) process to the sensitivity matrix **S.** This operation produces a diagonal matrix **W** of the same dimensions as **S**, and unitary matrices **U** and **V,** so that $S = U \,.\, W \,.\, V$.

F is the **SVD** filter function matrix defined in equation **A1.2**.

$$f = (\,(1 - (\,1 - t \,.\, w\,)^N\,)\,/\,w \qquad (15.14)$$

where:

f is one element of the filter matrix **F**

w is one element of the diagonal matrix **W**

t is a relaxation parameter (referred to in the main text as the Landweber transform parameter L).

N is the number of iterations.

Typical safe values for **L** are in the range 0.01 to 0.0001. Experience shows that high values of **L** (0.01) can give rise to spurious artefacts around the edges of the image, while low values of **L** appear to give results similar to those obtained using the simple **LBP algorithm**. Typical practical values for the number of iterations **N** are in the range 10 to 100.

To use the Landweber transform, all that is required is to replace the inverse transform used in the inverse problem equation (the transpose sensitivity matrix) by the Landweber transform.